Report
P-15-13
December 2016

KBS-3H – DETUM

Difference flow logging in boreholes K03009F01 and K08028F01

Jere Komulainen
Jari Pöllänen

SVENSK KÄRNBRÄNSLEHANTERING AB

SWEDISH NUCLEAR FUEL
AND WASTE MANAGEMENT CO

Box 250, SE-101 24 Stockholm
Phone +46 8 459 84 00
skb.se

SVENSK KÄRNBRÄNSLEHANTERING

ISSN 1651-4416
SKB P-15-13
ID 1466330

December 2016

KBS-3H – DETUM

Difference flow logging in boreholes K03009F01 and K08028F01

Jere Komulainen, Jari Pöllänen

Pöyry Finland Oy

Keywords: Äspö, Hydrogeology, Hydraulic tests, Difference flow measurements, Äspö Hard Rock Laboratory.

This report concerns a study which was conducted for Svensk Kärnbränslehantering AB (SKB). The conclusions and viewpoints presented in the report are those of the authors. SKB may draw modified conclusions, based on additional literature sources and/or expert opinions.

Data in SKB's database can be changed for different reasons. Minor changes in SKB's database will not necessarily result in a revised report. Data revisions may also be presented as supplements, available at www.skb.se.

A pdf version of this document can be downloaded from www.skb.se.

Abstract

The Posiva Flow Log, Difference Flow Method (PFL DIFF) uses a flowmeter that incorporates a flow guide and can be used for relatively quick determinations of transmissivity and hydraulic head in fractures/fractured zones in cored boreholes. This report presents the main principles of the method as well as the results of measurements carried out in underground boreholes K03009F01 and K08028F01 at the Äspö Hard Rock Laboratory, Sweden, in September 2014.

The flow logging measurements were done with 1 m and 5 m test sections and by moving the measurement tool in 0.1 m and 0.5 m steps, respectively. This method was used to flow log the entire measurable part of the two boreholes. Both boreholes were partially sealed at the collar during the measurements in order to obtain the desired pressure in a borehole, and keeping the boreholes filled with water. Pressure in the borehole was controlled by an adjustable control valve. The flow measurements were carried out at two different pressure states in the borehole.

The boreholes were closed using a new borehole sealing mechanism which was used for the first time in these measurements. The sealing mechanism was developed under a SKB-Posiva co-operation by Pöyry Finland Oy.

The electrical conductivity (EC) and temperature of borehole water were also measured. The EC measurements were used to study the occurrence of saline water in the borehole.

The outflow from the borehole was measured when the borehole was partially closed during the measurements.

The KBS-3H design has been developed jointly by SKB and Posiva since 2002. This report has been prepared within the project phase "KBS-3H – System Design 2011–2016".

Sammanfattning

Posiva Flow Log, Differensflödesloggning (PFL DIFF) är en snabb metod för bestämning av transmissiviteten och hydraulisk tryckhöjd i borrhålssektioner och sprickor/sprickzoner i kärnborrhål. Denna rapport presenterar huvudprinciperna för metoden och resultat av mätningar utförda i borrhål K03009F01 och K08028F01 inom Äspö Hard Rock Laboratoriet, Sverige, i september 2014.

Flödesmätningarna gjordes med en 1 m och 5 m lång testsektion som förflyttades successivt i steg om 0.1 m och 0.5 m i den mätbara delen av borrhålet. Borrhålet var delvis stängt under mätningarna. Trycket i borrhålet var justerat med reglerventil. Flödesmätningarna utfördes i två tryckförhållanden i borrhålet.

Borrhålet var stängt med en ny stängningsmekanism vilken användes för första gången. Denna stängning mekanism var utvecklad i samarbete med SKB, Posiva och Pöyry Finland AB.

Elektrisk konduktivitet (EC) och temperatur på borrhålsvattnet mättes också. EC-mätningarna användes för att studera förekomsten av saltvatten i borrhålet.

Utflödet från borrhålet mättes under tiden det var delvis stängt för mätningarna.

KBS-3H är en variant av KBS-3 metoden som utvecklas gemensamt av SKB och Posiva. Denna rapport har utarbetats under projektfasen ”KBS-3H – System Design 2011–2016”.

Contents

1 Introduction 9

2 Objective and scope 11

3 Principles of measurement and interpretation 13
3.1 Measurements 13
3.2 Interpretation 15

4 Equipment specification 17

5 Execution of measurements 19
5.1 General 19
5.2 Experimental premises 21
5.3 Measurement in an upward inclined borehole 21
5.4 Nonconformities 24

6 Results 25
6.1 Length calibration 25
6.1.1 SPR measurement 25
6.1.2 Estimated error in position of detected fractures 25
6.2 Electrical conductivity and temperature 25
6.2.1 Electrical conductivity and temperature of borehole water 25
6.3 Absolute pressure and outflow measurements 26
6.4 Flow logging 27
6.4.1 General comments on results 27
6.4.2 Hydraulic characteristics of borehole sections 27
6.4.3 Transmissivity of fractures 29
6.4.4 Theoretical and practical measurement limits of flow and transmissivity 30
6.4.5 Sensitivity of transmissivity and the formation head to the errors in flow and pressure measurements 31
6.4.6 Comments and further improvements of the used techniques 33

7 Summary of main findings 35

References 37

Appendix 1 SPR results after length correction 39
Appendix 2.1 Electrical conductivity of borehole water 41
Appendix 2.2 Temperature of borehole water 43
Appendices 3.1–3.5 Flow rate and single point resistance 45
Appendix 4 Explanations for the tables in Appendices 5, 7 and 9 55
Appendices 5.1–5.4 Results of sequential flow logging 57
Appendix 6.1 Flow rates of 1 m sections 65
Appendix 6.2 Transmissivity and head of 1 m sections 67
Appendix 6.3 Transmissivity and head of 1 m sections with error bars 69
Appendix 7 Results of sequential flow logging 71
Appendix 8.1 Flow rates of 5 m sections 73
Appendix 8.2 Transmissivity and head of 5 m sections 75
Appendix 8.3 Transmissivity and head of 5 m sections with error bars 77
Appendices 9.1–9.2 Inferred flow anomalies from overlapping flow logging 79
Appendix 10 Transmissivity and head of detected fractures 83
Appendices 11.1–11.2 Comparison between section transmissivity and fracture transmissivity 85

Appendix 12.1	Head in the borehole during flow logging	89
Appendix 12.2	Pressure in the borehole during flow logging	91
Appendix 12.3	Borehole pressure and outflow from the borehole	93
Appendix 13	SPR results after length correction	95
Appendix 14.1	Electrical conductivity of borehole water	97
Appendix 14.2	Temperature of borehole water	99
Appendices 15.1–15.5	Flow rate and single point resistance	101
Appendix 16	Explanations for the tables in Appendices 17, 19 and 21	111
Appendices 17.1–17.4	Results of sequential flow logging	113
Appendix 18.1	Flow rates of 1 m sections	121
Appendix 18.2	Transmissivity and head of 1 m sections	123
Appendix 18.3	Transmissivity and head of 1 m sections with error bars	125
Appendix 19	Results of sequential flow logging	127
Appendix 20.1	Flow rates of 5 m sections	129
Appendix 20.2	Transmissivity and head of 5 m sections	131
Appendix 20.3	Transmissivity and head of 5 m sections with error bars	133
Appendix 21	Inferred flow anomalies from overlapping flow logging	135
Appendix 22	Transmissivity and detected fractures	137
Appendices 23.1–23.2	Comparison between section transmissivity and fracture transmissivity	139
Appendix 24.1	Head in the borehole during flow logging	143
Appendix 24.2	Pressure in the borehole during flow logging	145
Appendix 24.3	Borehole pressure and outflow from the borehole	147

1 Introduction

The core-drilled boreholes K03009F01 and K08028F01 at Äspö, Sweden were measured using the Posiva Flow Log, Difference Flow Method (PFL DIFF) which provides a swift, multifaceted characterization of a borehole. The measurements were conducted between September 3 and September 7, 2014. The boreholes are located in the Äspö Expansion part (TASU tunnel) of the Äspö Hard Rock Laboratory (HRL).

The KBS-3H design has been developed jointly by SKB and Posiva since 2002. This report has been prepared within the project phase "KBS-3H – System Design 2011–2016".

K03009F01 is 100.92 m long and its inclination at its reference point at Z= −399.23 masl with a −0.37° (downward) inclination from the horizontal plane. K08028F01 is 94.39 m long and its reference point is at Z= −396.584 masl with a 2.18° (upward) inclination from the horizontal plane. The boreholes are cased within interval −0.24 m to 2.44 m in K03009F01 and within interval −0.35 m to 2.20 m in K08028F01 (rock surface being the reference level for length measurement). The inner diameter of the casing tube is 80 mm in K03009F01 and 76.2 mm in K08028F01. The rest of the boreholes is core drilled with a diameter of c. 75.8 mm.

The locations of K03009F01 and K08028F01 in the Äspö Expansion part of the Äspö Hard Rock Laboratory are illustrated in Figure 1-1.

The field work and the subsequent data interpretation were conducted by Pöyry Finland Oy. PFL DIFF has previously been employed in Posiva's site characterisation programme in Finland as well as at the Äspö HRL and in the SKB site investigations at Forsmark and Laxemar, Sweden.

This document reports the results acquired with PFL DIFF in boreholes K03009F01 and K08028F01. Measurements and results presented in this report were undertaken within the framework of the KBS-3H project, subproject KBS-3H Sub-system demonstration and the DETUM-1 subproject Large Fractures. This joint activity was also conducted in close collaboration with the DETUM-1 Methods and Instruments subproject and the SKB-Posiva co-operation project PFL development, sealing mechanism and measurement in upward inclined holes. The developed sealing mechanism applied at the borehole collar was used for the first time in these measurements.

The measurements were carried out in accordance with SKB's internal controlling document AP TD 3HDEMO-14-046. The controlling documents for performing according to this Activity Plan are listed in Table 1-1. The list of the controlling documents excludes the assignment-specific quality plans. Both the Activity Plan and the Method Descriptions are SKB's internal controlling documents. The measurement data and the results were delivered to the SKB site characterization database SICADA and are traceable by the Activity Plan number.

Table 1-1. SKB's internal controlling documents for the activities concerning this report.

Activity Plan	Number	Version
Difference flow logging in borehole K08028F01 and K03009F01	AP TD 3HDEMO-14-046	1.0
Method Descriptions	**Number**	**Version**
Method Description for Difference Flow Logging.	SKB MD 322.010e	2.0
Instruktion för rengöring av borrhålsutrustning och viss markbaserad utrustning.	SKB MD 600.004	1.0
Instruction for length calibration in investigation of core boreholes.	SKB MD 620.010e	2.0
Instruktion för analys av injektions- och enhålspumptester.	SKB MD 320.004	2.0

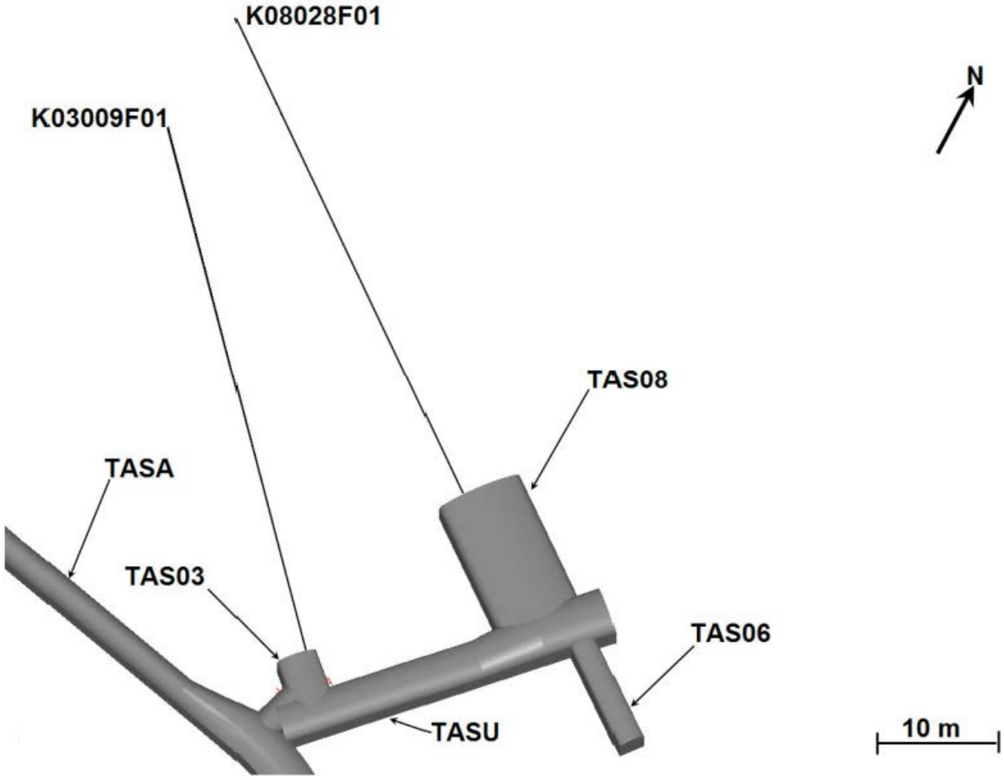

Figure 1-1. *Locations of boreholes K03009F01 and K08028F01 in the TASU tunnel at approximately −400 masl in the Äspö Hard Rock Laboratory.*

2 Objective and scope

The main objective of the PFL DIFF measurements in boreholes K03009F01 and K08028F01 was to characterize the rock with respect of its hydraulic properties, i.e. location of conductive fractures/zones and their transmissivity.

Besides difference flow logging, the measurement programme also included supporting measurements. These included measurement of the electrical conductivity (EC) and the temperature of the borehole fluid as well as the single-point resistance of the borehole wall. The flow measurement and the single-point resistance measurement can be used to locate flowing fractures and for length synchronization with other methods. Furthermore, the flow rate out from the partially closed borehole at top of the casing tube was recorded. This flow contains both non-intended leakage pass the sealing and intended flow through the control valve.

In conjunction with flow measurement absolute pressure along the borehole was measured with high-resolution absolute pressure. The fresh water head along the borehole is derived from the pressure measurement. The flow and pressure measurements in two different pressure conditions are used in calculation of hydraulic head and transmissivity of the formation.

Testing of the new borehole sealing mechanism and measuring in an upward inclined borehole were also part of the objectives of this measurement campaign.

3 Principles of measurement and interpretation

3.1 Measurements

The employed Posiva Flow Log (PFL) device is owned by Posiva Oy and operated by Pöyry Finland Oy. Unlike conventional borehole flowmeters which measure the total cumulative flow rate along a borehole, PFL DIFF probe measures the flow rate into or out of defined borehole sections. The advantage that follows from measuring the flow rate in isolated sections is improved detection of incremental changes of flow along the borehole. As these are generally very small, they can easily be missed when using conventional flowmeters.

Rubber sealing disks located at the top and bottom of the probe are used to isolate the flow of water in the test section from the flow in the rest of the borehole, see Figure 3-1. Flow inside the test section is directed through the flow sensor. Flow along the borehole is directed around the test section by means of a bypass pipe and is discharged at either the upper or lower end of the probe. The entire structure is called the flow guide.

Generally two separate measurements with two different section lengths (e.g. 5 m and 1 m) are used. The 5 m setup is usually used first to obtain a general picture of the flow distribution and possible anomalies. It is also good for measuring larger (less than 5 m thick along the borehole) fractured zones. The 1 m section setup can separate anomalies which are close to each other. There are also many other advantages to using different section lengths.

Flow rates into or out of the test section are monitored using thermistors, which track both the dilution (cooling) of an introduced thermal pulse and its transfer by way of the moving water (Öhberg and Rouhiainen 2000, pp 11–13). The thermal dilution method is used in measuring flow rates because it is faster than the thermal pulse method, and the latter is used only to determine flow direction within a given time frame. Both methods are used simultaneously at each measurement location.

In addition to incremental changes in flow, the PFL DIFF probe can also be used to measure:

- The electrical conductivity (EC) of both borehole water and fracture-specific water. The electrode used in EC measurements is located at the top of the flow sensor, see Figure 3-1.
- The single point resistance (SPR) of the borehole wall (grounding resistance). The electrode used for SPR measurements is located between the uppermost rubber sealing disks, see Figure 3-1, and is used for the high-resolution length determination of fractures and geological structures.
- The prevailing water pressure profile in the borehole. Located inside the watertight electronics assembly, the pressure sensor (transducer) is connected to the borehole water through a tube, see Figure 3-2.
- The temperature of the water in the borehole. The temperature sensor is part of the flow sensor, see Figure 3-1.

The principles behind PFL DIFF flow measurements are shown in Figure 3-3. The flow sensor consists of three thermistors (Figure 3-3 a). The central thermistor, A, is used both as a heating element and for registering temperature changes (Figures 3-3 b and c). The flanking thermistors, B1 and B2, serve as detectors of the moving thermal pulse caused by the heating of the central one (A).

Flow rate is measured by monitoring heat transients after constant power heating in thermistor A. The measurement begins by constant power (P_1) heating. After the power is cut off the flow rate is measured by monitoring transient thermal dilution (Figure 3-3 c). If the measured flow rate exceeds a certain limit, another constant power heating (P_2) period is started after which the flow rate is re-measured from the following heat transient.

Flows are measured when the probe is immobile. After transferring the probe to a new position, a waiting period (which can be adjusted according to the prevailing circumstances) is allowed to elapse before the heat pulse (Figure 3-3 b) is applied. The measurement period after the constant-power thermal pulse (normally 100 s each time the probe has moved a distance equal to the test section length and 10 s at every other location) can also be adjusted. The longer (100 s) measurement time is used to allow the direction of even the smallest measurable flows to be visible.

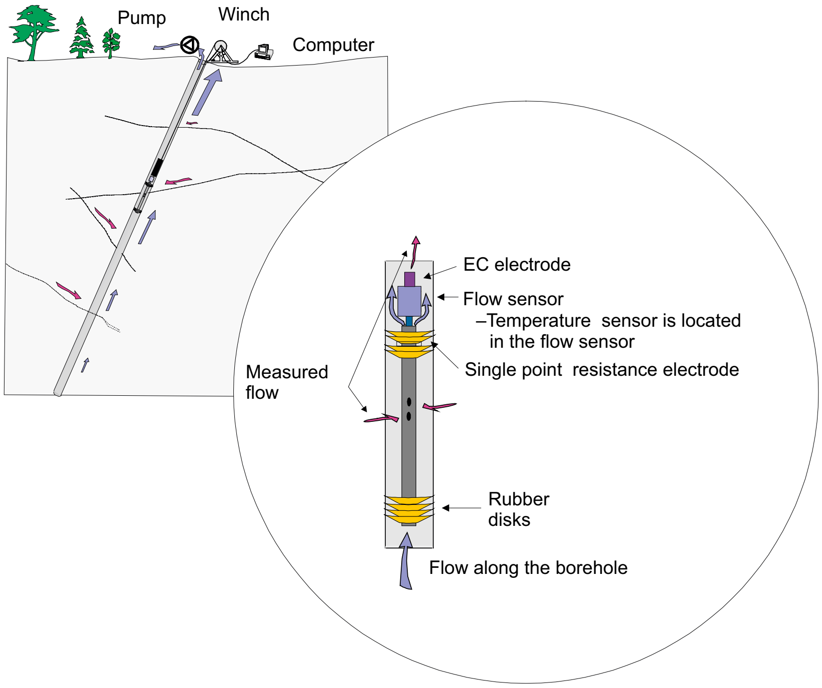

Figure 3-1. *Schematic of the probe used in the PFL DIFF.*

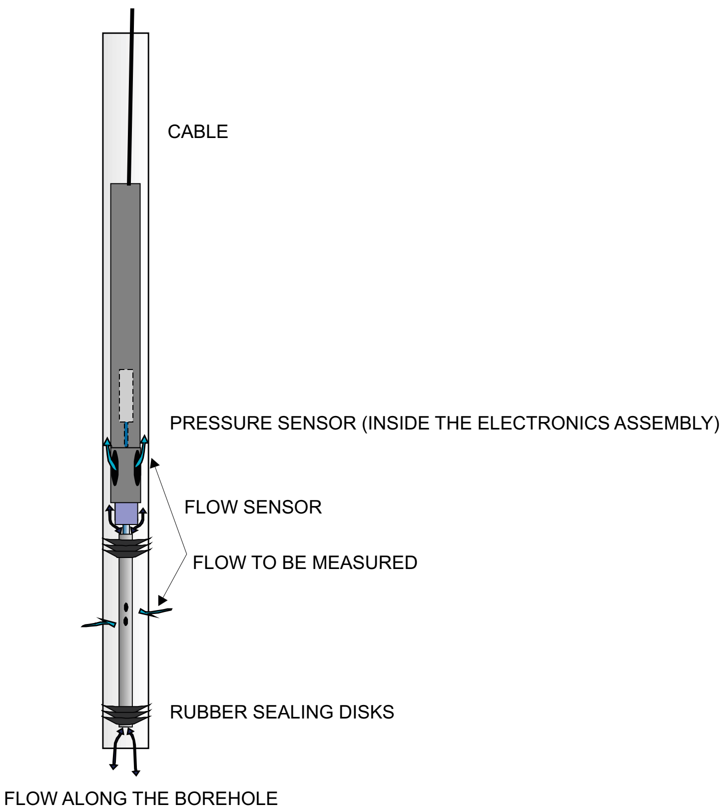

Figure 3-2. *The absolute pressure sensor is located inside the electronics assembly and connected to the borehole water through a tube.*

The flow rate measurement range is 30 mL/h–300 000 mL/h. The lower limit of measurement for the thermal dilution method is the theoretical lowest measurable value. Depending on conditions in the borehole, these flow limits may not always prevail. Examples of possible disturbances are drilling debris entrained in the borehole water, bubbles of gas in the water and high flow rates (some 30 L/min, i.e., 1 800 000 mL/h or more) along the borehole. If the disturbances encountered are significant, limits on practical measurements are calculated for each set of data.

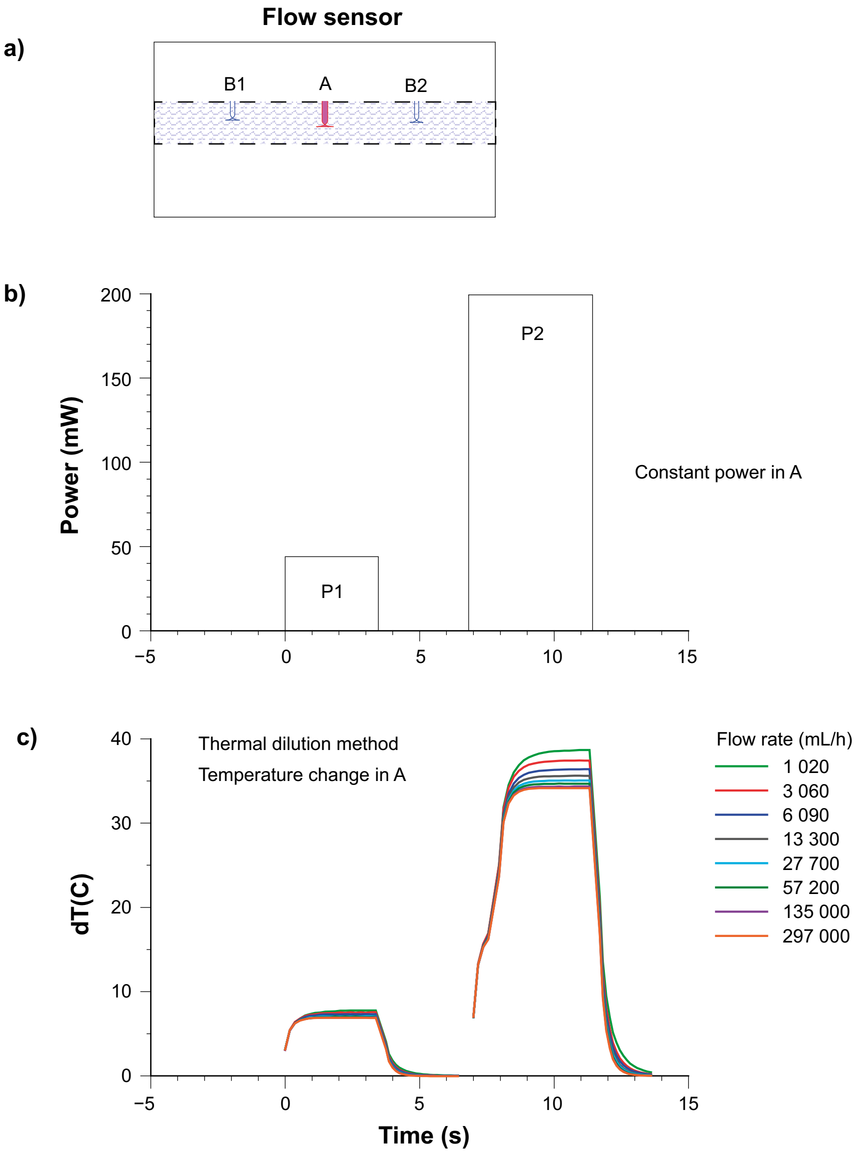

Figure 3-3. *Flow rate measurement.*

The device length reference point in the PFL DIFF is situated at the upper end of the test section.

3.2 Interpretation

The interpretation of data is based on Thiem's or Dupuit's formula, which describes a steady state and two-dimensional radial flow into the borehole (de Marsily 1986):

$h_S - h = Q/(T \cdot a)$ 3-1

where h is the hydraulic head in the vicinity of the borehole and $h = h_S$ at the radius of influence (R),

Q is the flow rate into the borehole,

T is the transmissivity of the test section,

a is a constant depending on the assumed flow geometry. For cylindrical flow, the constant a is:

$a = 2 \cdot \pi / \ln(R/r_0)$ 3-2

where

r_0 is the radius of the well and

R is the radius of influence, i.e., the zone inside which the effect of pumping is affecting the rock formation.

If measurements of flow rate are carried out using two levels of hydraulic head in the borehole, i.e. natural and pump-induced heads, the undisturbed (natural) hydraulic head and the transmissivity of the borehole sections tested can be calculated. Equation 3-1 can be reformulated in the following two ways:

$Q_{S0} = T_S \cdot a \cdot (h_S - h_0)$ 3-3

$Q_{S1} = T_S \cdot a \cdot (h_S - h_1)$ 3-4

where

h_0 and h_1 are the hydraulic heads in the borehole at the test levels,

Q_{S0} and Q_{S1} are the measured flow rates in the test section,

T_S is the transmissivity of the test section and

h_S is the undisturbed hydraulic head of the tested zone far from the borehole.

In general, since very little is known about the flow geometry, cylindrical flow without skin is assumed. Cylindrical flow geometry is also justified because the borehole is at a constant head, and no strong pressure gradients along the borehole exist except at its ends.

The radial distance R to the undisturbed hydraulic head h_S is not known and must be assumed. Here a value of 500 is selected for the quotient R/r_0.

The hydraulic head and the test section transmissivity can be deduced from the two measurements:

$h_S = (h_0 - b \cdot h_1)/(1-b)$ 3-5

$T_S = (1/a)\ (Q_{S0} - Q_{S1})/(h_1 - h_0)$ 3-6

where

$b = Q_{S0}/Q_{S1}$

The transmissivity (T_f) and hydraulic head (h_f) of individual fractures can be calculated provided that the flow rates at the individual fractures are known. Similar assumptions to those employed above must be used (a steady-state cylindrical flow regime without skin zones).

$h_f = (h_0 - b \cdot h_1)/(1-b)$ 3-7

$T_f = (1/a)\ (Q_{f0} - Q_{f1})/(h_1 - h_0)$ 3-8

where

Q_{f0} and Q_{f1} are the flow rates at a given fracture and h_f and T_f are the hydraulic head (far away from borehole) and transmissivity of the fracture, respectively.

Since the actual flow geometry and any skin effects are unknown, transmissivity values should only be considered as an indication of the prevailing (and relative) orders of magnitude. As the calculated hydraulic heads do not depend on geometrical properties but only on the ratio of the flows measured at different heads in the borehole, they should be less sensitive to unknown fracture geometry.
A discussion of potential uncertainties in the calculation of transmissivity and hydraulic head can be found in Ludvigson et al. (2002).

4 Equipment specification

In the PFL DIFF method, the flow of groundwater into or out of a borehole section is monitored using a flow guide which employs rubber sealing disks to isolate any such flow from the flow of water along the borehole. This flow guide defines the test section being measured without altering the hydraulic head. Groundwater flowing into or out of the test section is guided to the flow sensor, and flow is measured using the thermal pulse and thermal dilution methods. Measured values are transferred to a computer in digital form.

Type of instrument:	PFL DIFF probe (probe ID: PFL12).
Borehole diameters:	56 mm, 66 mm and 76 mm (or larger).
Length of test section:	The flow guide length can be varied.
Method of flow measurement:	Thermal pulse and thermal dilution.
Range and accuracy of measurement:	See Table 4-1.
Additional measurements:	Temperature, Single point resistance, Electrical conductivity of water, Water pressure.
Winch:	Mount Sopris Wna 10, 0.55 kW, conductors, Gerhard-Owen cable head.
Length determination:	Based on a digital distance counter (see Chapter 6.1.1).
Logging computer:	PC (Windows 7).
Software:	Based on MS Visual Basic.
Total power consumption:	1.5–2.5 kW depending on the type of pump employed.
Calibration of flow probe:	July 2014 (Probe ID: PFL12).

The range and accuracy of the sensors used is shown in Table 4-1.

Table 4-1. Range and accuracy of sensors.

Sensor	Range	Accuracy
Flow	30–300 000 mL/h	± 10% curr.value
Temperature (central thermistor)	0–50 °C	0.1 °C
Temperature difference (between outer thermistors)	−2 to +2 °C	0.0001 °C
Electrical conductivity of water (EC)	0.02–11 S/m	± 5 % curr.value
Single point resistance (SPR)	5–500 000 W	± 10 % curr.value
Groundwater level sensor	0–0.1 MPa	± 1 % full-scale
Air pressure sensor	800–1 060 hPa	± 5 hPa
Absolute pressure sensor	0–20 MPa	± 0.01 % full-scale

5 Execution of measurements

5.1 General

The work was performed according to Activity Plan AP TD 3HDEMO-14-046 following the SKB Method Description 322.010e, Version 2.0 (Method description for Difference Flow Logging), see Table 1-1. The Activity Plan and the Method Description are both SKB's internal controlling documents. Prior to the measurements, the downhole tools and the measurement cable were disinfected. Time was synchronized to local Swedish time, UTC +2 (Central European Summer Time). The activity schedule of the borehole measurements is presented in Table 5-1. The items and activities in Table 5-1 are the same as in the Activity Plan.

The outflow from the partially closed borehole was measured during the measurements.

The dummy logging (Item 6 and Item 13) of the borehole is done in order to assure that the measurement tools do not get stuck in the borehole. The dummy also collects solid material from the borehole wall. The solid material in the dummy is used for evaluation whether it is safe to continue with other logging tools.

The overlapping flow logging (Item 8, Item 9, Item 10, Item 14, Item 15 and Item 16) was carried out in the partially closed borehole at two different difference pressure states with 1 m and 5 m section lengths and employing 0.1 m and 0.5 m length increments (step length). Different pressure states in the borehole were established with an adjustable check valve. The boreholes were closed after the measurements.

The electrical conductivity (EC) and temperature of borehole water (Item 8, Item 9, Item 10, Item 14, Item 15 and Item 16) were measured during flow logging measurements.

The measuring arrangements are shown in Figures 5-1 and 5-2. The measurement trailer is seen mobilised at K08028F01 in Figure 5-1 and at K03009F01 in Figure 5-2.

Figure 5-1. *Measuring trailer mobilised at K08028F01.*

Figure 5-2. Measuring trailer mobilised at K03009F01.

Table 5-1. Flow logging and testing in K08028F01 and K03009F01. Activity schedule.

Item	Activity	Explanation	Date
2	Mobilisation at site (K08028F01)	Unpacking the trailer. Pressure in closed borehole was 3 100 kPa.	2014-09-01–2014-09-01
6	Dummy logging	Borehole stability/risk evaluation.	2014-09-02–2014-09-02
8	Overlapping flow logging – partially closed borehole	Section length L_w = 1 m. Step length dL = 0.1 m. Measurement at borehole length 93.06 m–1.36 m. Absolute pressure from 2 108 kPa to 2 803 kPa. Dp = 992 kPa–297 kPa.	2014-09-03–2014-09-04
10	Overlapping flow logging – partially closed borehole	Section length L_w = 5 m. Step length dL = 0.5 m. Measurement at borehole length 89.13 m–1.39 m. Absolute pressure from 462 kPa to 538 kPa. Dp = 2 638 kPa–2 562 kPa.	2014-09-04–2014-09-04
9	Overlapping flow logging – partially closed borehole	Section length L_w = 1 m. Step length dL = 0.1 m. Measurement at borehole length 93.13 m–1.38 m. Absolute pressure from 530 kPa to 603 kPa. Dp = 2 570 kPa–2 497 kPa.	2014-09-04–2014-09-05
	Demobilisation at K08028F01 and mobilisation at K03009F01	Packing the trailer and closing the borehole. Moving to K03009F01. Unpacking the trailer. Packers from borehole K03009F01 have just been removed and borehole was open. Pressure of 3 100 kPa in closed borehole was mentioned in risk assessment.	2014-09-05–2014-09-05
13	Dummy logging	Borehole stability/risk evaluation.	2014-09-05–2014-09-05
14	Overlapping flow logging – partially closed borehole	Section length L_w = 1 m. Step length dL = 0.1 m. Measurement at borehole length 99.66 m–1.45 m. Absolute pressure from 1 983 kPa to 2 224 kPa. Dp = 1 117 kPa–876 kPa.	2014-09-05–2014-09-06
15	Overlapping flow logging – partially closed borehole	Section length L_w = 1 m. Step length dL = 0.1 m. Measurement at borehole length 99.65 m–1.44 m. Absolute pressure from 463 kPa to 512 kPa. Dp = 2 637 kPa–2 588 kPa.	2014-09-06–2014-09-07
16	Overlapping flow logging – partially closed borehole	Section length L_w = 5 m. Step length dL = 0.5 m. Measurement at borehole length 95.65 m–1.45 m. Absolute pressure from 497 kPa to 560 kPa. Dp = 2 603 kPa–2 540 kPa.	2014-09-07–2014-09-07
17	Demobilisation	Packing the trailer. Closing the borehole.	2014-09-07–2014-09-07

Full borehole length could not be measured due to the structure of the probe (see Section 5.3).

5.2 Experimental premises

Since one of the objectives of the measurements was to test and evaluate alternative modes of performing PFL measurements two boreholes of alternate inclination were measured. The boreholes were also equipped with casing pipes such that the sealing mechanism could be used.

In borehole K03009F01 the length interval 4 m to 15.5 m has been grouted with close to 1 000 L of cementitious grout. This did not affect how the measurements were conducted but it should be noted that the transmissivity of the fractures in this length interval are affected by the grouting. The tunnel wall around the collar of borehole K03009F01 at a radial distance of a few meters leaked water when the borehole was closed. When the borehole was opened the leakage decreased significantly. After the sealing mechanism was mounted to the casing pipe and pressure in the borehole was controlled it was clearly noticed that the amount of the leakage on the wall varied in accord with to the pressure in the borehole. When the pressure was high the leakage on the tunnel wall was high. An attempt was made to measure the leakage from the tunnel wall. However, since the leakage came from different spots on the tunnel wall only a rough estimate of the leakage could be made. The estimate was about 5 L/min when borehole pressure was 2 200 kPa.

5.3 Measurement in an upward inclined borehole

The new borehole sealing mechanism was used for the first time in these measurements. A sealing mechanism was needed as the borehole K08028F01 is upward inclined. A sealing mechanism also makes it possible to measure a borehole in different pressure conditions. Previously employed sealing mechanisms have not worked well enough so that it could be used in boreholes where the outflow is low. Besides closing a borehole during a measurement, an upward inclined borehole has to be filled with water before measurement. Filling an upward inclined borehole requires that air is evacuated from the bottom of a borehole. The procedure and required devices to fulfil these requirements are presented below in the same order they were used.

The sealing mechanism is a flange which has a central hole (Figure 5-3). The hole has been dimensioned so that the cable connector goes through the hole. Therefore no parts of the PFL equipment have to be disassembled when the sealing mechanism is used. The cable is only led through the hole before the cable is connected to the probe.

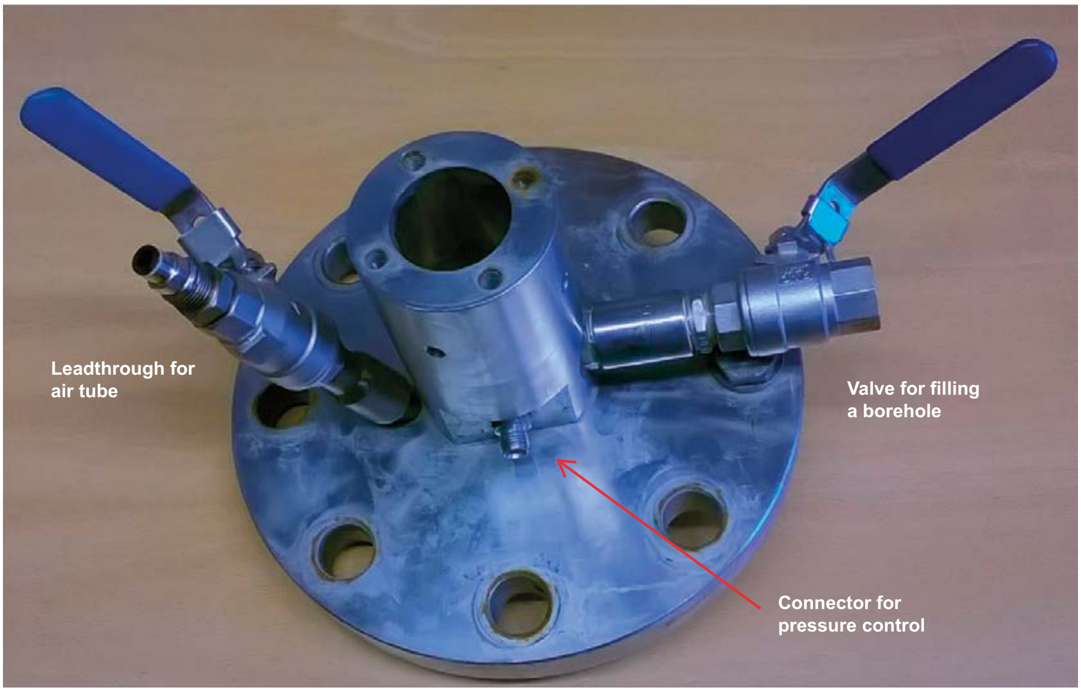

Figure 5-3. *Borehole sealing flange.*

The PFL probe has to be pushed to the bottom of the borehole before sealing it off. The tube for air removal is connected to the probe and goes to the bottom of the borehole with the probe. The Figure 5-4 shows the position of the air removal tube in principle. The other end of the tube is connected to its leadthrough at the sealing mechanism (Figure 5-3). There is a quick connector at the leadthrough so the tube stays in place without holding it.

When the PFL probe and air removal tube are at the bottom of the borehole and the push rods have been removed, the sealing mechanism is attached to its counterpart at the borehole casing (Figure 5-5). At this point the water from the borehole can flow through the hole in the flange. In order to seal the cable hole, three rubber rings are assembled around the cable and pushed inside the hole in the sealing unit (Figure 5-5).

The rubber seals are tightened inside the hole with four screws (Figure 5-6). The flow through the seal and the tension that is needed to move the probe depends on how tight are the screws tightened. The adequate tension for the winch can be adjusted when the rubber disks in the probe are flipped before starting a measurement. Flipping of rubber disks means that when probe is pushed the outer parts of rubber disks are bending towards the top of borehole and hence before starting the measurement the probe has to be pulled about 0.1 m in order to make the rubber disks bend towards the bottom of the borehole. In this position the rubber disks seal the measurement section. The tension can be adjusted at any point during the measurement by tightening or loosening the screws.

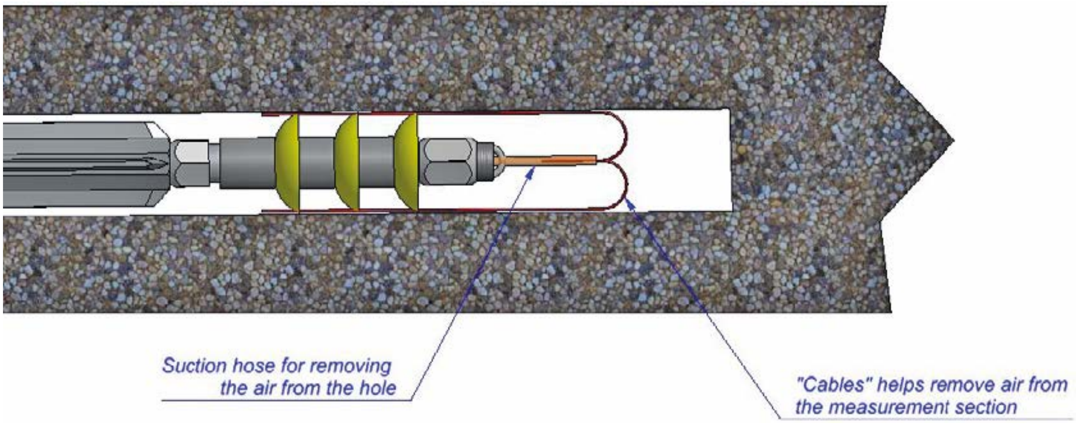

***Figure 5-4.** Principle sketch of air removal tube positioned at the bottom of a borehole.*

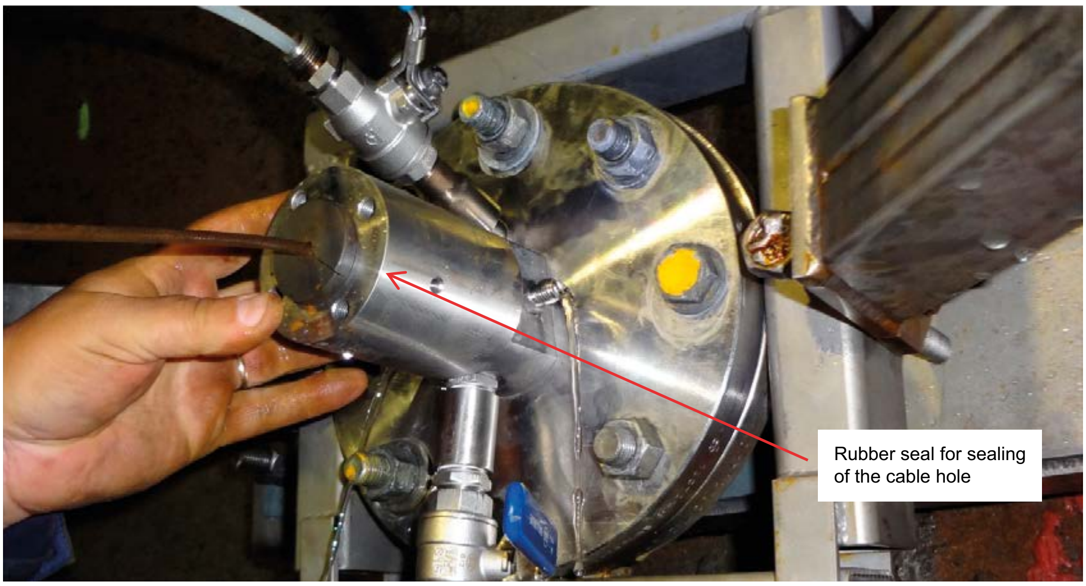

***Figure 5-5.** The sealing unit attached to a borehole casing.*

As the borehole is closed and the cable hole sealed filling of water to the borehole can start. The borehole is filled by pumping water into the borehole through a valve at the sealing unit. At the same time when the pumping is on the air removal tube is monitored as the air from the bottom of the borehole is evacuated. The water goes to bottom of a borehole through bypass pipe inside the probe but filling measurement section and cavities between rubber disks takes more time. This is why the pumping of water to the borehole should be continued for some period of time after water starts to flow out through the air removal tube.

When the borehole is full of water and air has been removed the air removing tube is pulled out of the borehole. The pumping should be on during removal the tube so that the pressure in a borehole stays high.

At this point the borehole is sealed and all valves can be closed. The desired pressure is obtained by adjusting the control valve. When the pressure is adjusted the measurement can start after a certain waiting period. The flow out of the measured borehole is measured during the flow logging. The flow out of the borehole includes both leakage flow through the sealing device and flow through the pressure controlling valve. The results of the borehole outflow measurements are presented in Appendices 12.3 and 24.3. The sealing unit during the measurement is presented in Figure 5-7.

Figure 5-6. *Seal tightening screws.*

Figure 5-7. *Sealing mechanism during the measurement.*

5.4 Nonconformities

In the first measurement (Item 8 in K08028F01) the installation of the probe and subsequent filling of the borehole with water was successful. However, when the air removal tube was removed from the sealing mechanism it was noticed that the plug for the air removal tube entry did not sustain the pressure. The sealing mechanism had to be fixed by adding a valve to the air removal tube entry so that it could be closed after the tube was removed. This caused one day delay of the measurement programme.

In K08028F01 the noise level was elevated throughout the measurements. In measurements conducted with 1 m section length the noise level was c. 200 ml/h. In measurements with 5 m section length the noise level was c. 2000 ml/h. The noise level did not change during individual measurements. The possible cause of elevated noise levels can be air in the measurement section as the borehole K08028F01 is upward inclined and the probe was pushed into dry borehole. The borehole was filled with water when the PFL probe was at the bottom of the borehole.

It was physically impossible to measure approximately one meter above of the respective bottom of the boreholes. There was a centralizer attached to the probe, which reduces the measured distance by c. 0.85 m. The rubber sealing disks in the device must also be flipped before the measurement begins. This reduces the measured distance by approximately 0.10 m.

6 Results

6.1 Length calibration

6.1.1 SPR measurement

An accurate length reference for the measurements is difficult to achieve in long boreholes. The main cause of the inaccuracy is the extension of the logging cable. The amount of extension depends on the tension on the cable, the magnitude of which in turn depends, among other things, on the inclination of the borehole and the roughness (friction properties) of the borehole wall. In these measurements boreholes were nearly horizontal so the tension of the measurement cable was low.

The length calibration was made based on borehole casing length and comparing the SPR and LateroLog (Tiensuu and Heikkinen 2016). The LateroLog data has been length matched with drill core data and the length accuracy is better than 5 cm (Lahti et al. 2011). The borehole casing length at the outermost end of the borehole was detected by single-point resistance (SPR) measurements using the SPR sensor of the PFL DIFF probe. LateroLog and SPR results were compared to find anomalies that can be used for length calibration. Anomalies that could be used for length matching were found well through the boreholes therefore the accuracy of the length matching is about 2 cm (point interval of SPR and LateroLog are 1 cm and 2 cm respectively). Overall total accuracy of the length calibrations in both boreholes is better than 7 cm. Results that are length corrected using SPR are shown in Appendices 1 and 13.

6.1.2 Estimated error in position of detected fractures

In spite of the length correction of the probe as described above, there can still be length errors in position of a detected fracture due to the following reasons:

1. The point interval in the overlapping mode flow measurements is 0.1 m. This could cause an error of ± 0.05 m.
2. The length of the test section is not exact. The specified section length denotes the distance between the nearest upper and lower rubber sealing disks. Effectively, the section length can be larger. At the upper end of the test section there are four rubber sealing disks. The distance between them is 5 cm. This will cause flow anomalies rounded in shape in the log: a flow may be detected already when a fracture is situated between the upper rubber sealing disks. These phenomena can cause an error of ± 0.05 m when the short step length (0.1 m) is used.

Rounded flow anomalies can also occur when orientation of a fracture is not perpendicular with the borehole. In these cases fracture might be in the measurement section on one side of the borehole but out of the section on the other side of the borehole. Fractures nearly parallel with the borehole might be even more problematic. Fracture location may be difficult to define accurately in such cases. In these measurements rounded flow anomalies were not found therefore it is most likely that orientation of a fracture does not increase the estimated error in position of a fracture.

In ideal case, when fracture is perpendicular to the borehole and the fracture aperture/thickness is very small, the total accuracy of the position of fracture is ± 12 cm comprising 7 cm error margin from position of the probe and an additional 5 cm due to 10 cm length interval in flow logging. There are no length marks in boreholes K03009F01 and K08028F01.

6.2 Electrical conductivity and temperature

6.2.1 Electrical conductivity and temperature of borehole water

The electrical conductivity of the borehole water (borehole EC) was measured during the flow logging measurements. The measurement was performed outwards, see Appendices 2.1 and 14.1.

When the flow is measured with the 1 m and 5 m test sections, the measurement is conducted using both the upper and lower rubber sealing disks. In this case the flow guide carries water with it and good flushing at the EC electrode and at the temperature sensor cannot be guaranteed. Therefore the measured EC and temperature conditions may not fully represent the actual conditions in the borehole.

Borehole K08028F01 was filled with water originating from another borehole (KA2598A) before starting the measurement, because the borehole is upward inclined. Therefore the electrical conductivity measurement does not represent the real conditions in the borehole.

In borehole K03009F01 the water was the actual borehole water and no water was added to the borehole. The EC profile was relatively constant during the measurements at the different borehole pressure states varying between 0.9 S/m–1.3 S/m. The borehole length interval between 28–32 m containing four flowing fractures can be readily seen as a region where borehole EC decreases, see Appendix 2.1.

The temperature of the borehole water was measured simultaneously with the EC and flow measurements. The EC values are corrected for temperature at 25 °C to make them comparable with other EC measurements (Heikkonen et al. 2002). There is an increase in temperature at the noted high flow fractures at about 30 m in K03009F01, see Appendix 2.2. In K08028F01 temperature of water coming from the fractures at 31.4 m and 37.6 m seems to be lower at higher pressure than at lower pressure conditions, see Appendix 14.2. The flow rates in fractures are also different at different pressure conditions, being higher at lower pressure conditions, which might affect the measured temperature

6.3 Absolute pressure and outflow measurements

Absolute pressure was registered together with the other measurements in Items 8 through 10 and 14 through 16. The pressure sensor measures the sum of the hydrostatic pressure in the borehole and air pressure. The hydraulic head along the borehole at natural and pumped conditions is determined in the following way. First, the monitored air pressure at the site is subtracted from the measured absolute pressure. The hydraulic head (h) at a certain elevation (z) is calculated according to the following expression:

$$h = (p_{abs} - p_b)/(\rho_{fw} \cdot g) + z \qquad 6\text{-}1$$

where

h is the hydraulic head (masl) according to the RHB70 reference system,

p_{abs} is the absolute pressure (Pa),

p_b is the barometric (air) pressure (Pa),

ρ_{fw} is the density of water, 1 000 kg/m^3

g is the acceleration due to gravity, 9.80665 m/s^2 and

z is the elevation of the outermost point in the measurement section (masl) according to the RHB70 reference system. All elevation data in the report are given in the RHB70 (The Swedish national elevation system).

The calculated head distributions are presented in Appendices 12.1 through 12.3 and 24.1 through 24.3. The exact z-coordinates are important in head calculation. A 10 cm error in the z-coordinate means a 10 cm error in the head.

Borehole outflow was measured during the measurements. The results are shown in Appendices 12.3 and 24.3. Two different pressure states in the boreholes were achieved by adjusting the pressure with a control valve. After the measurements the boreholes were closed.

6.4 Flow logging

6.4.1 General comments on results

The measurement programme comprised several flow logging sequences. The results were plotted on the same diagram with single-point resistance (right hand side), see Appendices 3.1–3.5 and 15.1–15.5. SPR usually shows a lower value for a fracture where flow is detected (e.g. length 37.6 m in K08028F01). The SPR usually shows a lower value for a fracture where flow is detected (e.g. length 37.6 m in K08028F01). But it is also possible that the SPR plot is devoid of an anomaly at the same length were flow is detected (e.g. at 92.9 m in K03009F01). Many other resistance anomalies result from other fractures and geological features. As the electrode of the SPR tool is located within the outermost rubber sealing disks of the probe, the locations of resistance anomalies associated with conductive fractures coincide with the innermost end of the flow anomalies.

The flow logging was performed with a 1 m and 5 m section length using 0.1 m and 0.5 m increments. The method (overlapping flow logging) gives the length and the thickness of conductive zones with a length resolution of 0.1 m. The 5 m section length and 0.5 m length increment was used to measure possible longer fractured sections that do not fit inside a 1 m section.

The direction of small flows (< 100 mL/h) cannot be detected in the normal overlapping mode (thermal dilution method). Therefore the measurement time was longer (so that the thermal pulse method could be used) at every section length (1 m and 5 m) interval.

The test section length determines the width of a flow anomaly of a single fracture as seen in the flow log. If the distance between flow yielding fractures is less than the section length, the anomalies will overlap, resulting in a stepwise flow data plot. The overlapping flow logging was conducted twice (at two different pressures, cf. Table 5-1) using a 1 m long test section with 0.1 m length increments and once using 5 m test section with 0.5 m length increments.

The positions (in terms of borehole length) of the detected fractures are shown on the length scale. Fracture locations are interpreted on the basis of the flow curves and therefore represent flowing fractures. A long line represents the location of a conductive fracture; a short line denotes that the existence of a conductive fracture is uncertain. The short line is used if the flow rate is less than 30 mL/h or the flow anomalies are overlapping or unclear because of effects of noise.

The coloured triangles show the magnitude and direction of the measured flows. The triangles have the same colour as the corresponding curves.

The explanations to the tables in Appendices 5.1–5.4, 7, 9.1–9.2, 17.1–17.4, 19, and 21 are given in Appendices 4 and 16.

6.4.2 Hydraulic characteristics of borehole sections

The both boreholes were flow logged with a 1 m section length and with 0.1 m length increments at two different pressure states. During the first measurement in K03009F01 the absolute pressure varied between 1 983 kPa (head −207 m) to 2 224 kPa (head −187 m) and in the second measurement from 463 kPa (head −362 m) to 512 kPa (head −357 m), see appendix 12.2. The flow logging using 5 m section length and 0.5 m length increments was conducted while pressure varied between 497 kPa (head −359 m) to 560 kPa (head −352 m). All head values are given in the RHB70 system.

The target pressure in the first measurement was 300–500 kPa below the ambient pressure in the borehole K03009F01. A pressure of 3 100 kPa was mentioned as an ambient measured pressure in the borehole's risk assessment form but when the borehole was closed with the sealing mechanism and flow out of the borehole was zero a pressure of 2 300 kPa was registered. The targeted pressure could not be reached as there was a leak between the casing and the rock. The pressure during the first measurement was c. 900 kPa below the ambient pressure. This increased the possible error in transmissivity and formation head calculations as the pressure difference between the measurements turned out smaller. Also the larger drawdown during the measurement may have caused disturbances like turbulent water flow.

In the first measurement with 1 m section length and with 0.1 m length increments in K08028F01 the absolute pressure varied between 2 108 kPa (head −193 m) to 2 803 kPa (head −124 m). The deviation is quite large but the pressure went below 2 400 kPa only when the length interval from 12 m to 1.36 m was measured. Fractures were not detected in this length interval. The pressure was between 2 400 and 2 700 kPa at the time when detected fractures were measured (see Appendix 24.2). During the second measurement absolute pressure varied from 530 kPa (head −356 m) to 603 kPa (head −346 m), see appendix 24.2. The flow logging with 5 m section length and with 0.5 m increments was conducted while the pressure varied from 462 kPa (head −361 m) to 538 kPa (head −355 m). The pressure in borehole while closed, and flow out of the borehole was zero, was 3 100 kPa.

The deviation of pressure during the first measurements in K08028F01 was larger than planned. The reason for deviation was mainly lack of experience how to use the new sealing mechanism. The first measurement was also the most demanding measurement in terms of pressure control as the outflow from the borehole was the smallest. This in turn means that even a small change in outflow can change the pressure in the borehole.

Two sets of flow measurements are needed for calculation of transmissivity as described in Equation 3-6. In this case the borehole was all the time partially closed at a different outflow and pressure state.

The results of the flow logging measurements with a 1 m section length are presented in the tables of Appendices 5.1–5.4 and 17.1–17.4. The results of measurements with 5 m section length are presented in the tables of Appendices 7 and 19. The measurements with 5 m section length were conducted only at one pressure condition. Therefore the corresponding 5 m sections at higher pressure were constructed from preceding 1 m section results. Using the 5 m sections the section transmissivities and formation head could be calculated for both 1 m and 5 m sections. All the borehole sections are shown in Appendices 3.1–3.5 and 15.1–15.5. Secup and Seclow in Appendices 5.1–5.4, 7, 17.1–17.4 and 19 are the distances along the borehole from the reference level (tunnel wall) to the outermost end of the test section and to the innermost end of the test section, respectively.

Pressure was measured and calculated as described in Section 6.3.The h1FW and h2FW in Appendices 5.1–5.4, 7, 17.1–17.4 and 19 represent heads in the borehole at different pressure states. All head values in the borehole and calculated heads in the formations or in fractures are given in the RHB70 system.

The flow rates are positive if the flow direction is from the bedrock into the borehole and negative for the reversed flow direction. Amongst the 1 m sections there were 41 sections in K03009F01 and 3 sections in K08028F01 which were flow yielding in the measurement when borehole pressure was maintained at low pressure (high drawdown). In the measurement when borehole pressure was the high, 39 sections in K03009F01 and 3 sections in K02028F01 were flow yielding. All of the flows were positive except the one in K03009F01 which actually was a leakage between the casing and rock (fracture at 2.5 m). The number of 5 m sections which were flow yielding was 14 in K03009F01 and 3 in K08028F01. In K08028F01 the noise level was so high during the 5 m section measurement that one section flow could not be detected.

The flow data from the 1 m logging is presented as a plot, see Appendices 6.1 and 18.1. The corresponding plots for 5 m sections are presented in Appendices 8.1 and 20.1. The left-hand plot in each diagram represents flow from the borehole into the bedrock from the respective test sections, while the right-hand plot represents flow from the bedrock into the borehole. If flow could not be detected (zero flow), no corresponding point will be visible in the logarithmic plots found in the appendices.

The lower and upper measurement limits of the flow rate are also presented in the plot (Appendices 6.1, 8.1, 18.1 and 20.1) and in the tables (see Appendices 5.1–5.4, 7, 17.1–17.4 and 19). There are theoretical and practical lower limits of flow rate, see Section 6.4.4.

The hydraulic head and transmissivity (TS) of borehole sections can be calculated from the flow data using the method described in Chapter 3. The results are illustrated in Appendices 6.2, 8.2, 18.2 and 20.2. The hydraulic head of the sections is presented in the plots if none of the two flow values at the same length is equal to zero. Transmissivity is presented if none or just one of the flows is equal to zero. Some of the calculated hydraulic heads were physically impossible, being way above the level of the ground surface. Therefore the sensitivities of transmissivity and hydraulic head values to errors in flow rate and pressure measurements were evaluated (see Section 6.4.5). The transmissivities and hydraulic heads of the sections with corresponding error limits have been presented in Appendices 6.3, 8.3, 18.3 and 20.3.

In K03009F01 the sum of all detected flows during the first measurement (Q0 in fractures table in Appendices 9.1–9.2) was 1.31×10^{-5} m^3/s (0.786 L/min). The outflow from the borehole was approximately 1 L/min during the first measurement. The sum of all detected flows during the second measurement (Q1 in fractures table Appendices 9.1–9.2) was 1.36×10^{-4} m^3/s (8.16 L/min). The outflow from the borehole was approximately 8 L/min during the second measurement. The sum of flows in 5 m sections (Q1 sections table Appendix 7) was 1.1×10^{-4} m^3/s (6.6 L/min). At section 18.23 m–23.23 m flow rate was above the measurement limit. Therefore the actual flow might be little bit higher. Also the sum of detected fracture flows in the same section in the same conditions is higher. The outflow from the borehole was approximately 8 L/min during the measurement conducted with 5 m measurement section. The sum of detected flows and outflow from the borehole are consistent with measurements conducted with a 1 m section.

In K03009F01 there was a leak between the casing and the rock which is presented as a fracture in the results. If this fracture is omitted from the sum of section flows the sum of all flows coming from bedrock into the borehole is 1.65×10^{-4} m^3/s (9.9 L/min) when borehole pressure was lower.

Most of the flow in borehole K03009F01 comes from section from 16 m to 32 m. Sum of section flows in this section is 1.6×10^{-4} m^3/s (9.6 L/min) when pressure in borehole is low. The sum of transmissivities in this section is 5.1×10^{-7} m^2/s. In other parts of the borehole inflow into the borehole is 3.7×10^{-6} m^3/s (0.22 L/min). Section from 48 to 92 m is quite solid in terms of water conductive fractures. There are few water conductive fractures but transmissivities of these fractures are smaller than 1×10^{-10} m^2/s.

In K08028F01 the sum of all detected flows during the first measurement (Q0 in fractures table Appendix 21) was 4.4×10^{-6} m^3/s (0.26 L/min). The outflow from the borehole was approximately 0.25 L/min during the first measurement. The sum of all detected flows during the third measurement (Q_1 in fractures table Appendices 21) was 1.41×10^{-5} m^3/s (0.846 L/min). The sum of flows in 5 m sections (Q_1 sections table Appendix 19) was 1.5×10^{-5} m^3/s (0.883 L/min). The outflow from the borehole was approximately 1.2 L/min during the third measurement and during the measurement conducted with 5 m measurement section. The sum of detected flows and outflow from the borehole are consistent when outflow was 0.25 L/min. When the pressure was lower and outflow higher the sum of detected fracture and section flows were not consistent with the outflow from the borehole. If there are flowing fractures at the immeasurable part of the borehole at the bottom this would explain the difference.

6.4.3 Transmissivity of fractures

An attempt was made to evaluate the magnitude of fracture-specific flow rates. The results for a 1 m section length and 0.1 m length increments were used for this purpose. The first step in this procedure was to identify the locations of individual flowing fractures and then evaluate their flow rates.

In cases where the distance between fractures is less than one metre, it may be difficult to evaluate the flow rate. There are such cases shown in Appendix 3.1. In these cases a stepwise increase or decrease in the flow data plot equals the flow rate of a specific fracture (filled triangles in the appendices).

The total number of detected flowing fractures was 49 in K03009F01 and 3 in K08028F01. These fractures were used for transmissivity estimations. The transmissivity of the fractures is presented in Appendices 9.1–9.2 and 21, respectively.

Some fracture-specific results were classified to be “uncertain.” The basis for this classification is either a small flow rate (< 30 mL/h) or unclear definition of the conductive fracture in the flow log. Anomalies are considered unclear if their nature is unclear because of noise or if fractures are so close to each other that they are difficult to interpret separately.

In K03009F01 the largest transmissivities can be found at fractures 19.0 m and 20.0 m. Both of the transmissivities are 1.4×10^{-7} m^2/s. There is also third fracture which have almost as high transmissivity as fractures mentioned previously. Transmissivity of fracture 19.7 m is 9.8×10^{-7} m^2/s. Sum of these three transmissivities is 3.78×10^{-7} m^2/s which is c. 71 % of transmissivity of entire borehole. The fracture at length of 2.5 m was not taken into account in these evaluations as it is a leak between casing pipe and the rock and should be considered as flow out of the borehole.

In K08028F01 there are two major fractures which dictate the transmissivity in the borehole. Transmissivity of both fractures is about 2×10^{-8} m^2/s. The fractures are located at lengths 31.4 m and 37.6 m along the borehole.

Summed up fracture-specific transmissivities were compared with transmissivities of the 1 m sections in Appendices 11.1 and 23.1 and with the 5 m section in Appendices 11.2 and 23.2. The 1 m section transmissivities were calculated using the same data that was used in calculations of fracture transmissivities. The section flows are summed up fracture flows inside a section. The head values that were used to calculate transmissivities are however a little bit different. That is why there are small differences between fracture and section transmissivities. The 5 m section transmissivities were calculated using 1 m section measurements at higher pressure and 5 m section measurement at lower pressure. There are some differences between the two transmissivities but nothing significant.

6.4.4 Theoretical and practical measurement limits of flow and transmissivity

The theoretical minimum for measurable flow rate is some 30 mL/h. The upper limit of flow measurement is 300 000 mL/h. As these upper and lower limits are determined by flow calibration, it is assumed that flows can be reliably detected between the upper and lower theoretical limits in otherwise favourable borehole conditions.

In practice, the minimum measurable flow rate may be much higher. Borehole conditions may have an influence on the flow base level (i.e. noise level). Noise levels can be evaluated in intervals along the borehole where there are no flowing fractures or other complicating structures, and may vary along a borehole.

There are several known reasons for increased noise in the flow:

- Roughness of the borehole wall.
- Solid particles such as clay or drilling debris in the water.
- Gas bubbles entrained in the water.
- High flow rate along the borehole.

Roughness of the borehole wall always results in high levels of noise, not only in the flow results, but also in the SPR results. The flow curve and SPR curves are typically spiky when the borehole wall is rough.

Drilling debris usually increases noise levels. This kind of noise is typical for both natural (un-pumped) and pumped conditions.

Pressure of flowing water is reduced when it enters into the borehole. This may lead to the release of dissolved gas and increase the quantity of gas bubbles entrained in the water. Some fractures may produce more gas than others. Sometimes, when the borehole is being measured, increased noise levels are observed just after certain fractures. The reason for this is assumed to be gas bubbles.

The effect of a high flow rate along the borehole can often be seen above fractures with a high flow. Any minor leakage in the seal provided by the lower rubber sealing disks will appear in the measurement as increased levels of noise.

A high level of noise in a flow usually masks the “real” flow if the flow is smaller than the noise. Experience indicates that high noise level (> 30 mL/h) can affect the flow rate measurement even if the measured flow value is larger than noise level. Magnitude of the effect is not clear therefore it can’t be taken into account in interpretation.

The practical minimum for measurable flow rate is presented in Appendices 3.1–3.5 and 15.1–15.5 using a grey dashed line (Lower limit of flow rate). The practical minimum level of the measurable flow was evaluated using the flow data obtained in the 1 m section length measurements with lower pressure conditions. The limit is an approximation. It is evaluated to obtain a limit below which there may be fractures or structures that remain undetected.

The noise level was 30 mL/h in K03009F01 and 200 mL/h in K08028F01. In K03009F01 the noise level is as low as it usually is but in K08028F01 noise level was elevated. The reason for elevated noise level is most probably air in the measurement section. This is one of the things that need to be improved, see Chapter 6.4.6. In good conditions it may be possible to detect flow anomalies below the limit of the thermal dilution method (30 mL/h). Nevertheless the noise line (grey dashed line) is chosen to be no less than 30 mL/h and anomalies below 30 mL/h are considered to be uncertain.

In some boreholes the upper limit of flow measurement (300 000 mL/h) may be exceeded. Such fractures or structures hardly remain undetected (as the fractures below the lower limit). There were such sections detected in K03009F01 during this campaign.

The practical minimum for measurable flow rate (Q-lower limit P) is also presented in Appendices 5.1–5.4, 7, 17.1–17.4 and 19 and is obtained from the plots in Appendices 3.1–3.5 and 15.1–15.5 (Lower limit of flow rate). The practical minimum of measurable transmissivity can be evaluated using Q-lower limit and the assumed head difference at each measurement location. The practical minimum of measurable transmissivity is c. 5×10^{-11} m^2/s in K03009F01 and c. 3×10^{-10} m^2/s in K08028F01, see Appendices 5.1–5.4, 7, 17.1–17.4 and 19 (T_D-measl$_{LP}$). The theoretical minimum for measurable transmissivity (T_D-measl$_{LT}$) is evaluated using a Q value of 30 mL/h (the minimum theoretical flow rate using the thermal dilution method). The theoretical minimum for measurable transmissivity in K03009F01 is the same as practical minimum and c. 4×10^{-10} m^2/s in K08028F01. The upper measurement limit for transmissivity can be evaluated using the maximum flow rate (300 000 mL/h) and the assumed head difference as above. The upper measurement limit for transmissivity is c. 5×10^{-7} m^2/s in K03009F01 and 4×10^{-7} m^2/s in K08028F01, see Appendices 5.1–5.4, 7, 17.1–17.4 and 19 (T_D-measl$_U$). These transmissivity limits are only qualitative because of the assumptions described in Section 6.4.2.

All three flow limits are plotted with the measured flow rates, see Appendices 6.1, 8.1, 18.1 and 20.1. The three transmissivity limits are also presented graphically, see Appendices 6.2, 8.2, 18.2 and 20.2.

Similar flow and transmissivity limits are not provided for the fracture-specific results as the limits for these are harder to define. The situation is similar for the upper flow limit. If several high-flowing fractures are positioned closer to one another than a distance of 1 m, the upper flow limit will depend on the sum of these flows, and this must be below 300 000 mL/h.

6.4.5 Sensitivity of transmissivity and the formation head to the errors in flow and pressure measurements

The aim was to measure flow rates in different pressure conditions in the borehole to achieve as large difference in flow rate as possible. The larger the difference in flow rates measured in different pressure condition the more insensitive the transmissivity and head interpretation is to errors in flow rate and pressure measurement. Therefore the two pressures at which measurements were conducted should be as far apart as possible to obtain large ratio of measured flows.

The Figure 6-1 shows how the ratio of flow rates affects the accuracy of transmissivity and formation head interpretation. The formation head is the head value at which the flow is zero. The slope of the line that has been drawn along the points is directly proportional to the transmissivity (Equation 3-1). Error in flow rate measurement is within ± 10 % of the measured value. Accuracy of absolute pressure sensor is ± 2 kPa which implies ± 0.2 m in head.

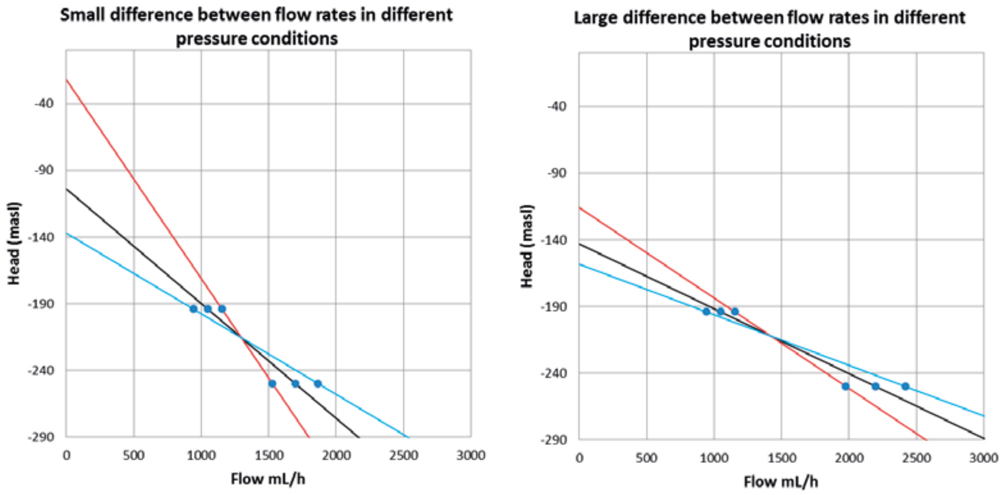

Figure 6-1. *Demonstrative plot how ratio of flow rates affects the accuracy of transmissivity and formation head interpretation.*

The black line represents the actual measurement assuming zero inaccuracy. The red line goes through points which have been obtained by adding 10 % to flow rate and 0.2 m to head at higher pressure conditions (head value higher) and subtracting 10 % from flow rate and 0.2 m from head at lower pressure conditions (head value lower). This is the worst case scenario to high formation head and low transmissivity value. The blue line goes through points which have been obtained by adding 10 % to flow rate and 0.2 m to head at lower pressure conditions (head value lower) and subtracting 10 % from flow rate and 0.2 m from head at higher pressure conditions (head value higher). This is the worst case scenario to low formation head and high transmissivity value.

When two of the figures are compared the difference between worst case highest and lowest values is much smaller when the ratio of flow rates is large than when the ratio is small.

The upper and lower limits for transmissivity and formation head have been calculated using formulas 3-5 and 3-6 with added errors to flow and pressure measurements.

$$h_{s\,upper\,limit} = ((h_0 + 0.2\text{ m}) - \frac{Q_{0s}\cdot 1.1}{Q_{1s}\cdot 0.9}\cdot (h_1 - 0.2\text{ m}))/(1 - \frac{Q_{0s}\cdot 1.1}{Q_{1s}\cdot 0.9}) \qquad 6\text{-}1$$

$$T_{s\,upper\,limit} = \frac{1}{a}\cdot (Q_{0s}\cdot 0.9 - Q_{1s}\cdot 1.1)/((h_1 + 0.2\text{ m}) - (h_0 - 0.2\text{ m})) \qquad 6\text{-}2$$

$$h_{s\,lower\,limit} = ((h_0 - 0.2\text{ m}) - \frac{Q_{0s}\cdot 0.9}{Q_{1s}\cdot 1.1}\cdot (h_1 + 0.2\text{ m}))/(1 - \frac{Q_{0s}\cdot 0.9}{Q_{1s}\cdot 1.1}) \qquad 6\text{-}3$$

$$T_{s\,lower\,limit} = \frac{1}{a}\cdot (Q_{0s}\cdot 1.1 - Q_{1s}\cdot 0.9)/((h_1 - 0.2\text{ m}) - (h_0 + 0.2\text{ m})) \qquad 6\text{-}4$$

These sensitivity calculations take into consideration only the accuracy of the measurements. In addition to all uncertainties in measurements there are also factors that can affect the flow rate measurement itself. Measurement at low pressure (i.e. large drawdown) introduces s a high pressure gradient near the borehole wall that might cause turbulence in flow out of the bedrock. If the turbulence increases with pressure gradient the flow/head ratio is not necessarily linear as presented in Figure 6-1. Also the real radius of influence might be different than assumed.

A small ratio of measured flows cause lower accuracies in transmissivity and head calculations and large difference in pressures may cause turbulence and other disturbances. Therefore measuring all fractures and sections in a borehole under the same pressure conditions is not necessarily the optimal solution for transmissivity and formation head estimation. Improved estimations of transmissivity and head can be obtained by measuring the fractures or sections, where calculated values are unreasonable, at multiple pressure conditions. From the larger set of flow measurements at different pressures it would be possible to select measurements that are not affected by turbulence or other disturbances or where the disturbances are smaller.

Appendices 6.3, 8.3, 18.3 and 20.3 show section transmissivities and head with upper and lower limits that are possible to achieve if ± 10% error in flow rate and ± 0.2 kPa error in pressure measurement are taken into account. Nevertheless some of the formation head values (e.g. fracture 23.9 m in K03009F01) are unreasonable even if error limits are considered.

6.4.6 Comments and further improvements of the used techniques

The borehole sealing mechanism worked as planned. The highest pressure at which the sealing unit was used was 2 700 kPa. At this pressure the leakage flow was about 250 mL/min through the sealing device and through the control valve which was used to control the pressure in the borehole. About half of the leakage came through the control valve so the leak through the sealing was about 125 mL/min when it was possible to move the cable. The tension at the cable was about 90 kg.

The pressure was set so that half of the leak came through the control valve and half through the sealing because it was expected that the leak through the sealing would increase during the measurement. It was observed that the leak indeed increased through the sealing when the sealing tightening screws were not tightened during the measurement. It is possible to tighten the screws during the measurement in order to keep the leak as small as possible but it would require continuous monitoring of the leak and tension at the cable. When choosing the higher pressure for the measurement it should also be remembered that if the flow rate out of the borehole is very small the fracture flows are also very small and may be difficult to detect.

Filling the upward inclined borehole and removing air from the bottom of the borehole was done using a small tube which was pushed to the borehole bottom with the PFL probe (see Figure 5-4) and pumping water into the borehole through the sealing unit. High noise level during the measurements indicates that there was air in the measurement section during the measurement. Removal of air from the bottom of the borehole and measurement section has to be improved because it is suspected that all air from the borehole and measurement section did not come out. The air removing hose needs a nozzle at the end of the probe that guarantees that all air will be removed from the end of the borehole. Air removal from the measurement section can be improved by enhancing the flow pass the rubber disks. In nearly horizontal boreholes there might be lot of small air bubbles all the way along the borehole which do not move. Removing these air bubbles could improve the measurement performance.

Removal of air from the measured borehole before the measurement is one precaution. However, gas coming from fractures during the measurement is an additional aspect that should be considered. In the event gas emanates from a fracture along with the flowing water there should be practical means to detect the gas in the measurement section and remove it. As the sealing mechanism works and it is possible to conduct measurements at different pressures it is now time to focus on how to select the conditions for the measurements. Choosing two pressures that are as far apart as possible should produce large difference in flow rates. This selection should minimise the errors inherited from flow rate measurement. The down side of using large deviation in pressures is that when the pressure is far from ambient formation pressure there may be turbulent inflow coming from the bedrock into the borehole. Other factors may also affect the flow rates at low pressure conditions when flows are supposed to be larger. In these measurements some of the calculated formation head values may turn out unreasonable, the reason is assumed to be turbulence during the flow measurement at lower pressure condition.

It is difficult to know what pressures will produce the best flow measurements because turbulence and some other disturbances are borehole and even fracture dependent. Therefore a definite and general solution for pressure selection is impossible to achieve. A possible approach to further investigate the disturbances is to set up a test measurement in which a large set of different pressures would be employed. Starting from high pressure, as close to ambient formation pressure as possible, and successively lowering the pressure by 2 000 kPa, 4 000 kPa, 8 000 kPa and so on. By comparing the transmissivity and formation head values calculated from the different measurements it could be possible to gain knowledge how to optimize the pressure selection.

Also measuring individual fractures at different pressures in such a way that probe is not moved but pressure is changed during the measurement would be beneficial. The pressure steps would be the same as mentioned above and change of pressure would be done after the flow has stabilized after the previous pressure change.

7 Summary of main findings

In this study the Posiva Flow Log Difference Flow Method was used to determine the location and flow rate of flowing fractures or structures in boreholes K03009F01 and K08028F01 in the Äspö HRL, Sweden. Both 1 m section length with 0.1 m increments and 5 m section length and 0.5 m increments were used in the measurements. The boreholes were partially closed during the measurements. The whole borehole was measured at two different pressure states by adjusting the pressure in the partially closed borehole using a control valve.

Measurements at two different pressures in the boreholes made it possible to interpret transmissivity and hydraulic head of fractures. The prerequisites for a reliable interpretation are e.g. that the measured flow rates are within the limits of measurements and that the ratio of the measured flow rates is large enough when measured at the same borehole length. The two pressures used were as far apart from each other as possible but still in some cases ratio of the measured flow were small. In the future more tests are needed to gain more experience how to select optimal pressures for measurements so that interpretation of formation head and transmissivity could be calculated reliably.

Length calibration was made by using the borehole's casing lower end as a length mark, the cable counter, the cable's length marks and comparing LateroLog with SPR. The single point resistance was measured simultaneously with the flow measurements, and thus all flow results could be length synchronized by synchronizing the single-point resistance logs.

In K03009F01 49 flow yielding fractures were found. In this borehole noise level was low (30 mL/h). Most of the flow comes from section from 16 m to 32 m. The sum of transmissivities in this section is about 5.1×10^{-7} m^2/s.

Most of the flow in K08028F01 comes from section from 30 m to 40 m. The transmissivity of the fractures in this section is about 2×10^{-8} m^2/s. The noise level was about 200 ml/h in this borehole therefore it is possible that smaller flows have not been detected.

Electrical conductivity and temperature of the borehole water were also logged during the flow measurements.

The new borehole sealing mechanism developed by Pöyry Finland Oy (contracted by SKB and Posiva) was used for the first time and it worked well. The sealing mechanism includes option to evacuate air from the bottom of a borehole which is needed in measurement of upward inclined borehole. The K08028F01 was the first upward inclined borehole which has been measured with PFL DIFF probe. The measurement went well but there is still need to improve air evacuation method.

References

SKB's (Svensk Kärnbränslehantering AB) publications can be found at www.skb.com/publications.

de Marsily G, 1986. Quantitative hydrogeology: groundwater hydrology for engineers. Orlando, FL: Academic Press.

Heikkonen J, Heikkinen E, Mäntynen M, 2002. Pohjaveden sähkönjohtavuuden lämpötilakorjauksen matemaattinen mallinnus synteettisten vesinäytteiden mittauksista (Mathematical modelling of temperature adjustment algorithm for groundwater electrical conductivity on basis of synthetic water sample analysis). Posiva Työraportti 2002-10, Posiva Oy, Finland. (In Finnish.)

Lahti M (ed), Pere T, Käpyaho E, Toropainen V, Tarvainen A-M, Pöllänen J, Pekkanen J. 2011. Drilling and associated drillhole measurements of the pilot hole ONK-PH12. Posiva Working Report 2011-02, Posiva Oy, Finland.

Ludvigson J-E, Hansson K, Rouhiainen P, 2002. Methodology study of Posiva difference flow meter in borehole KLX02 at Laxemar. SKB R-01-52, Svensk Kärnbränslehantering AB.

Tiensuu K, Heikkinen E, 2016. KBS-3H, Geophysical logging of borehole K08028F01. SKB P-15-15, Svensk Kärnbränslehantering AB.

Öhberg A, Rouhiainen P, 2000. Posiva groundwater flow measuring techniques. Posiva 2000-12, Posiva Oy, Finland.

SPR results after length correction

Äspö, borehole K03009F01

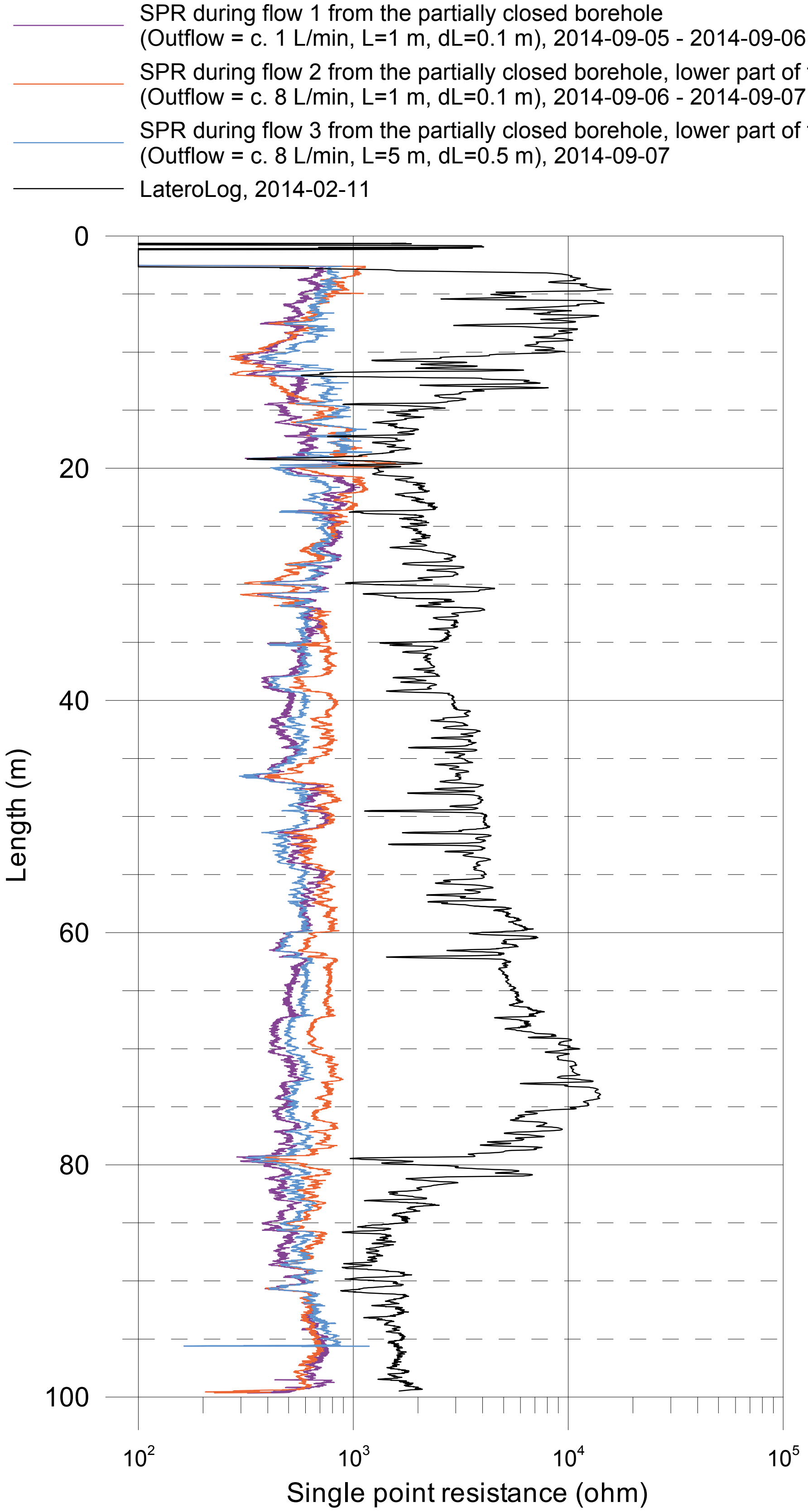

Electrical conductivity of borehole water

Äspö, borehole K03009F01

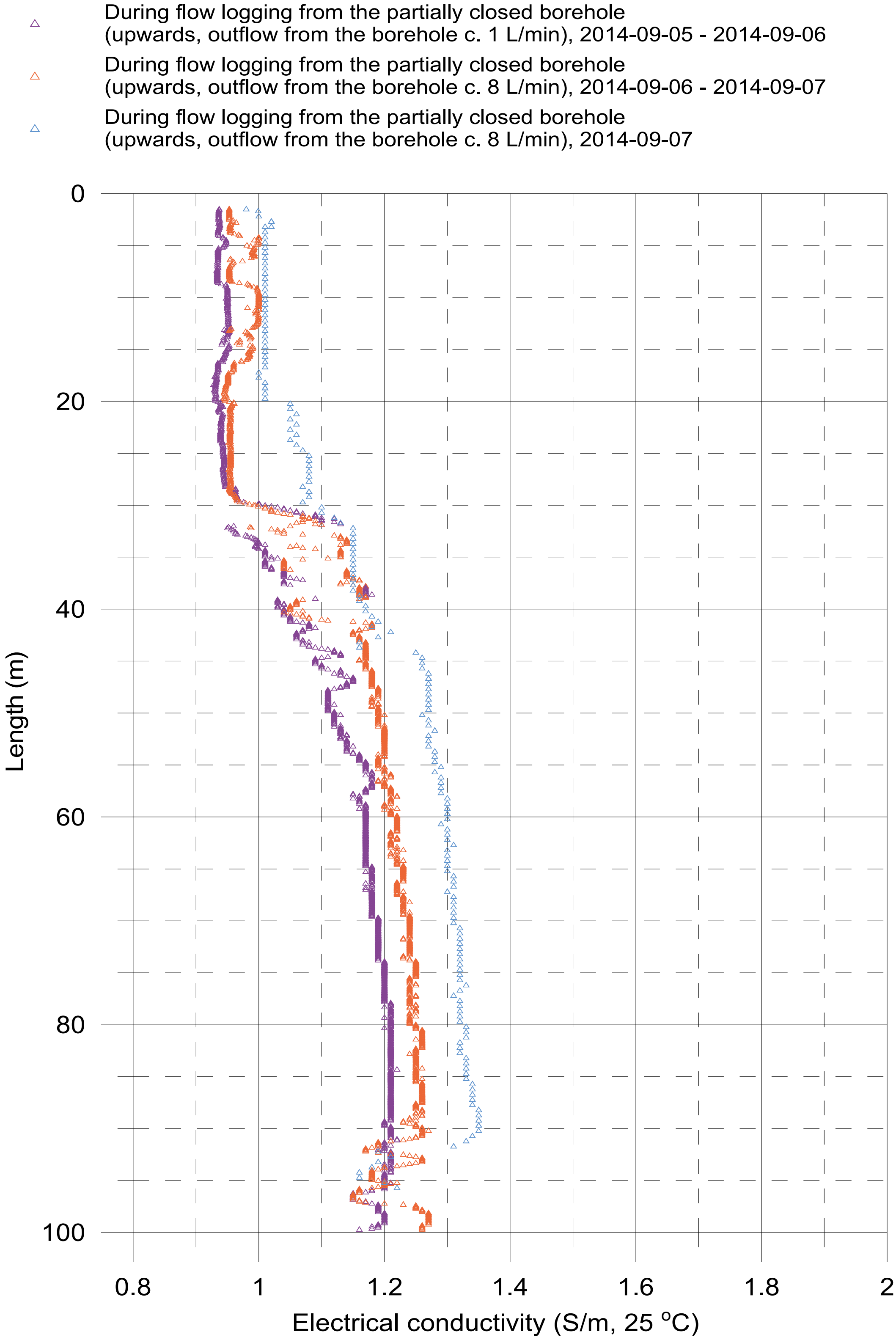

Temperature of borehole water

Äspö, borehole K03009F01

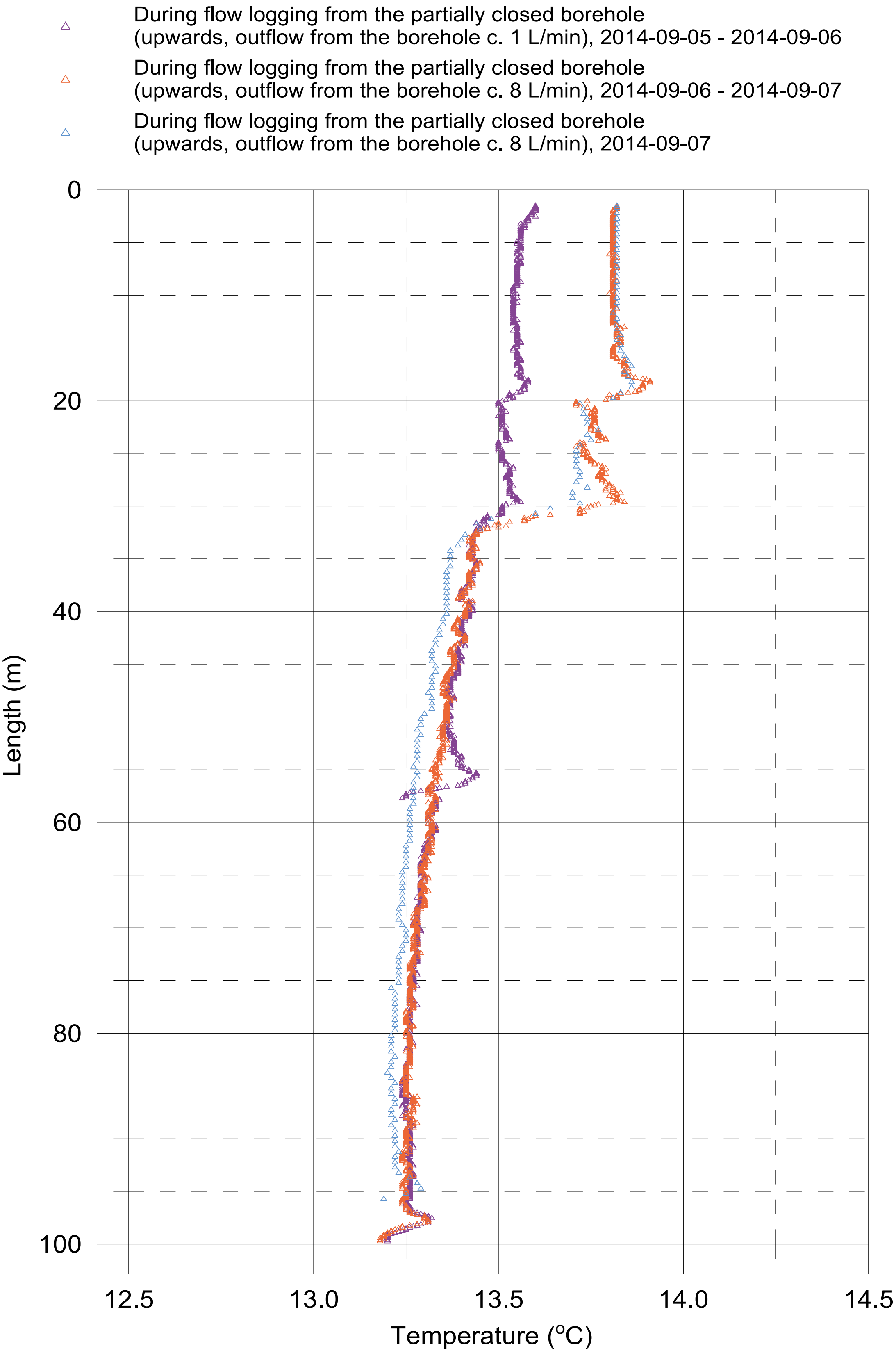

Flow rate and single point resistance

Äspö, borehole K03009F01

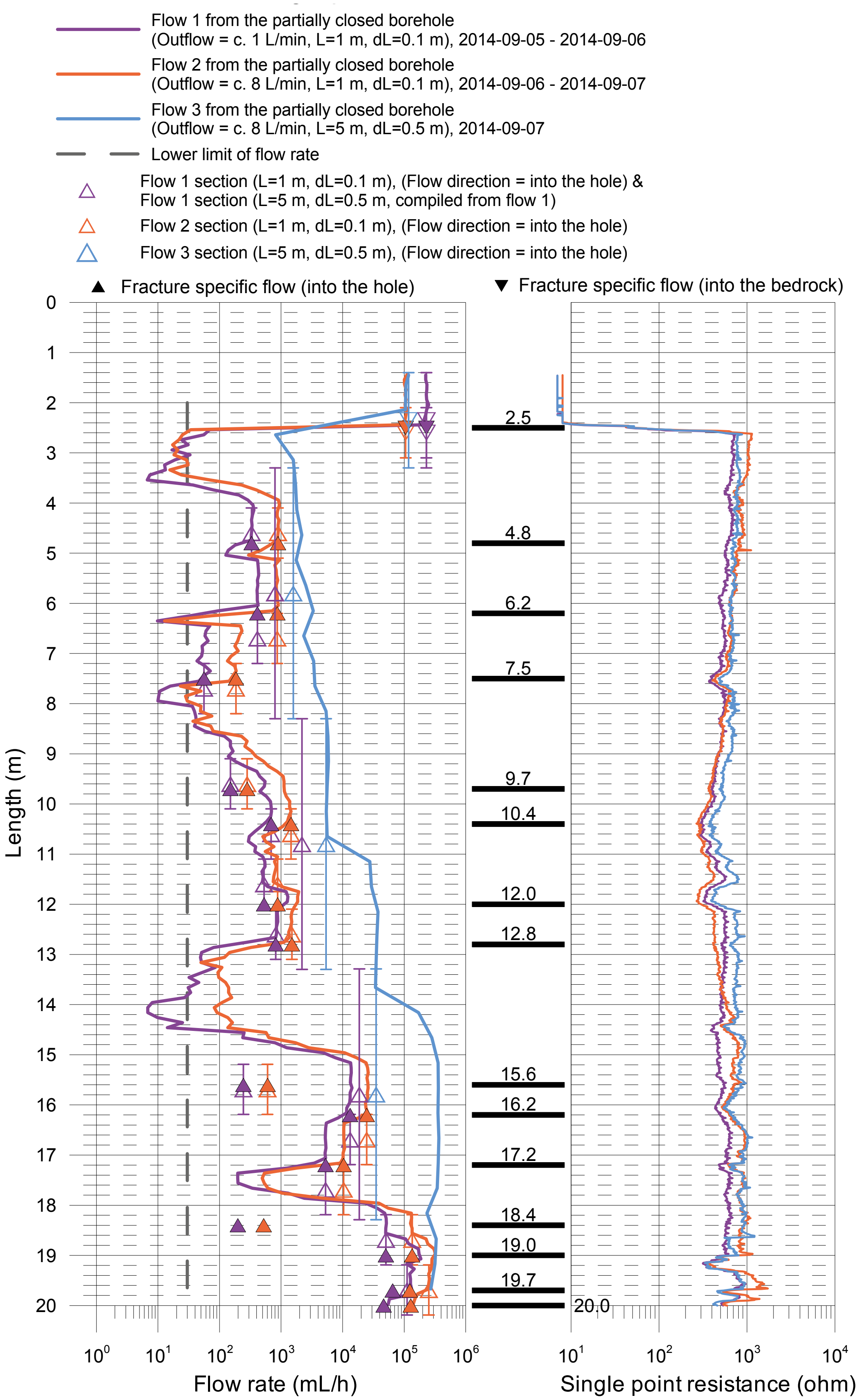

Flow rate and single point resistance

Äspö, borehole K03009F01

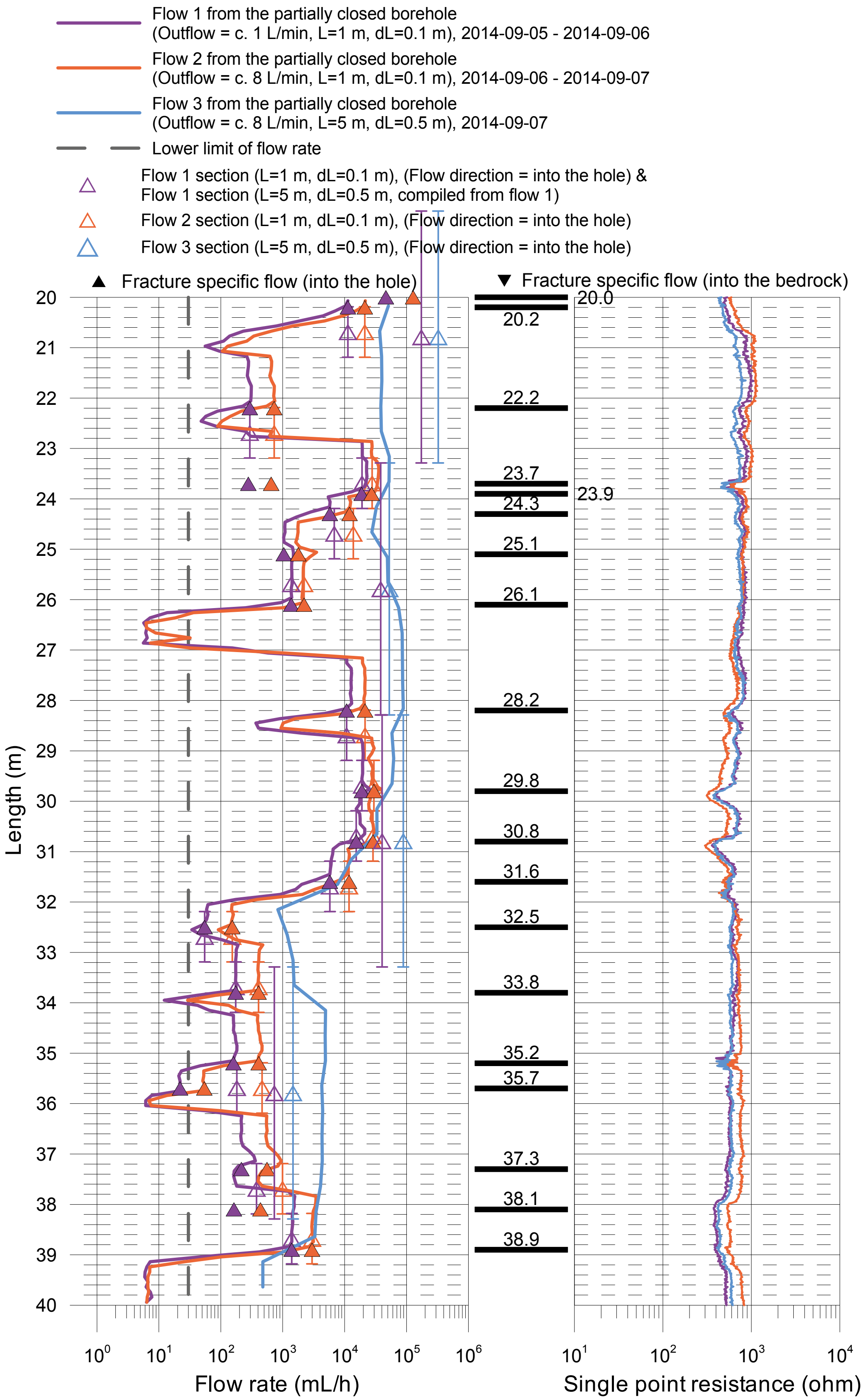

Flow rate and single point resistance

Äspö, borehole K03009F01

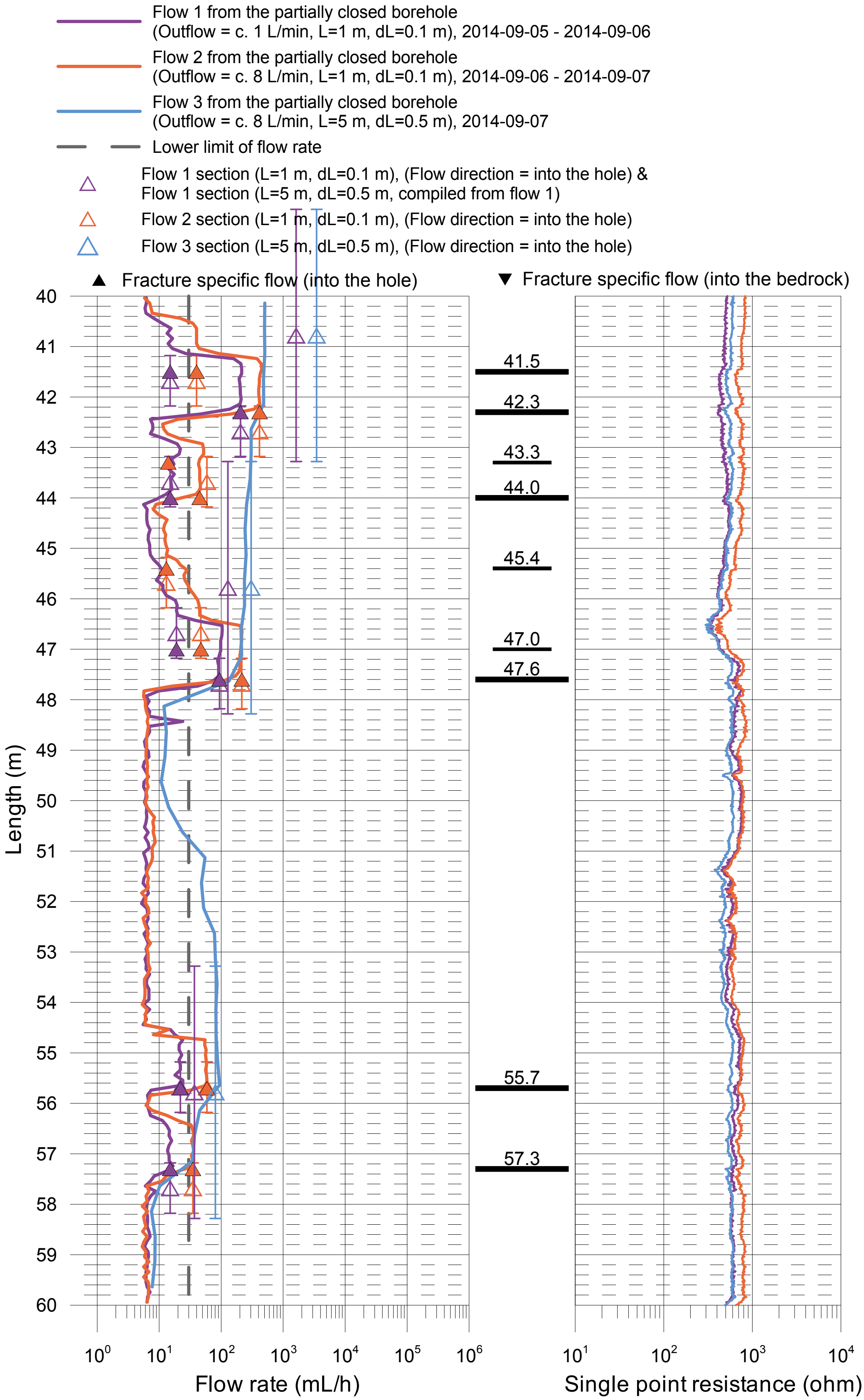

Flow rate and single point resistance

Äspö, borehole K03009F01

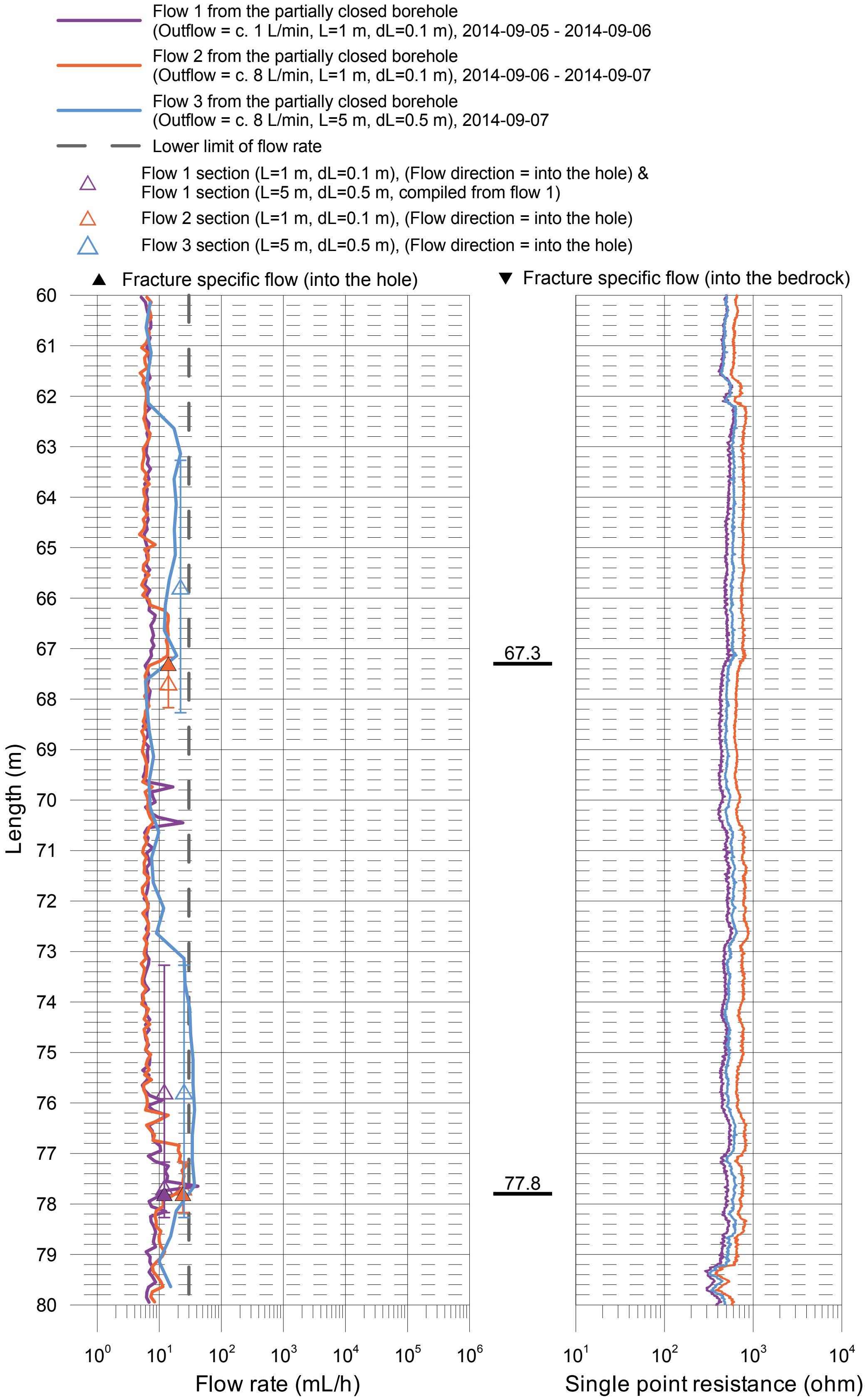

Flow rate and single point resistance

Äspö, borehole K03009F01

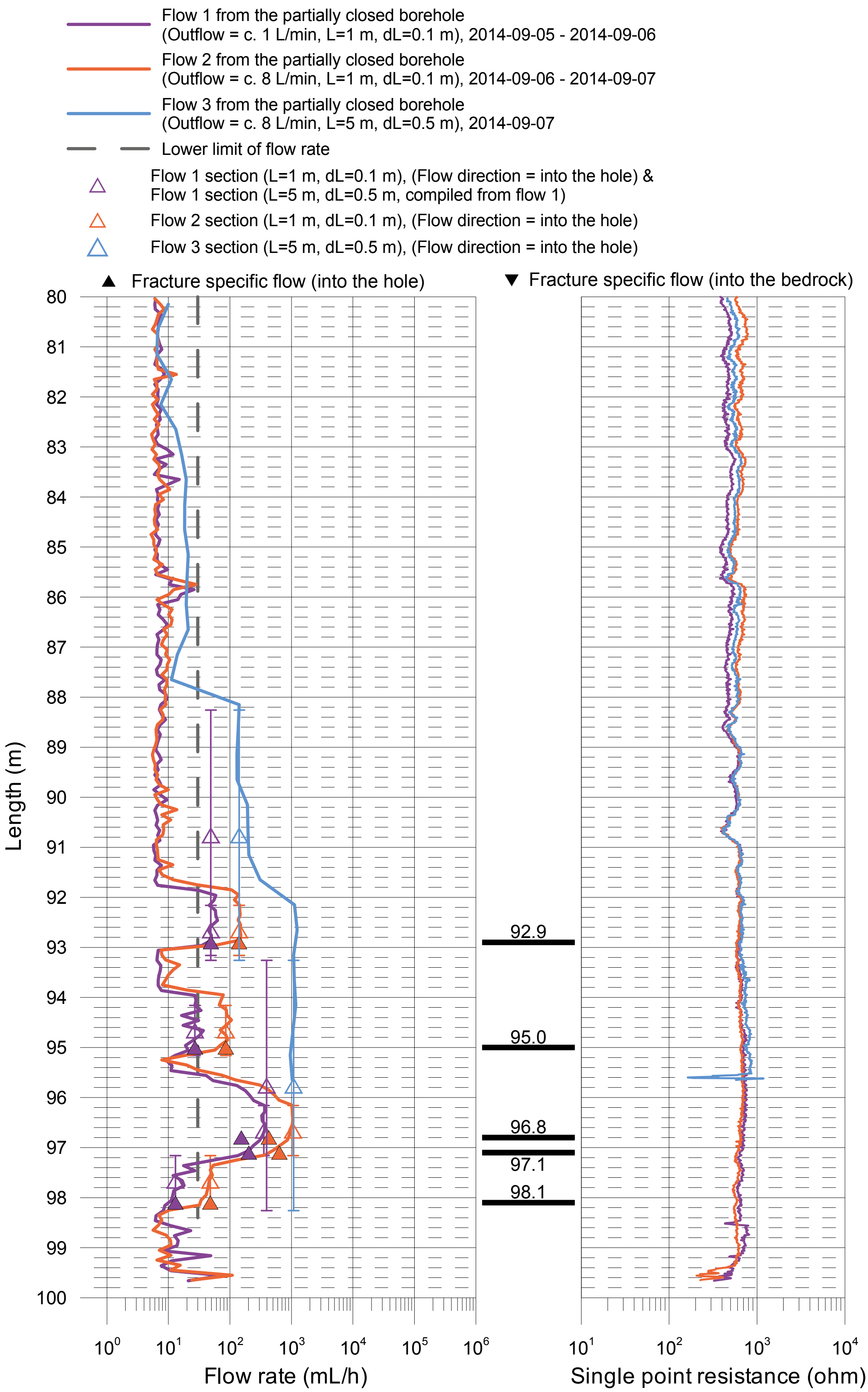

Appendix 4

Explanations for the tables in Appendices 5, 7 and 9

Header	Unit	Explanations
Borehole		ID for borehole.
Secup	m	Length along the borehole for the upper limit of the test section (based on corrected length L).
Seclow	m	Length along the borehole for the lower limit of the test section (based on corrected length L).
L	m	Corrected length along borehole based on SKB procedures for length correction.
Length to flow anom.	m	Length along the borehole to inferred flow anomaly during overlapping flow logging.
Test type (1-6)	(-)	1A: Pumping test – wire-line eq., 1B:Pumping test-submersible pump, 1C: Pumping test-airlift pumping, 2: Interference test, 3: Injection test, 4: Slug test, 5A: Difference flow logging -PFL-DIFF-Sequential, 5B: Difference flow logging -PFL-DIFF-Overlapping, 6: Flow logging-Impeller.
Date of test, start	YY-MM-DD	Date for start of pumping.
Time of test, start	hh:mm	Time for start of pumping.
Date of flowl., start .	YY-MM-DD	Date for start of the flow logging.
Time of flowl., start	hh:mm	Time for start of the flow logging.
Date of test, stop	YY-MM-DD	Date for stop of the test.
Time of test, stop	hh:mm	Time for stop of the test.
L_w	m	Section length used in the difference flow logging.
dL	m	Step length (increment) used in the difference flow logging.
Q_{p1}	m^3/s	Flow rate at surface by the end of the first pumping period of the flow logging.
Q_{p2}	m^3/s	Flow rate at surface by the end of the second pumping period of the flow logging.
t_{p1}	s	Duration of the first pumping period.
t_{p2}	s	Duration of the second pumping period.
t_{F1}	s	Duration of the first recovery period.
t_{F2}	s	Duration of the second recovery period.
h_0	m.a.s.l.	Initial hydraulic head before pumping. Elevation of water level in open borehole in the local co-ordinates system with z=0 m.
h_1	m.a.s.l.	Stabilized hydraulic head during the first pumping period. Elevation of water level in open borehole in the local co-ordinates system with z=0 m.
h_2	m.a.s.l.	Stabilized hydraulic head during the second pumping period. Elevation of water level in open borehole in the local co-ordinates system with z=0 m.
s_1	m	Drawdown of the water level in the borehole during first pumping period. Difference between the actual hydraulic head and the initial head (s1= h1−h0).
s_2	m	Drawdown of the water level in the borehole during second pumping period. Difference between the actual hydraulic head and the initial head (s2=h2−h0).
T	m^2/s	Transmissivity of the entire borehole.
Q_0	m^3/s	Measured flow rate through the test section or flow anomaly under natural conditions (no pumping) with h=h0 in the open borehole.
Q_1	m^3/s	Measured flow rate through the test section or flow anomaly during the first pumping period.

Q_2	m^3/s	Measured flow rate through the test section or flow anomaly during the second pumping period.
h_{0FW}	m.a.s.l.	Corrected initial hydraulic head along the hole due to e.g. varying salinity conditions of the borehole fluid before pumping.
h_{1FW}	m.a.s.l.	Corrected hydraulic head along the hole due to e.g. varying salinity conditions of the borehole fluid during the first pumping period.
h_{2FW}	m.a.s.l.	Corrected hydraulic head along the hole due to e.g. varying salinity conditions of the borehole fluid during the second pumping period.
EC_w	S/m	Measured electrical conductivity of the borehole fluid in the test section during difference flow logging.
Te_w	ºC	Measured borehole fluid temperature in the test section during difference flow logging.
EC_f	S/m	Measured fracture-specific electrical conductivity of the fluid in flow anomaly during difference flow logging.
Te_f	ºC	Measured fracture-specific fluid temperature in flow anomaly during difference flow logging.
T_D	m^2/s	Transmissivity of section or flow anomaly based on 2D model for evaluation of formation properties of the test section based on PFL-DIFF.
T-$measl_{LT}$	m^2/s	Estimated theoretical lower measurement limit for evaluated TD. If the estimated TD equals TD-measlim, the actual TD is considered to be equal or less than TD-measlim.
T-$measl_{LP}$	m^2/s	Estimated practical lower measurement limit for evaluated TD. If the estimated TD equals TD-measlim, the actual TD is considered to be equal or less than TD-measlim.
T-$meas_{lU}$	m^2/s	Estimated upper measurement limit for evaluated TD. If the estimated TD equals TD-measlim, the actual TD is considered to be equal or less than TD-measlim.
h_i	m.a.s.l.	Calculated relative, natural freshwater head for test section or flow anomaly (undisturbed conditions).
Q-lower limit P	mL/h	Practical minimum for measurable flow.

Results of sequential flow logging

Borehole ID	Secup L(m)	Seclow L(m)	L_w (m)	Q_0 (m^3/s)	h_{0FW} (masl)	Q_1 (m^3/s)	h_{1FW} (masl)	T_D (m^2/s)	h_i (masl)	Q-lower limit P (mL/h)	TD-measl$_{LT}$ (m^2/s)	TD-measl$_{LP}$ (m^2/s)	TD-measl$_U$ (m^2/s)	Comments
K03009F01	2.12	3.12	1	−6.39E-05	−188.50	−2.94E-05	−359.49	2.0E-07	−505.7	30	4.8E-11	4.8E-11	4.8E-07	
K03009F01	3.12	4.12	1	–	−191.49	–	−360.05	–	–	30	4.9E-11	4.9E-11	4.9E-07	
K03009F01	4.12	5.12	1	9.22E-08	−189.27	2.47E-07	−360.24	9.0E-10	−87.4	30	4.8E-11	4.8E-11	4.8E-07	
K03009F01	5.12	6.12	1	–	−193.38	–	−359.97	–	–	30	5.0E-11	5.0E-11	5.0E-07	
K03009F01	6.18	7.18	1	1.14E-07	−192.60	2.41E-07	−360.10	7.5E-10	−41.3	30	4.9E-11	4.9E-11	4.9E-07	
K03009F01	7.18	8.18	1	1.56E-08	−193.71	5.14E-08	−360.29	2.1E-10	−121.4	30	5.0E-11	5.0E-11	5.0E-07	
K03009F01	8.13	9.13	1	–	−193.98	–	−360.19	–	–	30	5.0E-11	5.0E-11	5.0E-07	
K03009F01	9.13	10.13	1	4.17E-08	−192.98	7.81E-08	−360.22	2.2E-10	−1.5	30	4.9E-11	4.9E-11	4.9E-07	
K03009F01	10.13	11.13	1	1.92E-07	−193.92	4.03E-07	−360.08	1.3E-09	−43.1	30	5.0E-11	5.0E-11	5.0E-07	
K03009F01	11.13	12.13	1	1.47E-07	−191.4	2.44E-07	−360.07	5.7E-10	63.8	30	4.9E-11	4.9E-11	4.9E-07	
K03009F01	12.13	13.13	1	2.28E-07	−193.56	4.17E-07	−359.99	1.1E-09	6.6	30	5.0E-11	5.0E-11	4.9E-07	
K03009F01	13.17	14.17	1	–	−195.73	–	−360.07	–	–	30	5.0E-11	5.0E-11	5.0E-07	
K03009F01	14.17	15.17	1	–	−194.07	–	−360.07	–	–	30	5.0E-11	5.0E-11	5.0E-07	
K03009F01	15.17	16.17	1	6.81E-08	−193.02	1.67E-07	−360.04	5.9E-10	−78.4	30	4.9E-11	4.9E-11	4.9E-07	
K03009F01	16.17	17.17	1	3.67E-06	−193.68	6.83E-06	−360.00	1.9E-08	−1.1	30	5.0E-11	5.0E-11	4.7E-07	
K03009F01	17.17	18.17	1	1.47E-06	−194.55	2.89E-06	−360.17	8.5E-09	−23.8	30	5.0E-11	5.0E-11	4.9E-07	
K03009F01	18.17	19.17	1	1.41E-05	−194.45	3.76E-05	−359.62	1.4E-07	−95.7	30	5.0E-11	5.0E-11	4.2E-07	
K03009F01	19.18	20.18	1	3.10E-05	−194.06	7.00E-05	−359.58	2.3E-07	−62.3	30	5.0E-11	5.0E-11	3.1E-07	
K03009F01	20.18	21.18	1	3.14E-06	−194.18	5.89E-06	−360.24	1.6E-08	−4.6	30	5.0E-11	5.0E-11	4.8E-07	
K03009F01	21.18	22.18	1	–	−194.50	–	−360.15	–	–	30	5.0E-11	5.0E-11	5.0E-07	
K03009F01	22.18	23.18	1	8.17E-08	−194.23	2.03E-07	−360.14	7.2E-10	−82.4	30	5.0E-11	5.0E-11	5.0E-07	
K03009F01	23.18	24.18	1	5.33E-06	−194.49	7.76E-06	−360.10	1.5E-08	167.6	30	5.0E-11	5.0E-11	4.7E-07	
K03009F01	24.18	25.18	1	1.89E-06	−193.99	3.83E-06	−360.47	1.2E-08	−31.1	30	5.0E-11	5.0E-11	4.8E-07	
K03009F01	25.18	26.18	1	3.81E-07	−195.28	6.17E-07	−360.53	1.4E-09	71.1	30	5.0E-11	5.0E-11	5.0E-07	
K03009F01	26.18	27.18	1	–	−194.19	–	−360.20	–	–	30	5.0E-11	5.0E-11	5.0E-07	
K03009F01	27.18	28.18	1	–	−194.77	–	−360.32	–	–	30	5.0E-11	5.0E-11	5.0E-07	
K03009F01	28.18	29.18	1	3.00E-06	−193.25	5.94E-06	−360.29	1.7E-08	−23.1	30	4.9E-11	4.9E-11	4.8E-07	

Appendix 5.2

Results of sequential flow logging

Borehole ID	Secup L(m)	Seclow L(m)	L_w (m)	Q_0 (m^3/s)	h_{0FW} (masl)	Q_1 (m^3/s)	h_{1FW} (masl)	T_D (m^2/s)	h_i (masl)	Q-lower limit P (mL/h)	TD-measl$_{LT}$ (m^2/s)	TD- measl$_{LP}$ (m^2/s)	TD- measl$_U$ (m^2/s)	Comments
K03009F01	29.17	30.17	1	5.31E-06	−194.47	8.28E-06	−360.41	1.8E-08	101.7	30	5.0E-11	5.0E-11	4.7E-07	
K03009F01	30.17	31.17	1	4.28E-06	−193.91	7.97E-06	−360.43	2.2E-08	−1.1	30	5.0E-11	5.0E-11	4.7E-07	
K03009F01	31.17	32.17	1	1.61E-06	−193.50	3.28E-06	−360.38	9.9E-09	−32.7	30	4.9E-11	4.9E-11	4.8E-07	
K03009F01	32.17	33.17	1	1.53E-08	−193.80	4.25E-08	−360.35	1.6E-10	−100.3	30	5.0E-11	5.0E-11	5.0E-07	
K03009F01	33.17	34.17	1	4.83E-08	−193.03	1.13E-07	−360.35	3.8E-10	−68.6	30	4.9E-11	4.9E-11	4.9E-07	
K03009F01	34.17	35.17	1	–	−193.65	–	−360.32	–	–	30	5.0E-11	5.0E-11	5.0E-07	
K03009F01	35.17	36.17	1	5.06E-08	−192.67	1.29E-07	−360.21	4.6E-10	−84.2	30	4.9E-11	4.9E-11	4.9E-07	
K03009F01	36.17	37.17	1	–	−192.75	–	−360.21	–	–	30	4.9E-11	4.9E-11	4.9E-07	
K03009F01	37.17	38.17	1	1.05E-07	−194.00	2.76E-07	−360.51	1.0E-09	−91.8	30	5.0E-11	5.0E-11	4.9E-07	
K03009F01	38.16	39.16	1	3.89E-07	−192.88	8.28E-07	−360.26	2.6E-09	−44.6	30	4.9E-11	4.9E-11	4.9E-07	
K03009F01	39.16	40.16	1	–	−193.13	–	−360.25	–	–	30	4.9E-11	4.9E-11	4.9E-07	
K03009F01	40.16	41.16	1	–	−195.24	–	−360.34	–	–	30	5.0E-11	5.0E-11	5.0E-07	
K03009F01	41.16	42.16	1	4.17E-09	−193.66	1.11E-08	−360.39	4.1E-11	−93.6	30	4.9E-11	4.9E-11	4.9E-07	*
K03009F01	42.16	43.16	1	5.69E-08	−194.61	1.16E-07	−360.36	3.5E-10	−34.3	30	5.0E-11	5.0E-11	5.0E-07	
K03009F01	43.16	44.16	1	4.17E-09	−194.77	1.64E-08	−360.33	7.3E-11	−138.3	30	5.0E-11	5.0E-11	5.0E-07	*
K03009F01	44.16	45.16	1	–	−193.88	–	−360.34	–	–	30	5.0E-11	5.0E-11	5.0E-07	
K03009F01	45.16	46.16	1	–	−191.83	3.61E-09	−360.25	2.1E-11	–	30	4.9E-11	4.9E-11	4.9E-07	*
K03009F01	46.16	47.16	1	5.28E-09	−192.99	1.31E-08	−360.32	4.6E-11	−79.4	30	4.9E-11	4.9E-11	4.9E-07	*
K03009F01	47.16	48.16	1	2.61E-08	−194.43	5.97E-08	−360.50	2.0E-10	−65.4	30	5.0E-11	5.0E-11	5.0E-07	
K03009F01	48.16	49.16	1	–	−194.52	–	−360.39	–	–	30	5.0E-11	5.0E-11	5.0E-07	
K03009F01	49.16	50.16	1	–	−194.02	–	−360.25	–	–	30	5.0E-11	5.0E-11	5.0E-07	
K03009F01	50.16	51.16	1	–	−194.14	–	−360.34	–	–	30	5.0E-11	5.0E-11	5.0E-07	
K03009F01	51.16	52.16	1	–	−193.90	–	−360.32	–	–	30	5.0E-11	5.0E-11	5.0E-07	
K03009F01	52.16	53.16	1	–	−193.45	–	−360.25	–	–	30	4.9E-11	4.9E-11	4.9E-07	
K03009F01	53.16	54.16	1	–	−194.84	–	−360.36	–	–	30	5.0E-11	5.0E-11	5.0E-07	
K03009F01	54.16	55.16	1	–	−193.96	–	−360.31	–	–	30	5.0E-11	5.0E-11	5.0E-07	
K03009F01	55.16	56.16	1	6.11E-09	−193.82	1.64E-08	−360.33	6.1E-11	−94.8	30	5.0E-11	5.0E-11	5.0E-07	*

Appendix 5.3

Results of sequential flow logging

Borehole ID	Secup L(m)	Seclow L(m)	L_w (m)	Q_0 (m^3/s)	h_{0FW} (masl)	Q_1 (m^3/s)	h_{1FW} (masl)	T_D (m^2/s)	h_i (masl)	Q-lower limit P (mL/h)	TD-measl$_{LT}$ (m^2/s)	TD- measl$_{LP}$ (m^2/s)	TD- measl$_U$ (m^2/s)	Comments
K03009F01	56.16	57.16	1	–	−194.14	–	−360.29	–	–	30	5.0E-11	5.0E-11	5.0E-07	
K03009F01	57.16	58.16	1	4.17E-09	−195.13	9.72E-09	−360.01	3.3E-11	−71.5	30	5.0E-11	5.0E-11	5.0E-07	*
K03009F01	58.16	59.16	1	–	−192.29	–	−360.18	–	–	30	4.9E-11	4.9E-11	4.9E-07	
K03009F01	59.16	60.16	1	–	−191.11	–	−360.10	–	–	30	4.9E-11	4.9E-11	4.9E-07	
K03009F01	60.16	61.16	1	–	−191.81	–	−360.09	–	–	30	4.9E-11	4.9E-11	4.9E-07	
K03009F01	61.16	62.16	1	–	−192.26	–	−360.23	–	–	30	4.9E-11	4.9E-11	4.9E-07	
K03009F01	62.16	63.16	1	–	−191.76	–	−360.14	–	–	30	4.9E-11	4.9E-11	4.9E-07	
K03009F01	63.16	64.16	1	–	−191.91	–	−360.23	–	–	30	4.9E-11	4.9E-11	4.9E-07	
K03009F01	64.16	65.16	1	–	−192.32	–	−360.24	–	–	30	4.9E-11	4.9E-11	4.9E-07	
K03009F01	65.16	66.16	1	–	−191.82	–	−360.18	–	–	30	4.9E-11	4.9E-11	4.9E-07	
K03009F01	66.16	67.16	1	–	−192.31	–	−360.29	–	–	30	4.9E-11	4.9E-11	4.9E-07	
K03009F01	67.16	68.16	1	–	−193.38	3.89E-09	−360.38	2.3E-11	–	30	4.9E-11	4.9E-11	4.9E-07	*
K03009F01	68.16	69.16	1	–	−192.48	–	−360.29	–	–	30	4.9E-11	4.9E-11	4.9E-07	
K03009F01	69.16	70.16	1	–	−192.06	–	−360.29	–	–	30	4.9E-11	4.9E-11	4.9E-07	
K03009F01	70.16	71.16	1	–	−192.04	–	−360.19	–	–	30	4.9E-11	4.9E-11	4.9E-07	
K03009F01	71.16	72.16	1	–	−192.21	–	−360.26	–	–	30	4.9E-11	4.9E-11	4.9E-07	
K03009F01	72.16	73.16	1	–	−191.97	–	−360.17	–	–	30	4.9E-11	4.9E-11	4.9E-07	
K03009F01	73.16	74.16	1	–	−191.82	–	−360.18	–	–	30	4.9E-11	4.9E-11	4.9E-07	
K03009F01	74.16	75.16	1	–	−191.73	–	−360.14	–	–	30	4.9E-11	4.9E-11	4.9E-07	
K03009F01	75.16	76.16	1	–	−191.11	–	−360.21	–	–	30	4.9E-11	4.9E-11	4.9E-07	
K03009F01	76.16	77.16	1	–	−191.43	–	−360.17	–	–	30	4.9E-11	4.9E-11	4.9E-07	
K03009F01	77.16	78.16	1	3.33E-09	−185.7	6.67E-09	−359.53	1.9E-11	−11.9	30	4.7E-11	4.7E-11	4.7E-07	*
K03009F01	78.16	79.16	1	–	−191.48	–	−360.07	–	–	30	4.9E-11	4.9E-11	4.9E-07	
K03009F01	79.16	80.16	1	–	−191.86	–	−360.09	–	–	30	4.9E-11	4.9E-11	4.9E-07	
K03009F01	80.16	81.16	1	–	−191.20	–	−360.03	–	–	30	4.9E-11	4.9E-11	4.9E-07	
K03009F01	81.16	82.16	1	–	−191.97	–	−360.06	–	–	30	4.9E-11	4.9E-11	4.9E-07	
K03009F01	82.16	83.16	1	–	−191.54	–	−360.14	–	–	30	4.9E-11	4.9E-11	4.9E-07	

Appendix 5.4

Results of sequential flow logging

Borehole ID	Secup L(m)	Seclow L(m)	L_w (m)	Q_0 (m^3/s)	h_{0FW} (masl)	Q_1 (m^3/s)	h_{1FW} (masl)	T_D (m^2/s)	h_i (masl)	Q-lower limit P (mL/h)	TD-measl$_{LT}$ (m^2/s)	TD- measl$_{LP}$ (m^2/s)	TD- measl$_U$ (m^2/s)	Comments
K03009F01	83.16	84.16	1	–	−192.77	–	−360.19	–	–	30	4.9E-11	4.9E-11	4.9E-07	
K03009F01	84.16	85.16	1	–	−192.74	–	−360.22	–	–	30	4.9E-11	4.9E-11	4.9E-07	
K03009F01	85.16	86.16	1	–	−193.28	–	−360.38	–	–	30	4.9E-11	4.9E-11	4.9E-07	
K03009F01	86.16	87.16	1	–	−193.74	–	−360.39	–	–	30	5.0E-11	5.0E-11	5.0E-07	
K03009F01	87.16	88.16	1	–	−190.65	–	−360.10	–	–	30	4.9E-11	4.9E-11	4.9E-07	
K03009F01	88.16	89.16	1	–	−191.54	–	−360.04	–	–	30	4.9E-11	4.9E-11	4.9E-07	
K03009F01	89.16	90.16	1	–	−190.89	–	−360.20	–	–	30	4.9E-11	4.9E-11	4.9E-07	
K03009F01	90.16	91.16	1	–	−190.65	–	−360.06	–	–	30	4.9E-11	4.9E-11	4.9E-07	
K03009F01	91.16	92.16	1	–	−191.42	–	−360.18	–	–	30	4.9E-11	4.9E-11	4.9E-07	
K03009F01	92.16	93.16	1	1.36E-08	−190.5	3.92E-08	−360.25	1.5E-10	−100.1	30	4.9E-11	4.9E-11	4.9E-07	
K03009F01	93.16	94.16	1	–	−188.28	–	−360.17	–	–	30	4.8E-11	4.8E-11	4.8E-07	
K03009F01	94.16	95.16	1	7.50E-09	−188.86	2.39E-08	−360.19	9.5E-11	−110.5	30	4.8E-11	4.8E-11	4.8E-07	*
K03009F01	95.16	96.16	1	–	−187.44	–	−360.70	–	–	30	4.8E-11	4.8E-11	4.8E-07	
K03009F01	96.16	97.16	1	9.89E-08	−191.05	2.96E-07	−360.15	1.2E-09	−106.0	30	4.9E-11	4.9E-11	4.9E-07	
K03009F01	97.16	98.16	1	3.61E-09	−190.77	1.33E-08	−360.09	5.7E-11	−127.9	30	4.9E-11	4.9E-11	4.9E-07	*
K03009F01	98.16	99.16	1	–	−191.84	–	−360.46	–	–	30	4.9E-11	4.9E-11	4.9E-07	
K03009F01	99.16	100.16	1	–	−193.01	–	−360.51	–	–	30	4.9E-11	4.9E-11	4.9E-07	

* Uncertain = The flow rate Q1 and/or Q2 is less than 30 mL/h or the flow anomalies are overlapping or they are unclear because of noise.

Flow rates of 1 m sections

Äspö, borehole K03009F01

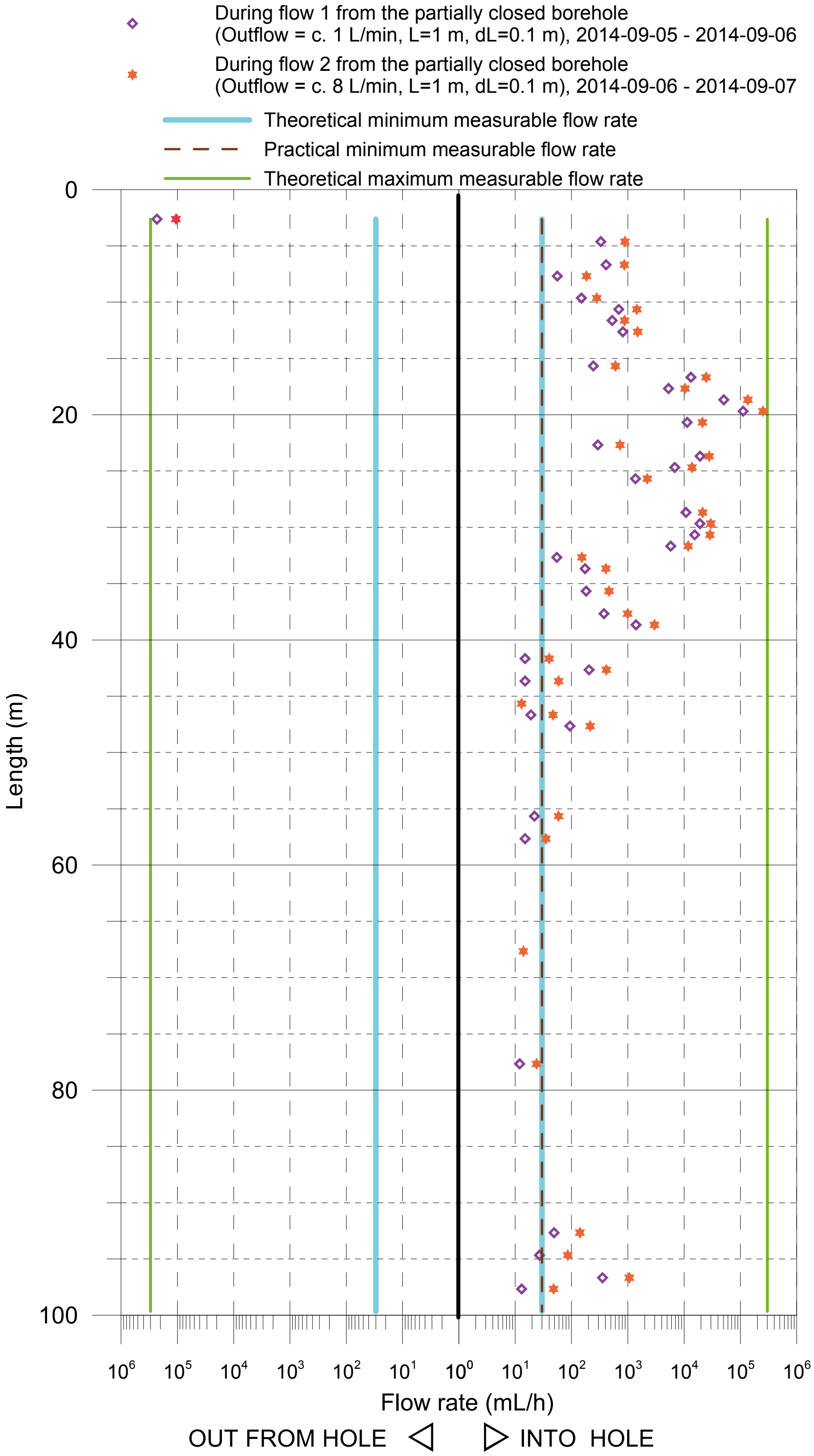

Transmissivity and head of 1 m sections

Äspö, borehole K03009F01

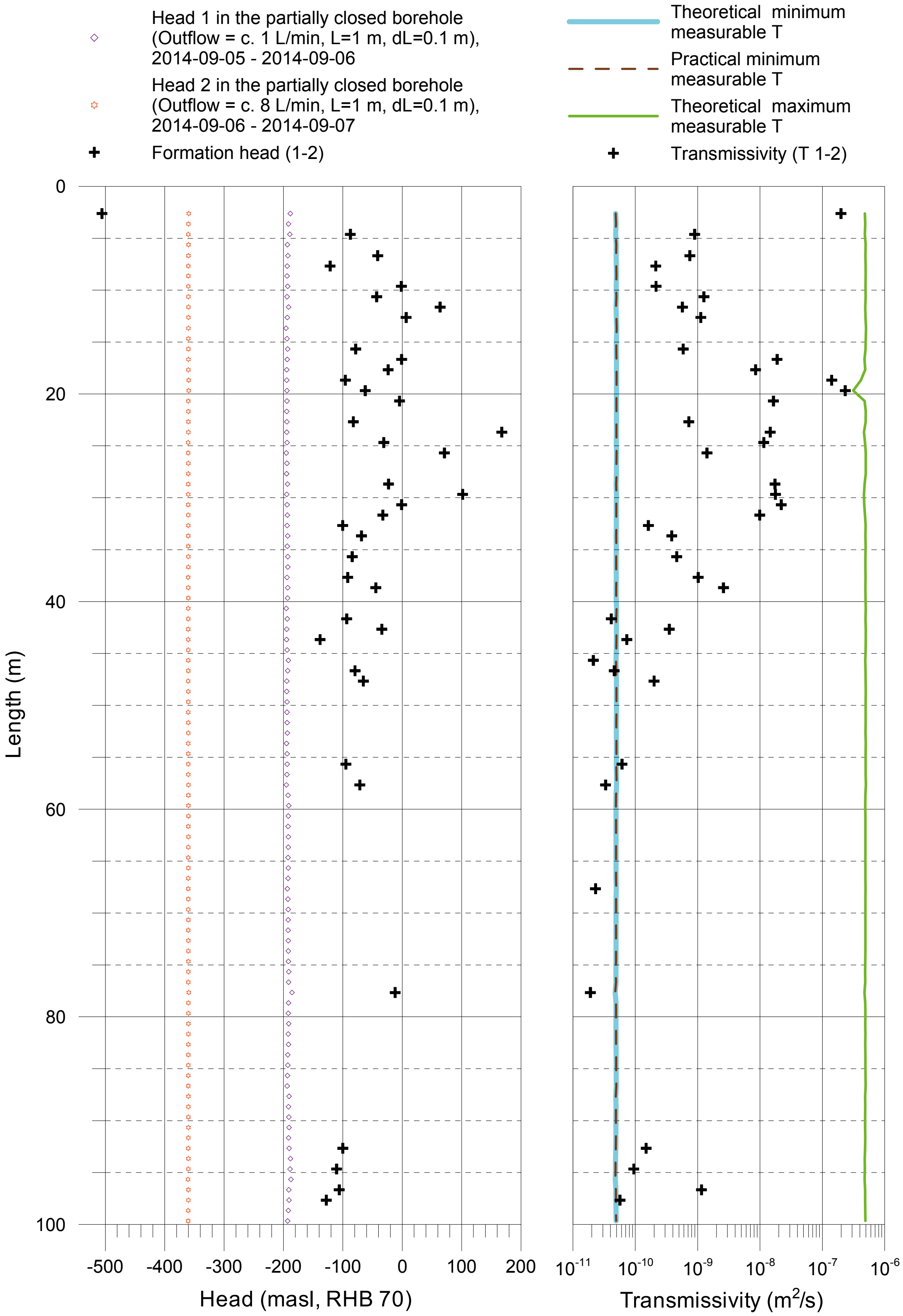

Transmissivity and head of 1 m sections

Äspö, borehole K03009F01

Error bars assuming ±10 % errors in flow rates
and ±0.2 m in head in worst combination

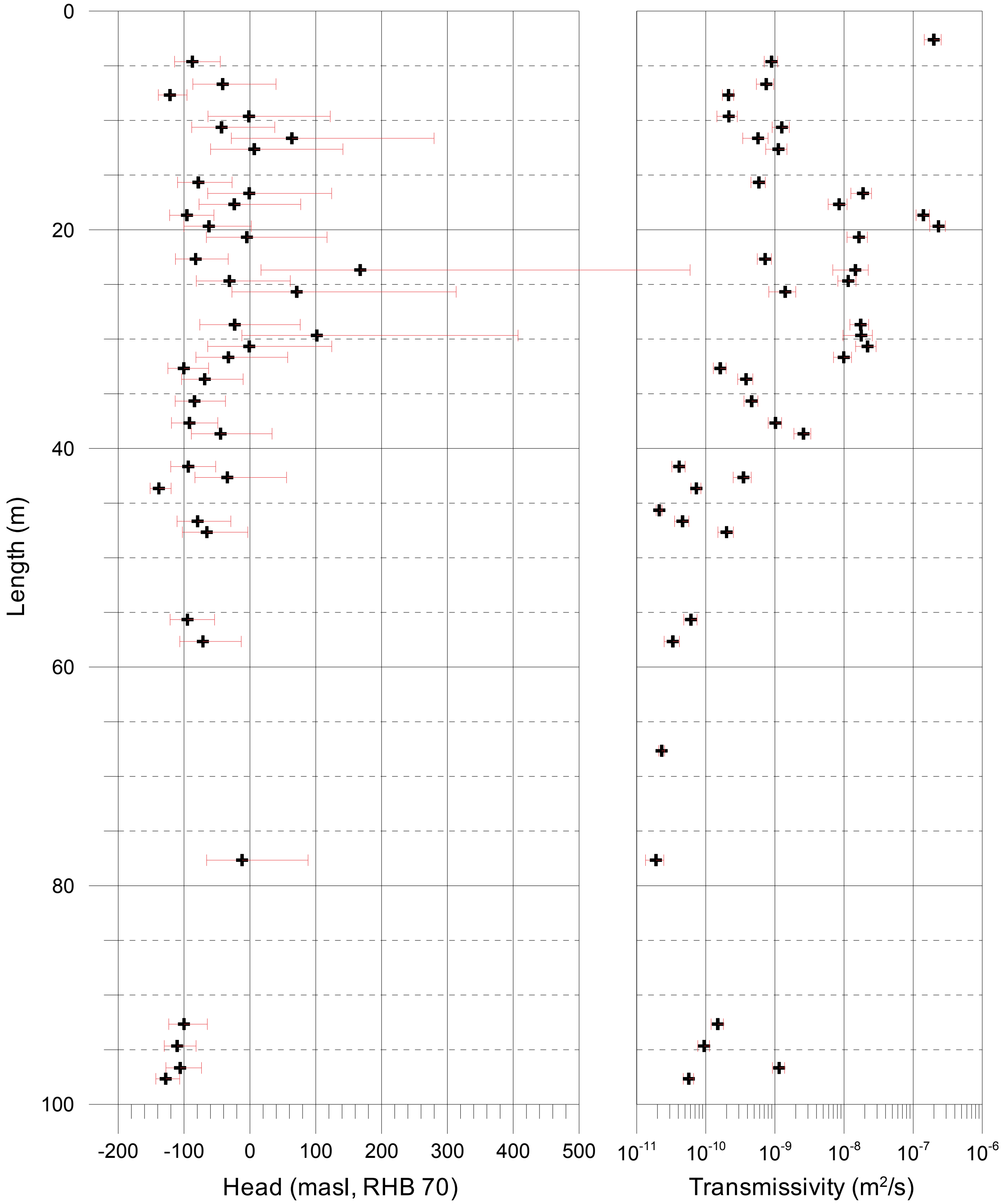

Appendix 7

Results of sequential flow logging

Borehole ID	Secup L(m)	Seclow L(m)	L_w (m)	Q_0 (m^3/s)	h_{0FW} (masl)	Q_1 (m^3/s)	h_{1FW} (masl)	T_D (m^2/s)	h_i (masl)	Q-lower limit P (mL/h)	TD-measl_{LT} (m^2/s)	TD- measl_{LP} (m^2/s)	TD- measl_U (m^2/s)	Comments
3009F01	1.40	3.30	1.9	−6.39E-05	−195.61	−3.28E-05	−352.97	2.0E-07	−518.7	30	5.2E-11	5.2E-11	5.2E-07	**
3009F01	3.22	8.22	5	2.22E-07	−193.38	4.38E-07	−357.96	1.3E-09	−24.2	30	5.0E-11	5.0E-11	5.0E-07	
3009F01	8.23	13.23	5	6.08E-07	−192.68	1.49E-06	−358.28	5.3E-09	−79.2	30	5.0E-11	5.0E-11	4.9E-07	
3009F01	13.23	18.23	5	5.20E-06	−193.17	9.74E-06	−356.52	2.8E-08	−5.8	30	5.1E-11	5.1E-11	4.7E-07	
3009F01	18.23	23.23	5	4.83E-05	−193.39	9.03E-05	−358.36	2.5E-07	−3.5	30	5.0E-11	5.0E-11	2.1E-07	***
3009F01	23.23	28.23	5	1.06E-05	−194.06	1.47E-05	−358.32	2.4E-08	235.7	30	5.0E-11	5.0E-11	4.4E-07	
3009F01	28.23	33.23	5	1.12E-05	−193.82	2.46E-05	−358.28	8.1E-08	−56.5	30	5.0E-11	5.0E-11	4.3E-07	
3009F01	33.22	38.22	5	2.04E-07	−193.03	4.07E-07	−358.07	1.2E-09	−27.3	30	5.0E-11	5.0E-11	5.0E-07	
3009F01	38.21	43.21	5	4.50E-07	−194.09	9.63E-07	−358.34	3.1E-09	−50.0	30	5.0E-11	5.0E-11	5.0E-07	
3009F01	43.21	48.21	5	3.56E-08	−193.97	8.44E-08	−358.11	3.0E-10	−74.6	30	5.0E-11	5.0E-11	5.0E-07	
3009F01	48.21	53.21	5	−	−193.09	−	−358.23	−	−	30	5.0E-11	5.0E-11	5.0E-07	
3009F01	53.21	58.21	5	1.03E-08	−193.70	2.25E-08	−358.26	7.4E-11	−55.3	30	5.0E-11	5.0E-11	5.0E-07	
3009F01	58.21	63.21	5	−	−191.33	−	−358.20	−	−	30	4.9E-11	4.9E-11	4.9E-07	
3009F01	63.21	68.21	5	−	−191.27	6.11E-09	−358.18	3.6E-11	−	30	4.9E-11	4.9E-11	4.9E-07	*
3009F01	68.21	73.21	5	−	−191.85	−	−358.22	−	−	30	5.0E-11	5.0E-11	5.0E-07	
3009F01	73.21	78.21	5	3.33E-09	−191.40	6.94E-09	−358.29	2.1E-11	−37.4	30	4.9E-11	4.9E-11	4.9E-07	*
3009F01	78.21	83.21	5	−	−191.08	−	−358.11	−	−	30	4.9E-11	4.9E-11	4.9E-07	
3009F01	83.21	88.21	5	−	−192.63	−	−358.27	−	−	30	5.0E-11	5.0E-11	5.0E-07	
3009F01	88.21	93.21	5	1.36E-08	−190.85	3.94E-08	−358.08	1.5E-10	−102.7	30	4.9E-11	4.9E-11	4.9E-07	
3009F01	93.21	98.21	5	1.10E-07	−188.33	3.01E-07	−359.49	1.1E-09	−89.7	30	4.8E-11	4.8E-11	4.8E-07	

* Uncertain = The flow rate Q_0 and/or Q_1 is less than 30 mL/h or the flow anomalies are overlapping or they are unclear because of noise.

** Smaller section length at top of borehole.

*** Q_1 over the measurement limit.

Flow rates of 5 m sections

Äspö, borehole K03009F01

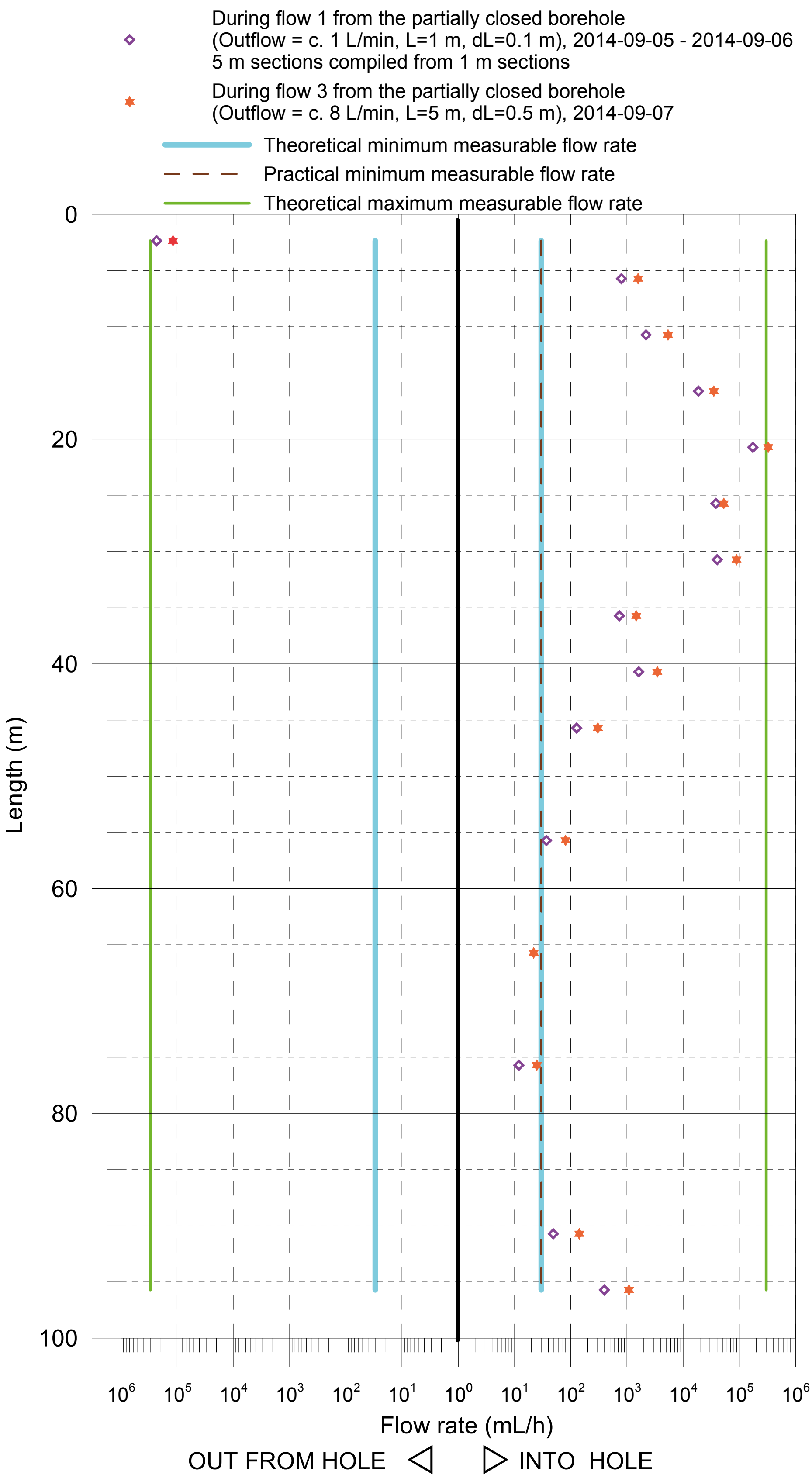

Transmissivity and head of 5 m sections

Äspö, borehole K03009F01

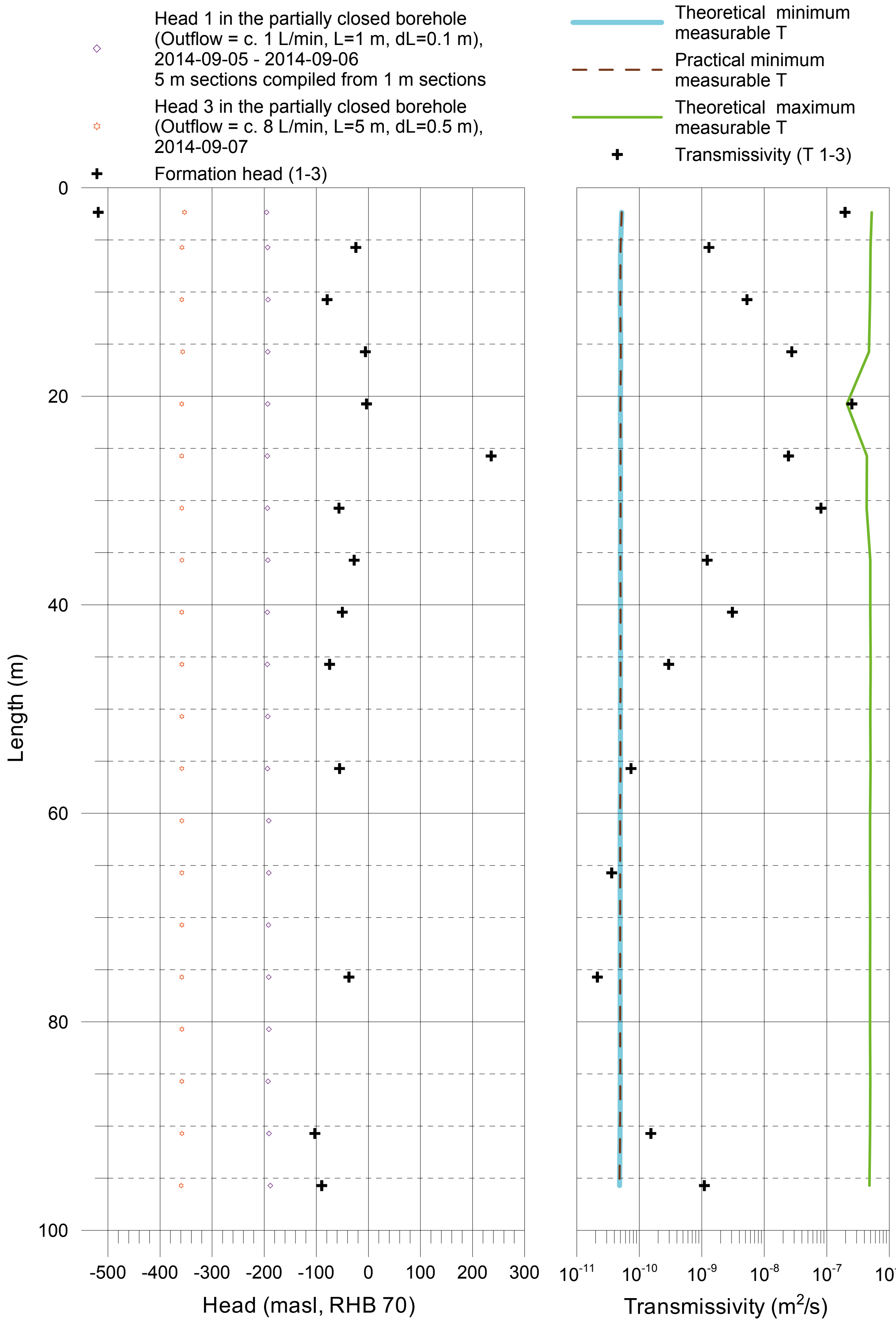

Transmissivity and head of 5 m sections

Äspö, borehole K03009F01

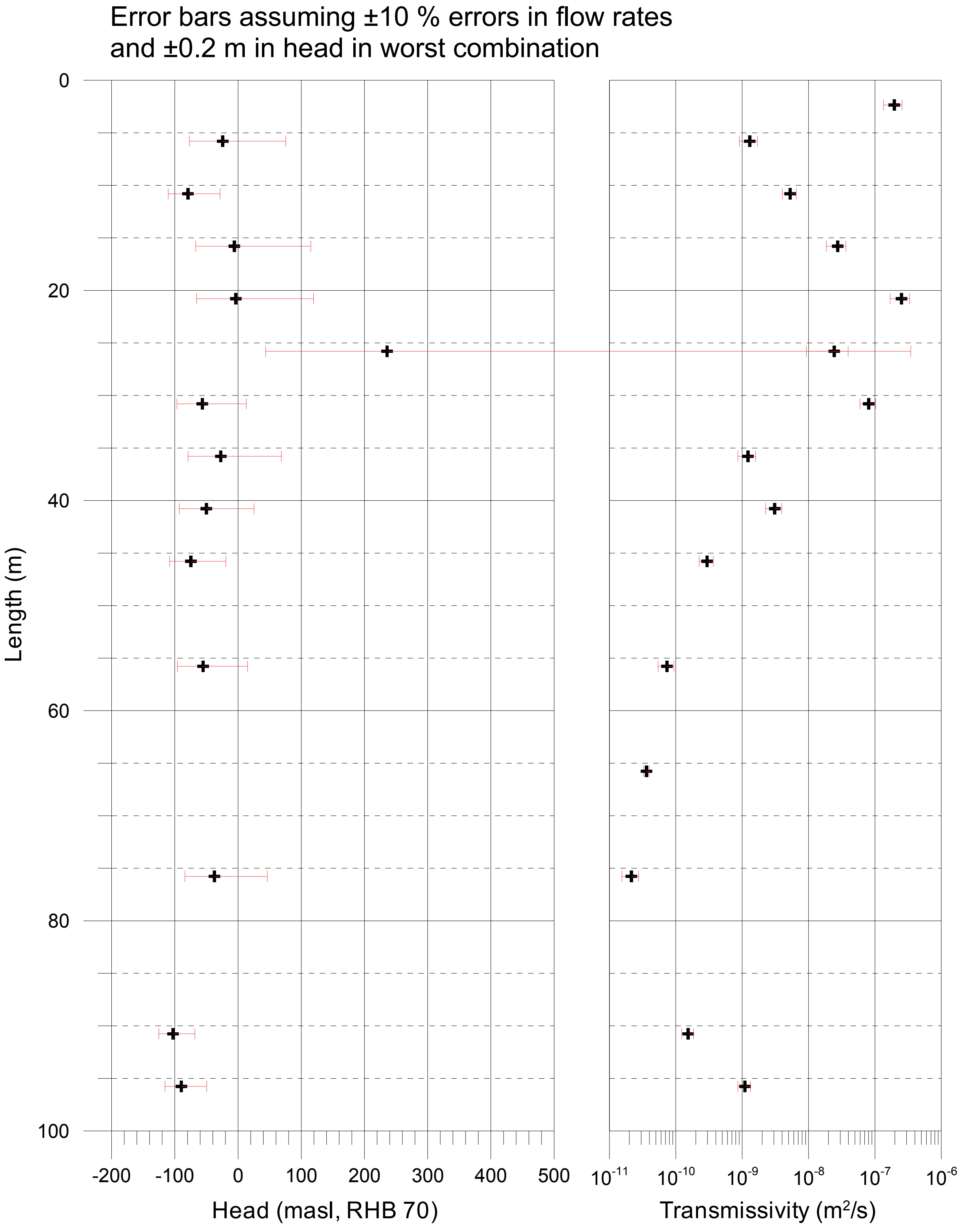

Appendix 9.1

Inferred flow anomalies from overlapping flow logging

Borehole ID	Length to flow anom. L (m)	L_w (m)	dL (m)	Q_0 (m^3/s)	h_{0FW} (masl)	Q_1 (m^3/s)	h_{1FW} (masl)	T_D (m^2/s)	h_i (masl)	Comments
K03009F01	2.5	1	0.1	−6.39E-05	−189.49	−2.94E-05	−359.53	2.0E-07	−504.9	
K03009F01	4.8	1	0.1	9.22E-08	−190.92	2.47E-07	−360.09	9.1E-10	−90.1	
K03009F01	6.2	1	0.1	1.14E-07	−192.60	2.41E-07	−360.00	7.5E-10	−41.4	
K03009F01	7.5	1	0.1	1.56E-08	−193.17	5.14E-08	−360.14	2.1E-10	−120.7	
K03009F01	9.7	1	0.1	4.17E-08	−192.43	7.81E-08	−359.97	2.2E-10	−0.6	
K03009F01	10.4	1	0.1	1.92E-07	−191.51	4.03E-07	−359.93	1.2E-09	−38.6	
K03009F01	12.0	1	0.1	1.47E-07	−192.80	2.44E-07	−359.94	5.7E-10	60.1	
K03009F01	12.8	1	0.1	2.28E-07	−192.47	4.17E-07	−359.99	1.1E-09	9.0	
K03009F01	15.6	1	0.1	6.81E-08	−192.80	1.67E-07	−359.83	5.9E-10	−78.2	
K03009F01	16.2	1	0.1	3.67E-06	−194.87	6.83E-06	−359.93	1.9E-08	−3.8	
K03009F01	17.2	1	0.1	1.47E-06	−194.69	2.89E-06	−359.83	8.5E-09	−24.4	
K03009F01	18.4	1	0.1	5.50E-08	−194.27	1.45E-07	−359.66	5.4E-10	−92.9	
K03009F01	19.0	1	0.1	1.40E-05	−192.88	3.75E-05	−358.72	1.4E-07	−94.1	
K03009F01	19.7	1	0.1	1.81E-05	−193.85	3.44E-05	−359.29	9.8E-08	−10.4	
K03009F01	20.0	1	0.1	1.29E-05	−193.24	3.56E-05	−359.55	1.4E-07	−98.4	
K03009F01	20.2	1	0.1	3.14E-06	−193.68	5.89E-06	−359.73	1.6E-08	−4.2	
K03009F01	22.2	1	0.1	8.17E-08	−192.78	2.03E-07	−359.62	7.2E-10	−80.3	
K03009F01	23.7	1	0.1	7.72E-08	−193.80	1.80E-07	−359.70	6.1E-10	−69.5	
K03009F01	23.9	1	0.1	5.25E-06	−194.38	7.58E-06	−359.77	1.4E-08	177.8	
K03009F01	24.3	1	0.1	1.61E-06	−194.07	3.33E-06	−359.71	1.0E-08	−40.2	
K03009F01	25.1	1	0.1	2.89E-07	−194.01	4.97E-07	−360.09	1.2E-09	36.3	
K03009F01	26.1	1	0.1	3.81E-07	−194.10	6.17E-07	−359.79	1.4E-09	73.0	
K03009F01	28.2	1	0.1	3.00E-06	−194.32	5.94E-06	−359.95	1.8E-08	−25.6	
K03009F01	29.8	1	0.1	5.31E-06	−193.62	8.28E-06	−359.86	1.8E-08	103.1	
K03009F01	30.8	1	0.1	4.28E-06	−193.20	7.97E-06	−359.89	2.2E-08	−0.2	
K03009F01	31.6	1	0.1	1.61E-06	−193.10	3.28E-06	−359.80	9.9E-09	−32.5	
K03009F01	32.5	1	0.1	1.53E-08	−191.75	4.25E-08	−359.84	1.6E-10	−97.4	
K03009F01	33.8	1	0.1	4.83E-08	−192.66	1.13E-07	−359.70	3.9E-10	−68.5	
K03009F01	35.2	1	0.1	4.44E-08	−193.47	1.14E-07	−359.86	4.1E-10	−86.6	
K03009F01	35.7	1	0.1	6.11E-09	−192.18	1.50E-08	−359.61	5.3E-11	−77.1	
K03009F01	37.3	1	0.1	5.97E-08	−193.30	1.54E-07	−359.72	5.6E-10	−88.4	
K03009F01	38.1	1	0.1	4.53E-08	−193.06	1.22E-07	−359.68	4.5E-10	−94.3	
K03009F01	38.9	1	0.1	3.89E-07	−191.43	8.28E-07	−359.51	2.6E-09	−42.5	
K03009F01	41.5	1	0.1	4.17E-09	−193.05	1.11E-08	−359.68	4.1E-11	−93.1	
K03009F01	42.3	1	0.1	5.69E-08	−193.59	1.16E-07	−359.75	3.5E-10	−32.9	
K03009F01	43.3	1	0.1	–	−194.00	3.89E-09	−359.69	2.3E-11	–	*
K03009F01	44.0	1	0.1	4.17E-09	−193.89	1.25E-08	−359.70	5.0E-11	−111.0	
K03009F01	45.4	1	0.1	–	−193.77	3.61E-09	−359.66	2.2E-11	–	*
K03009F01	47.0	1	0.1	5.28E-09	−193.14	1.31E-08	−359.60	4.6E-11	−80.2	*
K03009F01	47.6	1	0.1	2.61E-08	−193.39	5.97E-08	−359.52	2.0E-10	−64.3	
K03009F01	55.7	1	0.1	6.11E-09	−193.07	1.64E-08	−359.44	6.1E-11	−94.2	
K03009F01	57.3	1	0.1	4.17E-09	−194.00	9.72E-09	−359.43	3.3E-11	−69.9	
K03009F01	67.3	1	0.1	–	−191.68	3.89E-09	−359.24	2.3E-11	–	*
K03009F01	77.8	1	0.1	3.33E-09	−189.96	6.67E-09	−358.63	2.0E-11	−21.3	*
K03009F01	92.9	1	0.1	1.36E-08	−186.79	3.92E-08	−358.65	1.5E-10	−95.3	

Appendix 9.2

Inferred flow anomalies from overlapping flow logging

Borehole ID	Length to flow anom. L (m)	L_w (m)	dL (m)	Q_0 (m^3/s)	h_{0FW} (masl)	Q_1 (m^3/s)	h_{1FW} (masl)	T_D (m^2/s)	h_i (masl)	Comments
K03009F01	95.0	1	0.1	7.50E-09	−186.04	2.39E-08	−358.56	9.4E-11	−107.1	
K03009F01	96.8	1	0.1	4.25E-08	−189.32	1.19E-07	−358.65	4.5E-10	−95.1	
K03009F01	97.1	1	0.1	5.64E-08	−189.32	1.77E-07	−358.82	7.0E-10	−109.9	
K03009F01	98.1	1	0.1	3.61E-09	−190.41	1.33E-08	−358.73	5.7E-11	−127.9	

* Uncertain = The flow rate is less than 30 mL/h or the flow anomalies are overlapping or they are unclear because of noise.

Transmissivity and head of detected fractures

Äspö, borehole K03009F01

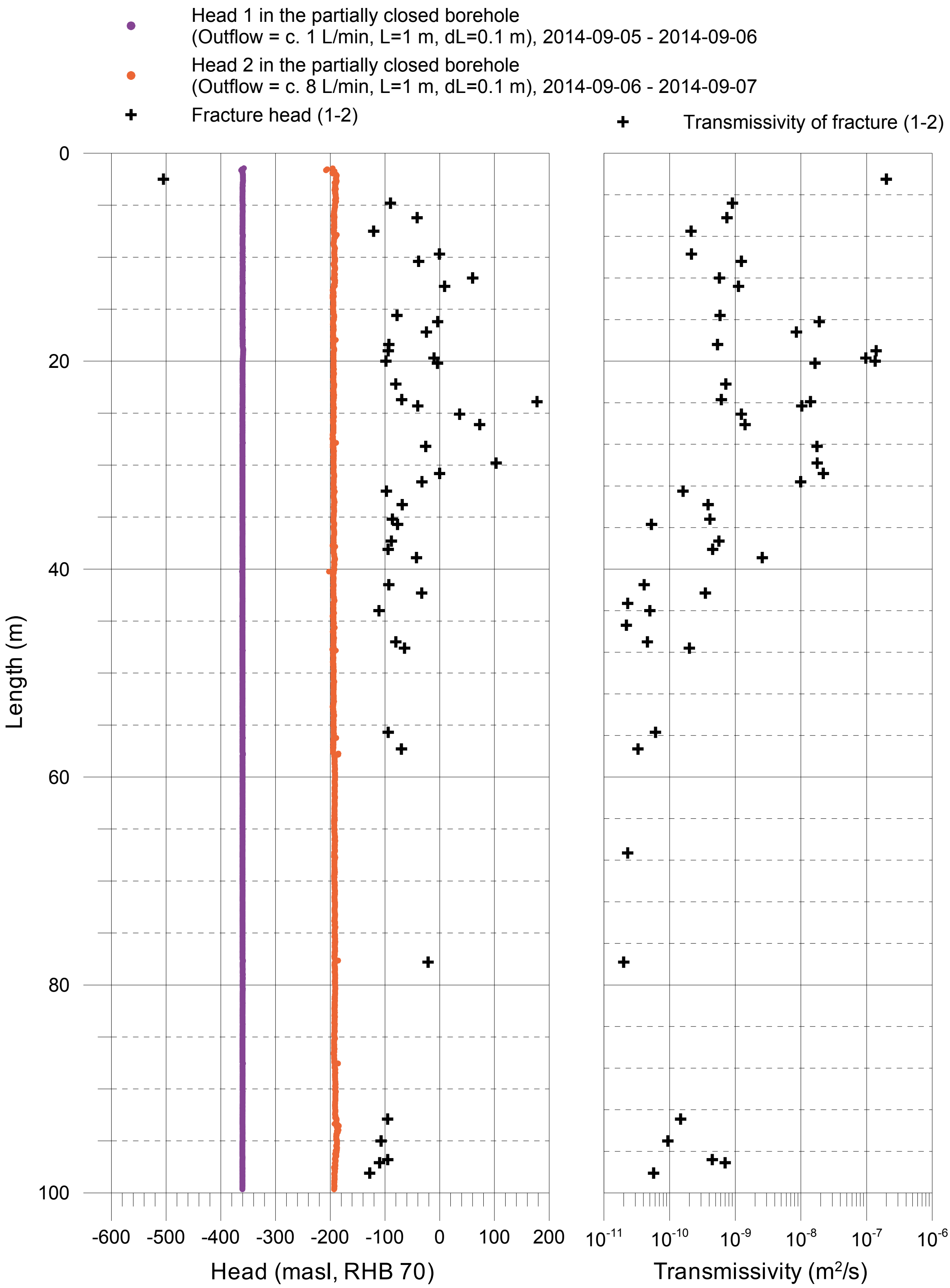

Comparison between section transmissivity and fracture transmissivity

Äspö, borehole K03009F01

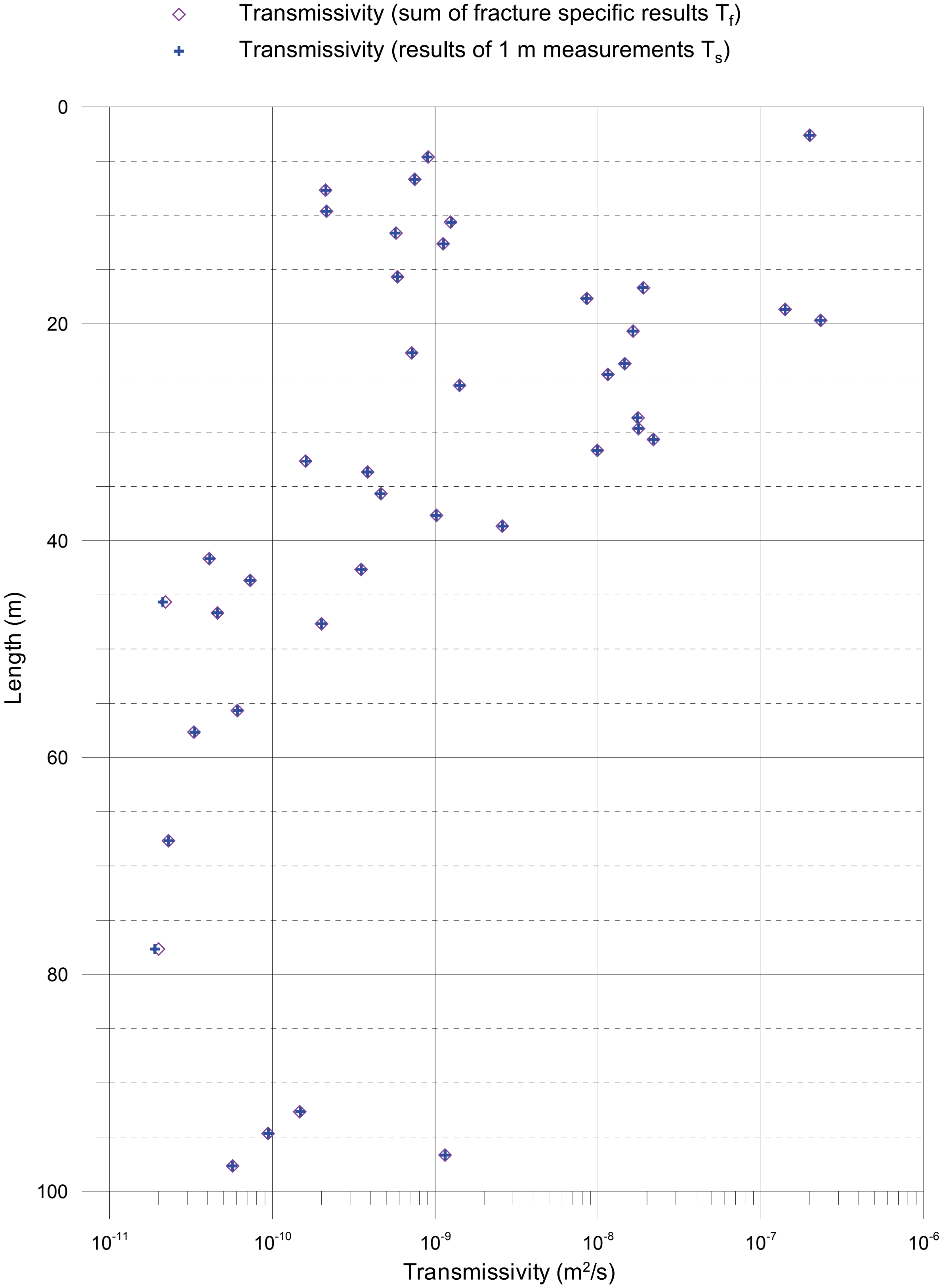

Comparison between section transmissivity and fracture transmissivity

Äspö, borehole K03009F01

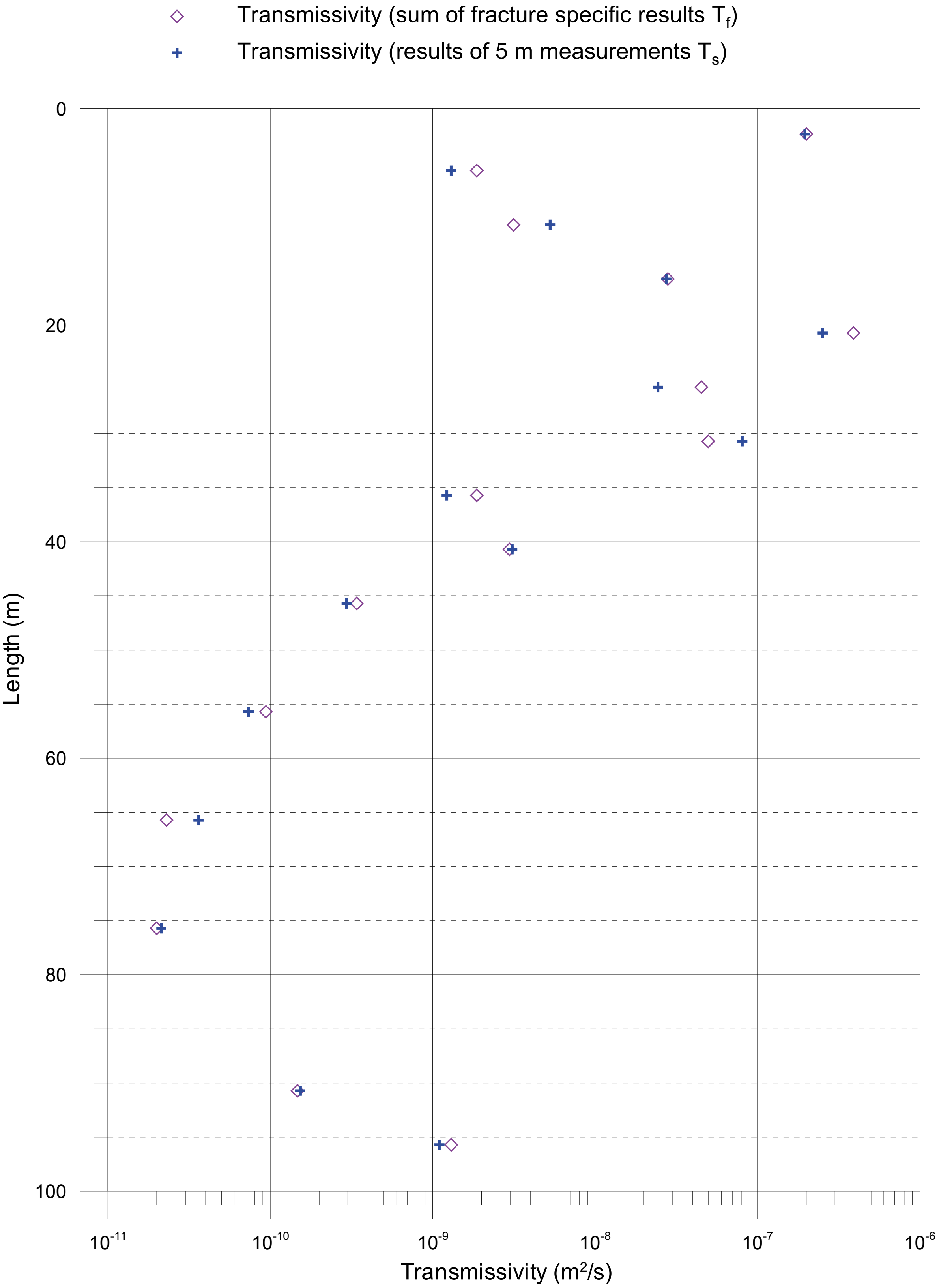

Head in the borehole during flow logging

Äspö, borehole K03009F01

Head(masl)= (Absolute pressure (Pa) - Airpressure (Pa) + Offset) /(1000 kg/m^3 * 9.80665 m/s^2) + Elevation (m)
Offset = 2600 Pa (Correction for absolute pressure sensor)

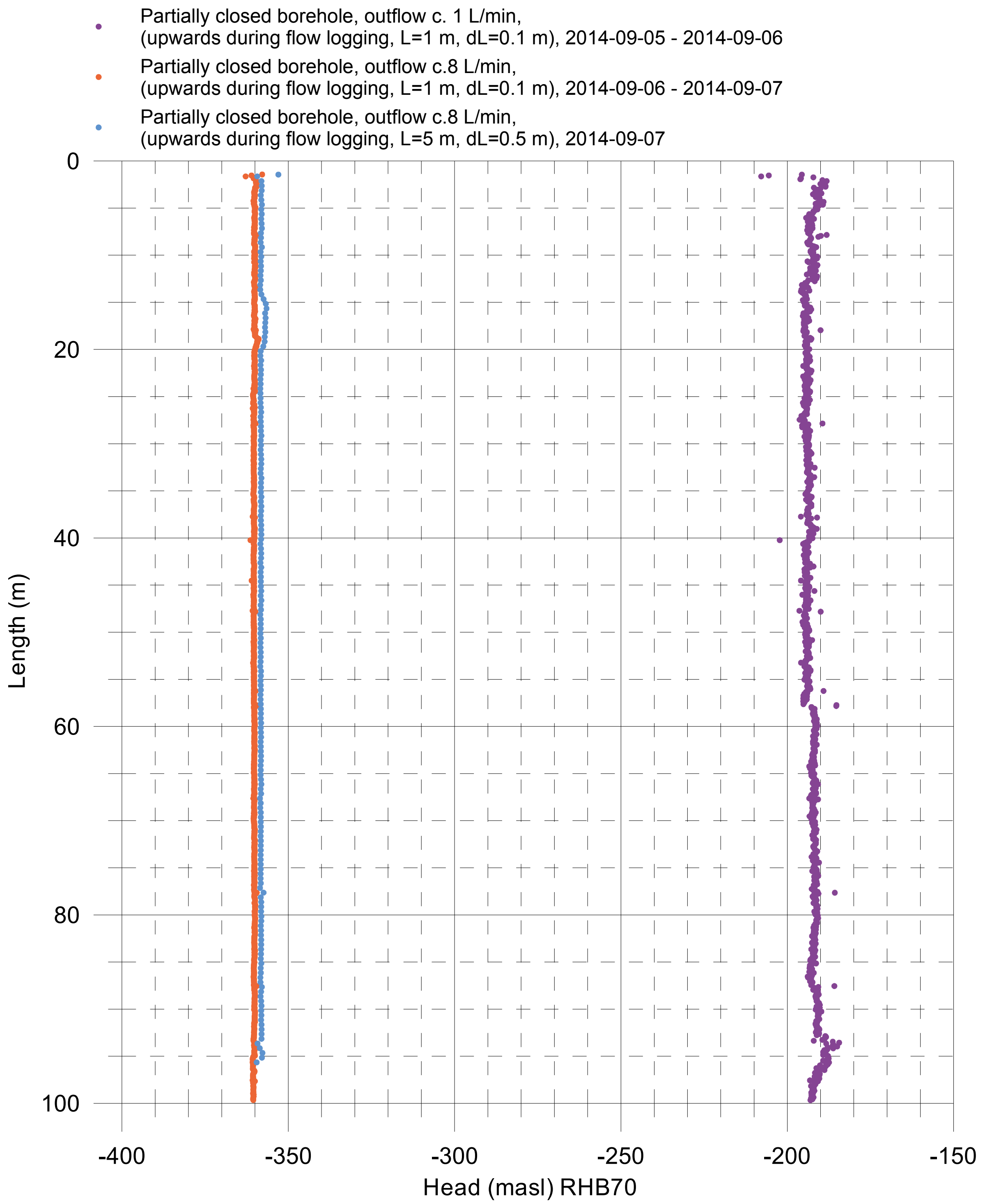

Pressure in the borehole during flow logging

Äspö, borehole K03009F01

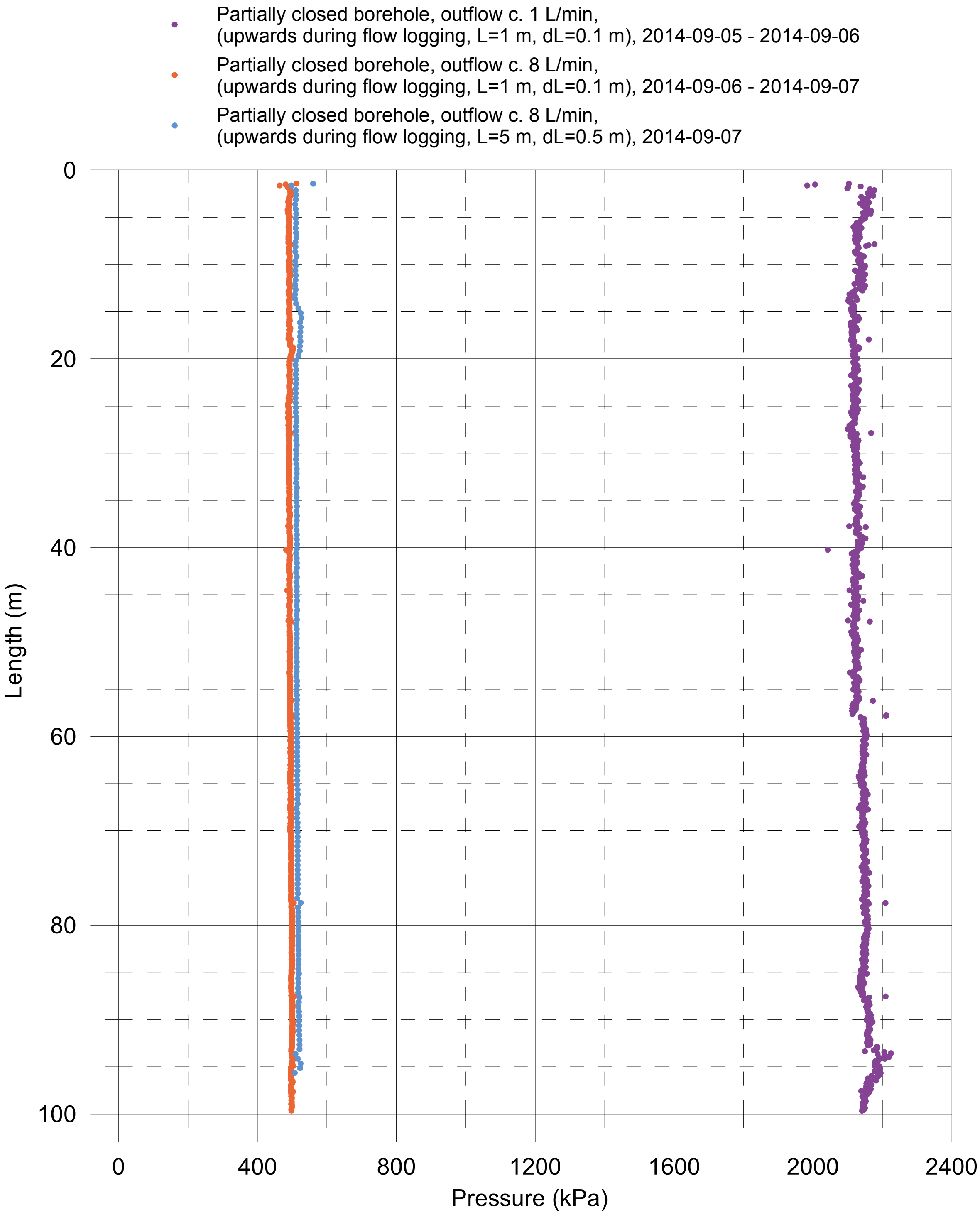

Borehole pressure and outflow from the borehole

Äspö, borehole K03009F01

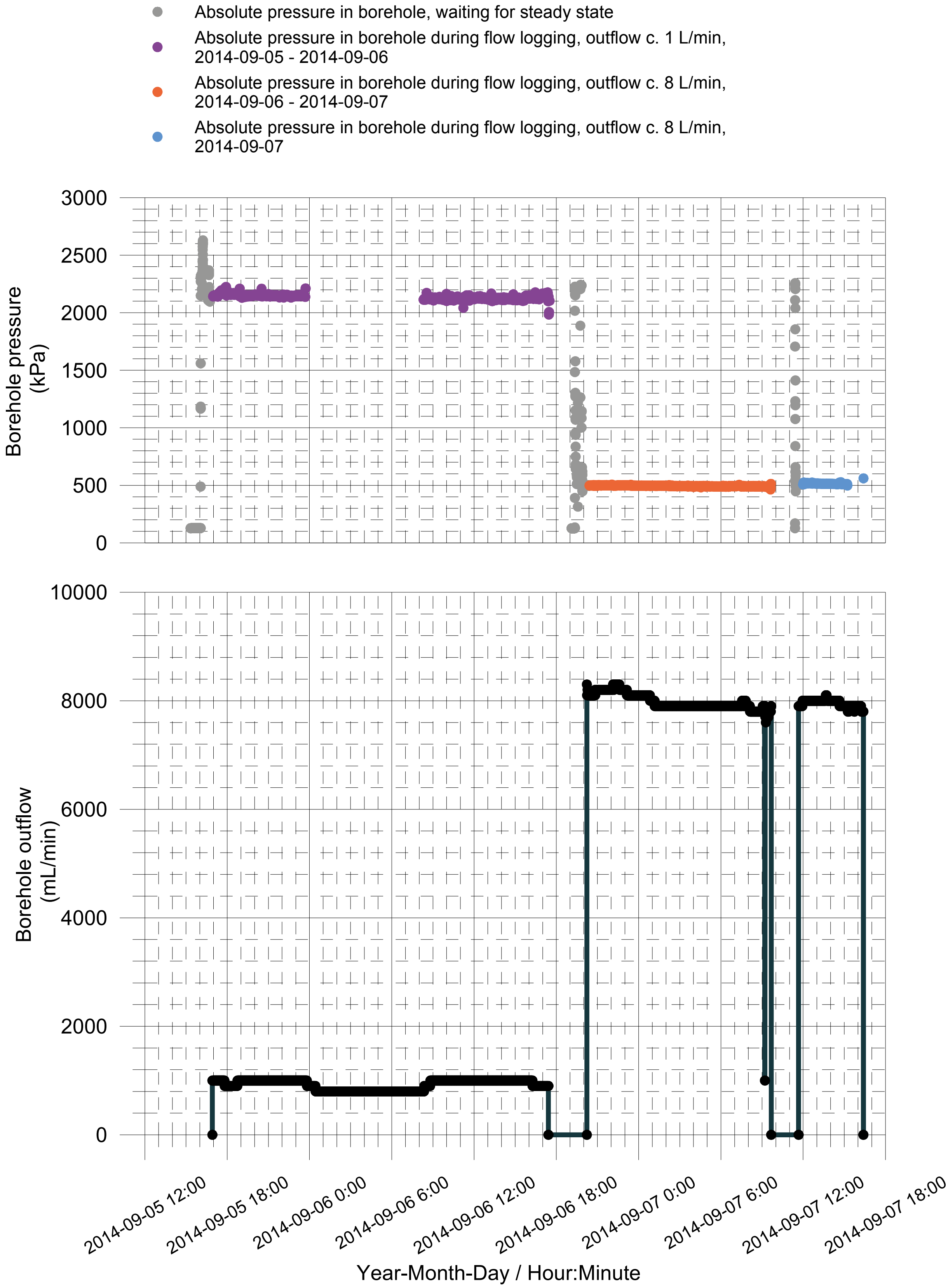

SPR results after length correction

Äspö, borehole K08028F01

SPR during flow 1 from the partially closed borehole
(Outflow = c. 0.25 L/min, L=1 m, dL=0.1 m), 2014-09-03 - 2014-09-04

SPR during flow 2 from the partially closed borehole, lower part of the borehole,
(Outflow = c. 1.2 L/min, L=5 m, dL=0.5 m), 2014-09-04

SPR during flow 3 from the partially closed borehole, lower part of the borehole,
(Outflow = c. 1.2 L/min, L=1 m, dL=0.1 m), 2014-09-04 - 2014-09-05

LateroLog, 2014-08-28

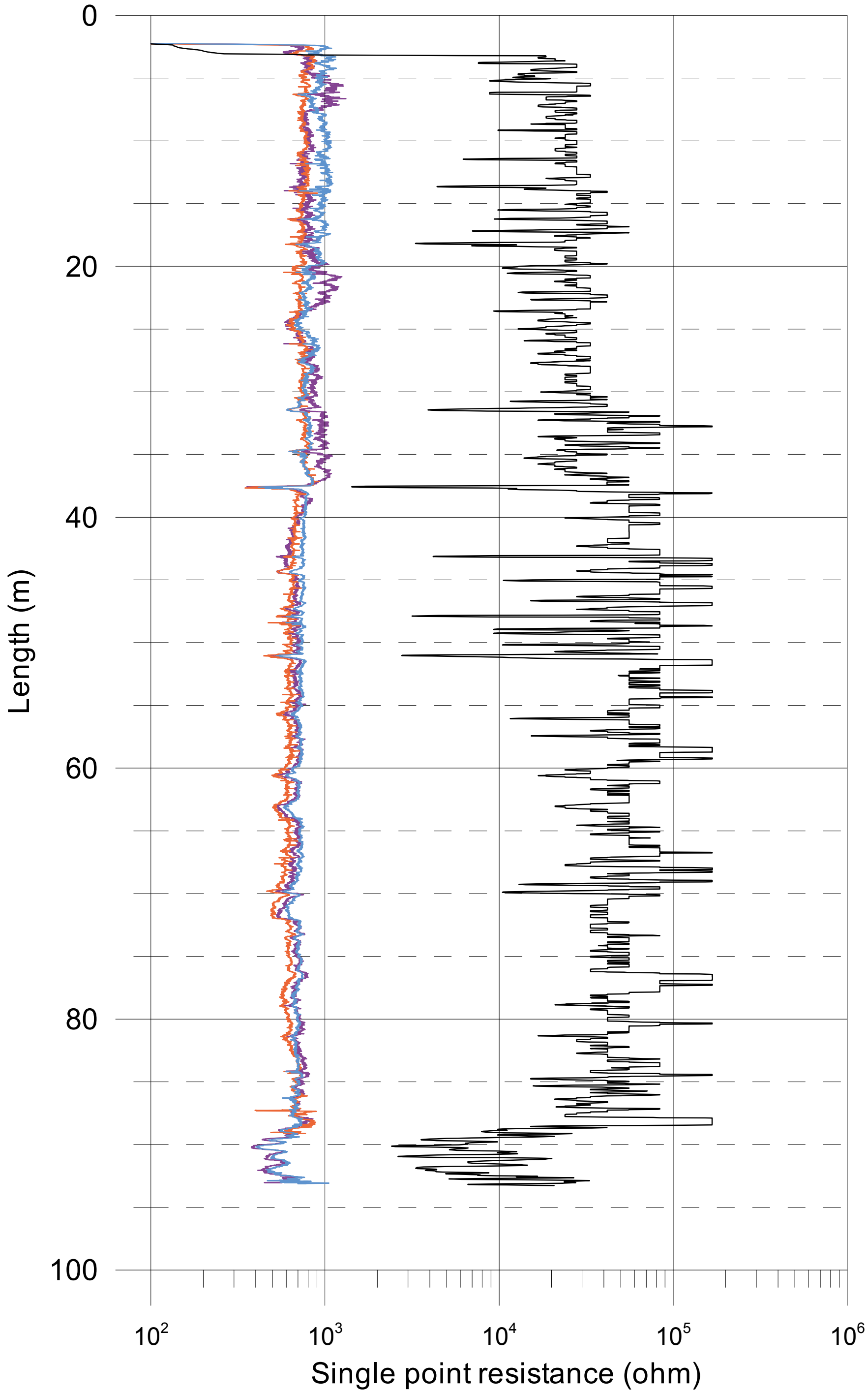

Electrical conductivity of borehole water

Äspö, borehole K08028F01

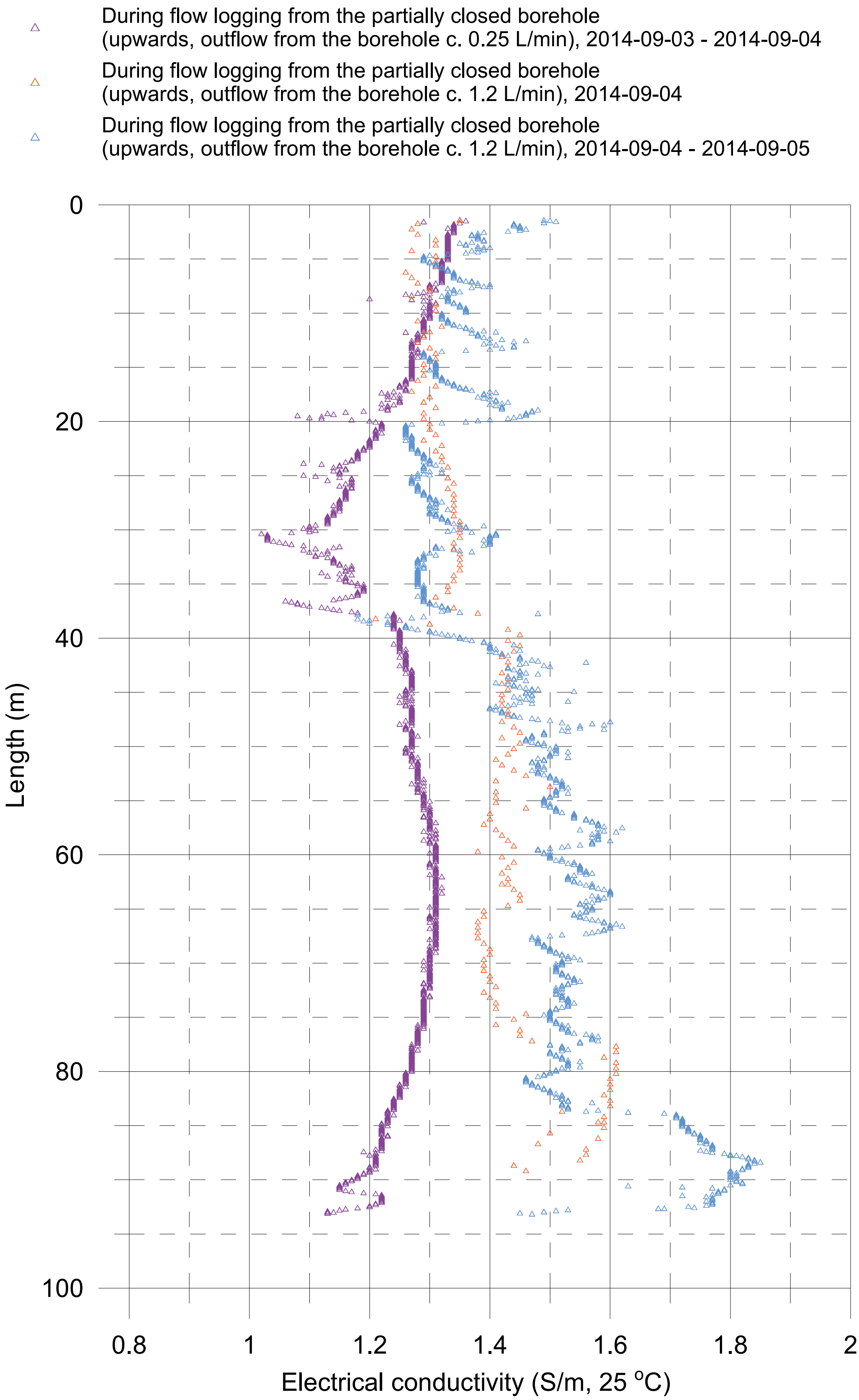

Temperature of borehole water

Äspö, borehole K08028F01

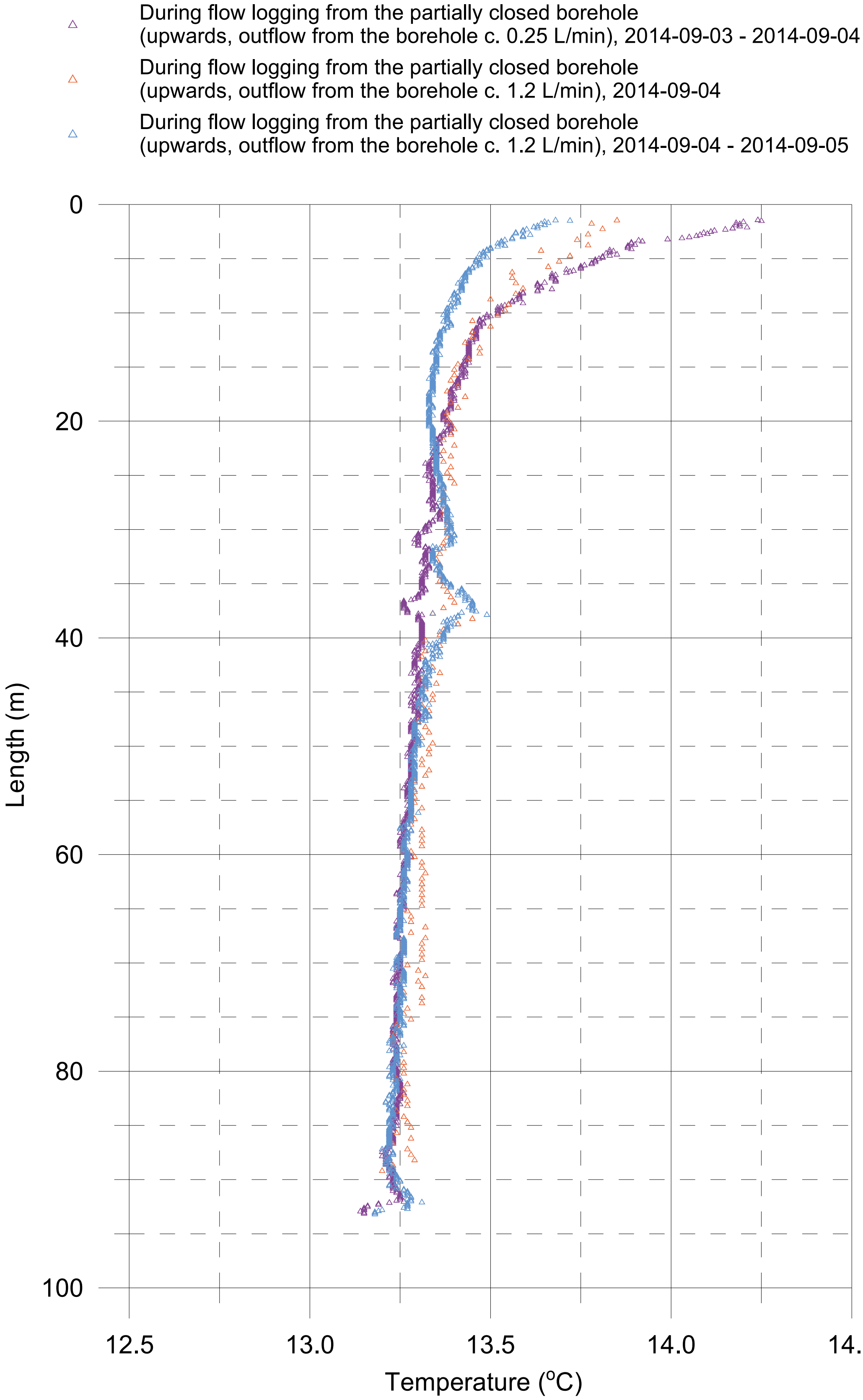

Flow rate and single point resistance

Äspö, borehole K08028F01

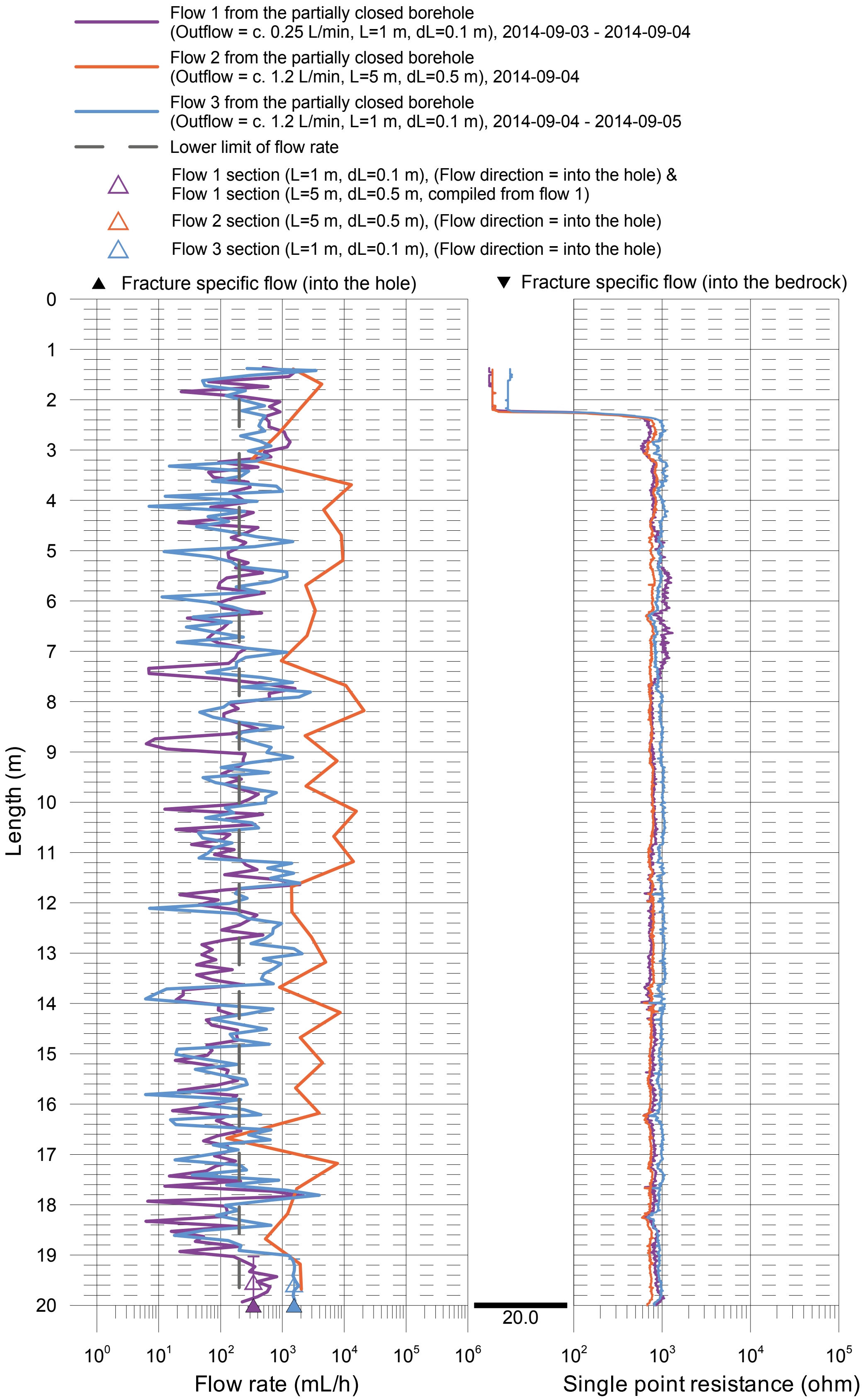

Flow rate and single point resistance

Äspö, borehole K08028F01

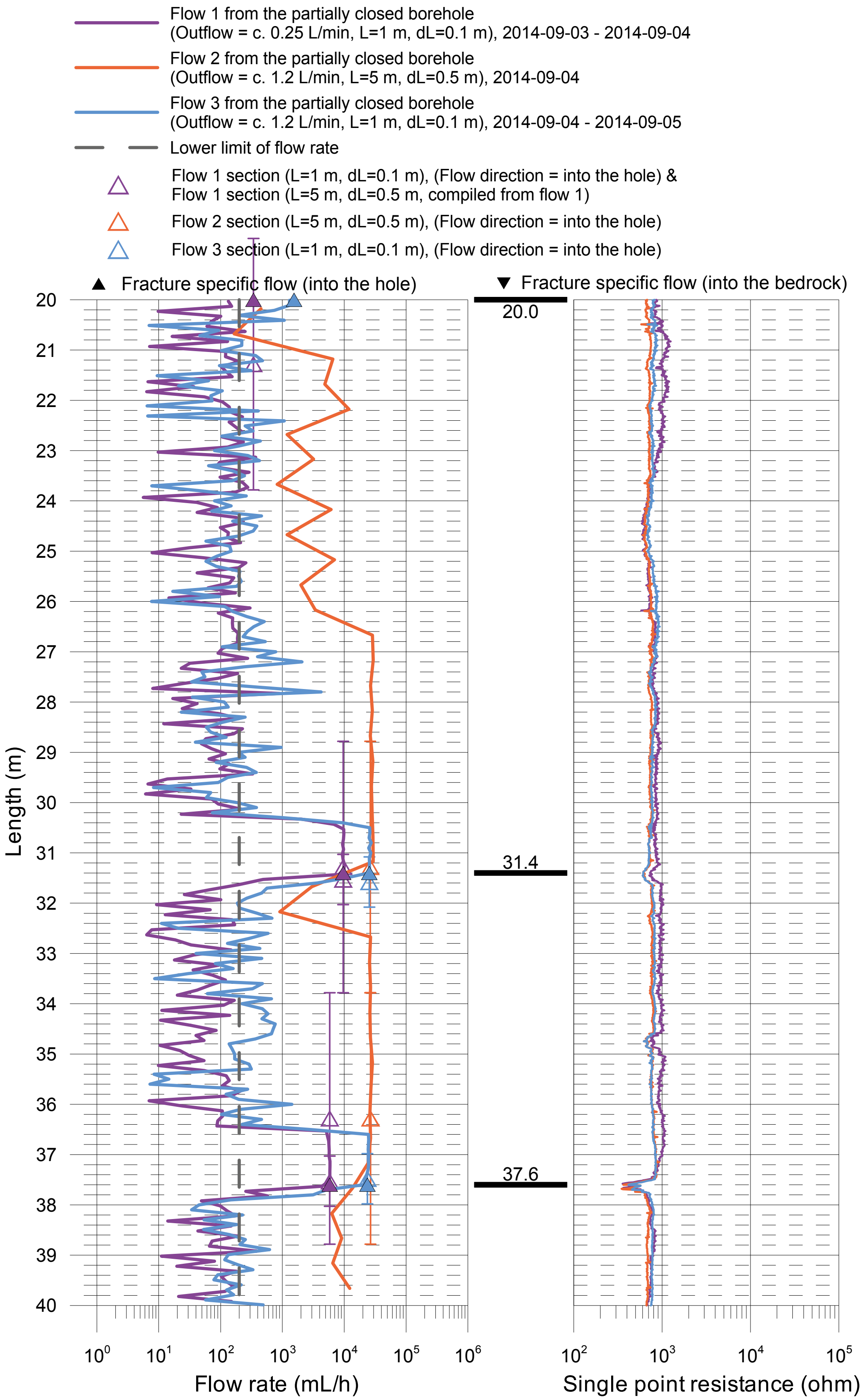

Flow rate and single point resistance

Äspö, borehole K08028F01

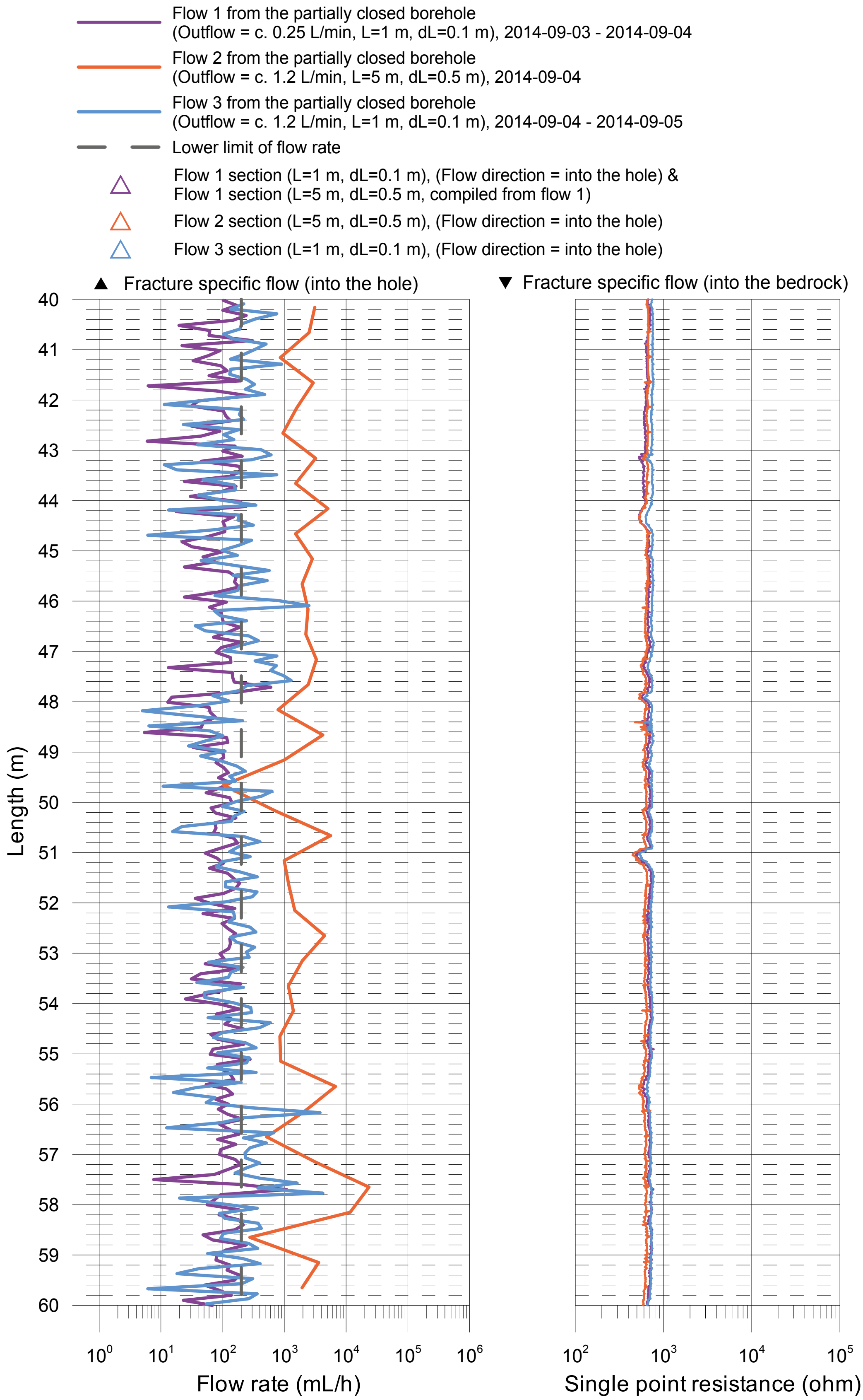

Flow rate and single point resistance

Äspö, borehole K08028F01

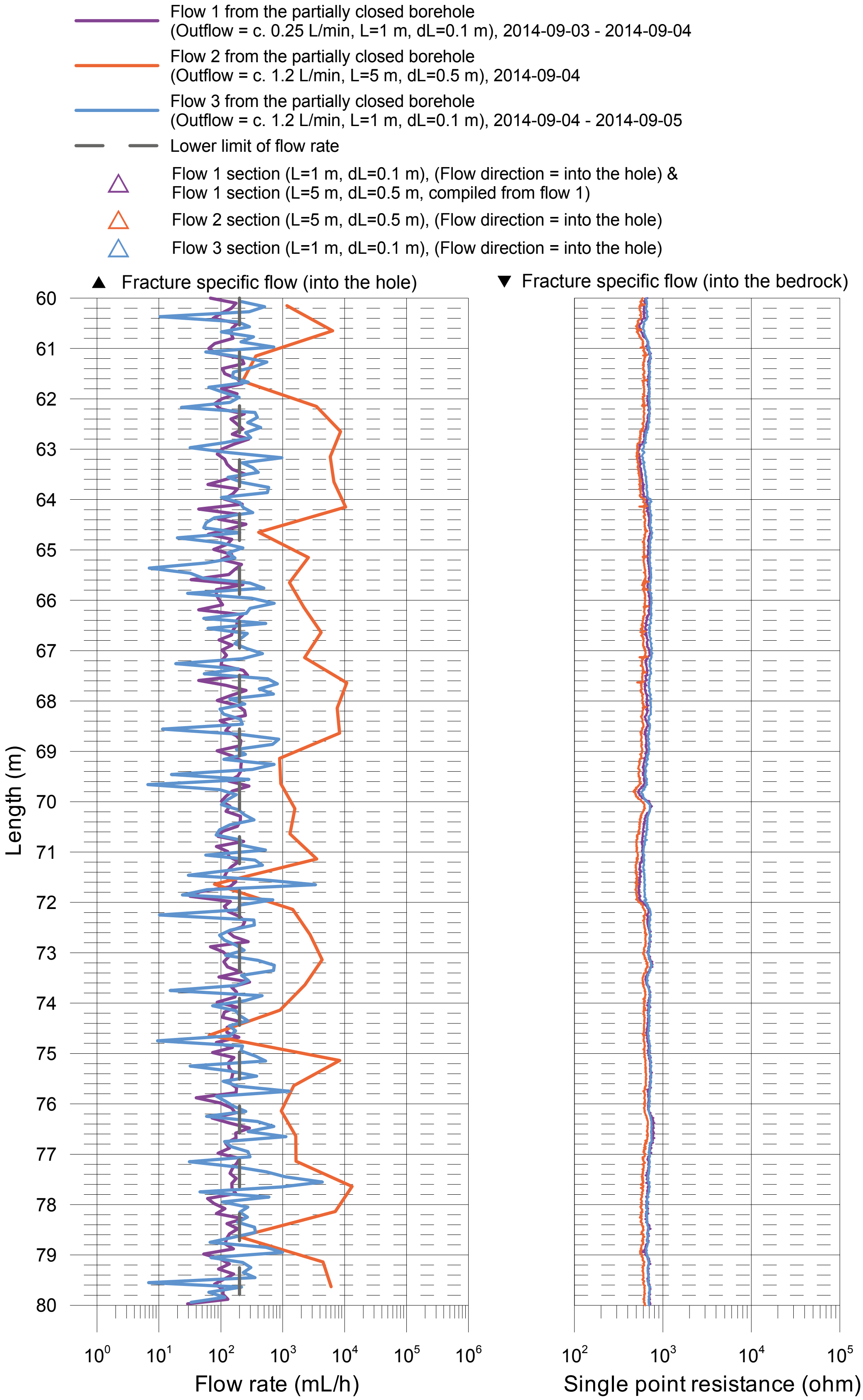

Flow rate and single point resistance

Äspö, borehole K08028F01

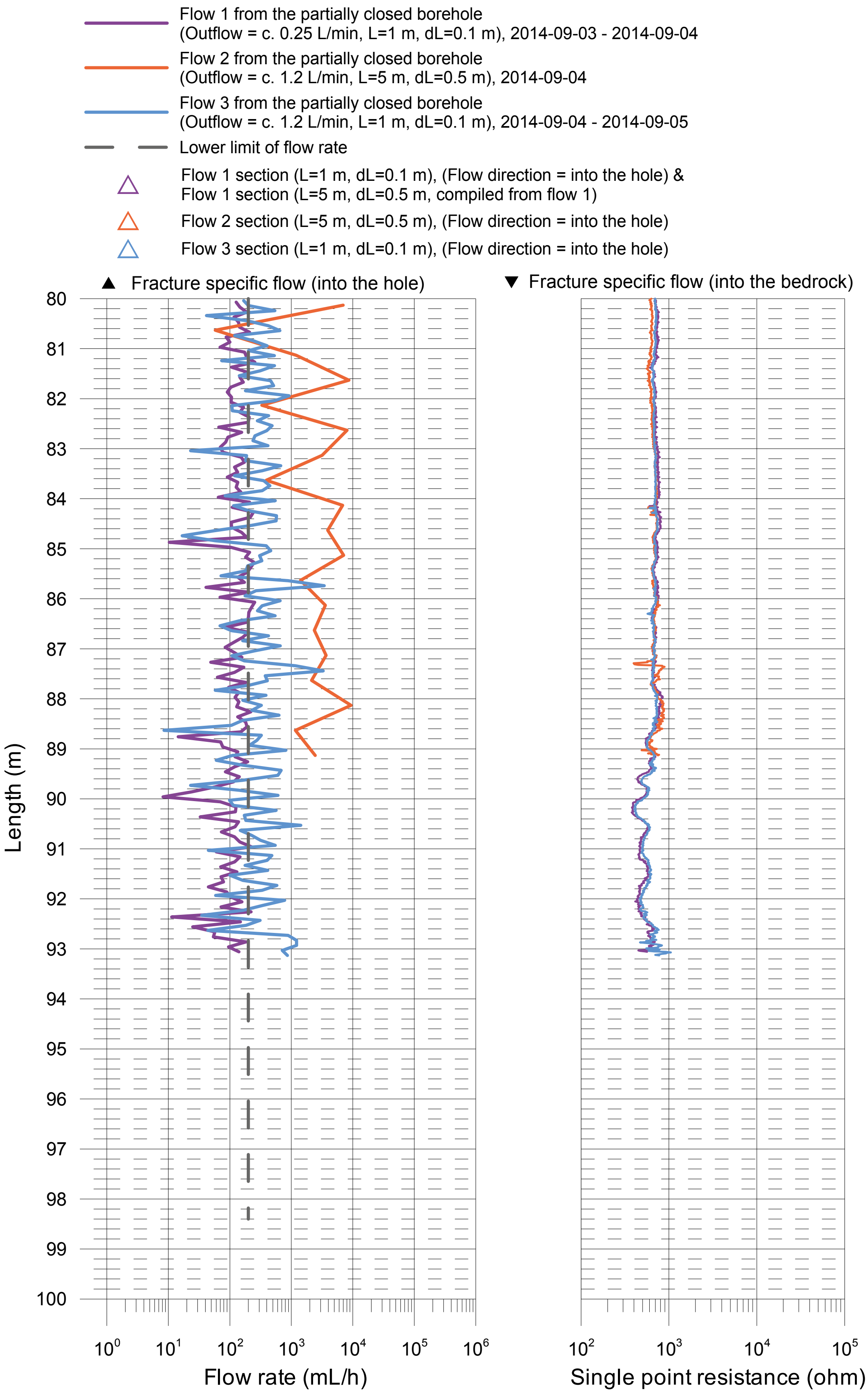

Appendix 16

Explanations for the tables in Appendices 17, 19 and 21

Header	Unit	Explanations
Borehole		ID for borehole.
Secup	m	Length along the borehole for the upper limit of the test section (based on corrected length L).
Seclow	m	Length along the borehole for the lower limit of the test section (based on corrected length L).
L	m	Corrected length along borehole based on SKB procedures for length correction.
Length to flow anom.	m	Length along the borehole to inferred flow anomaly during overlapping flow logging.
Test type (1–6)	(–)	1A: Pumping test – wire-line eq., 1B:Pumping test-submersible pump, 1C: Pumping test-airlift pumping, 2: Interference test, 3: Injection test, 4: Slug test, 5A: Difference flow logging -PFL-DIFF-Sequential, 5B: Difference flow logging -PFL-DIFF-Overlapping, 6: Flow logging-Impeller.
Date of test, start	YY-MM-DD	Date for start of pumping.
Time of test, start	hh:mm	Time for start of pumping.
Date of flowl., start .	YY-MM-DD	Date for start of the flow logging.
Time of flowl., start	hh:mm	Time for start of the flow logging.
Date of test, stop	YY-MM-DD	Date for stop of the test.
Time of test, stop	hh:mm	Time for stop of the test.
L_w	m	Section length used in the difference flow logging.
dL	m	Step length (increment) used in the difference flow logging.
Q_{p1}	m^3/s	Flow rate at surface by the end of the first pumping period of the flow logging.
Q_{p2}	m^3/s	Flow rate at surface by the end of the second pumping period of the flow logging.
t_{p1}	s	Duration of the first pumping period.
t_{p2}	s	Duration of the second pumping period.
t_{F1}	s	Duration of the first recovery period.
t_{F2}	s	Duration of the second recovery period.
h_0	m.a.s.l.	Initial hydraulic head before pumping. Elevation of water level in open borehole in the local co-ordinates system with z=0 m.
h_1	m.a.s.l.	Stabilized hydraulic head during the first pumping period. Elevation of water level in open borehole in the local co-ordinates system with z=0 m.
h_2	m.a.s.l.	Stabilized hydraulic head during the second pumping period. Elevation of water level in open borehole in the local co-ordinates system with z=0 m.
s_1	m	Drawdown of the water level in the borehole during first pumping period. Difference between the actual hydraulic head and the initial head (s1= h1−h0).
s_2	m	Drawdown of the water level in the borehole during second pumping period. Difference between the actual hydraulic head and the initial head (s2=h2−h0).
T	m^2/s	Transmissivity of the entire borehole.
Q_0	m^3/s	Measured flow rate through the test section or flow anomaly under natural conditions (no pumping) with h=h0 in the open borehole.

Header	Unit	Explanations
Q_1	m^3/s	Measured flow rate through the test section or flow anomaly during the first pumping period.
Q_2	m^3/s	Measured flow rate through the test section or flow anomaly during the second pumping period.
h_{0FW}	m.a.s.l.	Corrected initial hydraulic head along the hole due to e.g. varying salinity conditions of the borehole fluid before pumping.
h_{1FW}	m.a.s.l.	Corrected hydraulic head along the hole due to e.g. varying salinity conditions of the borehole fluid during the first pumping period.
h_{2FW}	m.a.s.l.	Corrected hydraulic head along the hole due to e.g. varying salinity conditions of the borehole fluid during the second pumping period.
EC_w	S/m	Measured electrical conductivity of the borehole fluid in the test section during difference flow logging.
Te_w	°C	Measured borehole fluid temperature in the test section during difference flow logging.
EC_f	S/m	Measured fracture-specific electrical conductivity of the fluid in flow anomaly during difference flow logging.
Te_f	°C	Measured fracture-specific fluid temperature in flow anomaly during difference flow logging.
T_D	m^2/s	Transmissivity of section or flow anomaly based on 2D model for evaluation of formation properties of the test section based on PFL-DIFF.
T-$measl_{LT}$	m^2/s	Estimated theoretical lower measurement limit for evaluated TD. If the estimated TD equals TD-measlim, the actual TD is considered to be equal or less than TD-measlim.
T-$measl_{LP}$	m^2/s	Estimated practical lower measurement limit for evaluated TD. If the estimated TD equals TD-measlim, the actual TD is considered to be equal or less than TD-measlim.
T-$meas_{lU}$	m^2/s	Estimated upper measurement limit for evaluated TD. If the estimated TD equals TD-measlim, the actual TD is considered to be equal or less than TD-measlim.
h_i	m.a.s.l.	Calculated relative, natural freshwater head for test section or flow anomaly (undisturbed conditions).
Q-lower limit P	mL/h	Practical minimum for measurable flow.

Results of sequential flow logging

Borehole ID	Secup L(m)	Seclow L(m)	L_w (m)	Q_0 (m^3/s)	h_{0FW} (masl)	Q_1 (m^3/s)	h_{1FW} (masl)	T_D (m^2/s)	h_i (masl)	Q-lower limit P (mL/h)	TD-measl$_{LT}$ (m^2/s)	TD- measl$_{LP}$ (m^2/s)	TD- measl$_U$ (m^2/s)	Comments
K08028F01	2.07	3.07	1	–	−144.53	–	−347.13	–	–	200	4.1E-11	2.7E-10	4.1E-07	
K08028F01	3.07	4.07	1	–	−156.81	–	−347.86	–	–	200	4.3E-11	2.9E-10	4.3E-07	
K08028F01	4.02	5.02	1	–	−153.16	–	−348.52	–	–	200	4.2E-11	2.8E-10	4.2E-07	
K08028F01	5.07	6.07	1	–	−165.42	–	−348.59	–	–	200	4.5E-11	3.0E-10	4.5E-07	
K08028F01	6.07	7.07	1	–	−163.81	–	−348.69	–	–	200	4.5E-11	3.0E-10	4.5E-07	
K08028F01	7.07	8.07	1	–	−155.83	–	−348.32	–	–	200	4.3E-11	2.9E-10	4.3E-07	
K08028F01	8.07	9.07	1	–	−166.85	–	−349.28	–	–	200	4.5E-11	3.0E-10	4.5E-07	
K08028F01	9.07	10.07	1	–	−162.88	–	−350.21	–	–	200	4.4E-11	2.9E-10	4.4E-07	
K08028F01	10.07	11.07	1	–	−167.71	–	−350.21	–	–	200	4.5E-11	3.0E-10	4.5E-07	
K08028F01	11.07	12.07	1	–	−171.85	–	−351.26	–	–	200	4.6E-11	3.1E-10	4.6E-07	
K08028F01	12.07	13.07	1	–	−159.27	–	−349.91	–	–	200	4.3E-11	2.9E-10	4.3E-07	
K08028F01	13.06	14.06	1	–	−153.08	–	−350.36	–	–	200	4.2E-11	2.8E-10	4.2E-07	
K08028F01	14.06	15.06	1	–	−154.15	–	−350.55	–	–	200	4.2E-11	2.8E-10	4.2E-07	
K08028F01	15.06	16.06	1	–	−154.91	–	−350.42	–	–	200	4.2E-11	2.8E-10	4.2E-07	
K08028F01	16.06	17.06	1	–	−154.87	–	−350.27	–	–	200	4.2E-11	2.8E-10	4.2E-07	
K08028F01	17.06	18.06	1	–	−151.61	–	−351.48	–	–	200	4.1E-11	2.8E-10	4.1E-07	
K08028F01	18.06	19.06	1	–	−153.09	–	−350.60	–	–	200	4.2E-11	2.8E-10	4.2E-07	
K08028F01	19.06	20.06	1	9.47E-08	−149.96	4.31E-07	−350.18	1.7E-09	−93.5	200	4.1E-11	2.7E-10	4.1E-07	
K08028F01	20.06	21.06	1	–	−148.78	–	−350.44	–	–	200	4.1E-11	2.7E-10	4.1E-07	
K08028F01	21.06	22.06	1	–	−151.96	–	−350.56	–	–	200	4.2E-11	2.8E-10	4.2E-07	
K08028F01	22.06	23.06	1	–	−150.90	–	−350.44	–	–	200	4.1E-11	2.8E-10	4.1E-07	
K08028F01	23.06	24.06	1	–	−152.36	–	−350.77	–	–	200	4.2E-11	2.8E-10	4.2E-07	
K08028F01	24.06	25.06	1	–	−151.78	–	−351.01	–	–	200	4.1E-11	2.8E-10	4.1E-07	
K08028F01	25.06	26.06	1	–	−147.27	–	−350.63	–	–	200	4.1E-11	2.7E-10	4.1E-07	
K08028F01	26.06	27.06	1	–	−145.89	–	−350.75	–	–	200	4.0E-11	2.7E-10	4.0E-07	
K08028F01	27.06	28.06	1	–	−145.89	–	−351.57	–	–	200	4.0E-11	2.7E-10	4.0E-07	
K08028F01	28.06	29.06	1	–	−140.50	–	−351.18	–	–	200	3.9E-11	2.6E-10	3.9E-07	

Appendix 17.2

Results of sequential flow logging

Borehole ID	Secup L(m)	Seclow L(m)	L_w (m)	Q_0 (m^3/s)	h_{0FW} (masl)	Q_1 (m^3/s)	h_{1FW} (masl)	T_D (m^2/s)	h_i (masl)	Q-lower limit P (mL/h)	TD-measl$_{LT}$ (m^2/s)	TD-measl$_{LP}$ (m^2/s)	TD-measl$_U$ (m^2/s)	Comments
K08028F01	29.06	30.06	1	–	−146.39	–	−351.44	–	–	200	4.0E-11	2.7E-10	4.0E-07	
K08028F01	30.06	31.06	1	–	−141.71	–	−350.91	–	–	200	3.9E-11	2.6E-10	3.9E-07	
K08028F01	31.06	32.06	1	2.68E-06	−141.02	7.08E-06	−351.24	2.1E-08	−13.2	200	3.9E-11	2.6E-10	3.8E-07	
K08028F01	32.00	33.00	1	–	−142.91	–	−351.53	–	–	200	4.0E-11	2.6E-10	4.0E-07	
K08028F01	33.00	34.00	1	–	−137.83	–	−351.33	–	–	200	3.9E-11	2.6E-10	3.9E-07	
K08028F01	34.00	35.00	1	–	−139.38	–	−351.55	–	–	200	3.9E-11	2.6E-10	3.9E-07	
K08028F01	35.00	36.00	1	–	−137.08	–	−351.01	–	–	200	3.9E-11	2.6E-10	3.9E-07	
K08028F01	36.00	37.00	1	–	−137.60	–	−351.27	–	–	200	3.9E-11	2.6E-10	3.9E-07	
K08028F01	37.00	38.00	1	1.62E-06	−141.10	6.58E-06	−352.05	2.3E-08	−72.1	200	3.9E-11	2.6E-10	3.8E-07	
K08028F01	38.04	39.04	1	–	−136.30	–	−350.66	–	–	200	3.8E-11	2.6E-10	3.8E-07	
K08028F01	39.04	40.04	1	–	−134.43	–	−350.89	–	–	200	3.8E-11	2.5E-10	3.8E-07	
K08028F01	40.04	41.04	1	–	−142.52	–	−351.63	–	–	200	3.9E-11	2.6E-10	3.9E-07	
K08028F01	41.05	42.05	1	–	−140.86	–	−351.73	–	–	200	3.9E-11	2.6E-10	3.9E-07	
K08028F01	42.05	43.05	1	–	−141.19	–	−351.84	–	–	200	3.9E-11	2.6E-10	3.9E-07	
K08028F01	43.05	44.05	1	–	−144.02	–	−352.38	–	–	200	4.0E-11	2.6E-10	4.0E-07	
K08028F01	44.05	45.05	1	–	−140.55	–	−352.18	–	–	200	3.9E-11	2.6E-10	3.9E-07	
K08028F01	45.05	46.05	1	–	−138.92	–	−352.22	–	–	200	3.9E-11	2.6E-10	3.9E-07	
K08028F01	46.05	47.05	1	–	−140.79	–	−351.45	–	–	200	3.9E-11	2.6E-10	3.9E-07	
K08028F01	47.05	48.05	1	–	−143.23	–	−353.48	–	–	200	3.9E-11	2.6E-10	3.9E-07	
K08028F01	47.99	48.99	1	–	−141.95	–	−352.90	–	–	200	3.9E-11	2.6E-10	3.9E-07	
K08028F01	48.99	49.99	1	–	−142.78	–	−352.93	–	–	200	3.9E-11	2.6E-10	3.9E-07	
K08028F01	49.99	50.99	1	–	−142.09	–	−353.21	–	–	200	3.9E-11	2.6E-10	3.9E-07	
K08028F01	50.99	51.99	1	–	−139.78	–	−353.05	–	–	200	3.9E-11	2.6E-10	3.9E-07	
K08028F01	51.99	52.99	1	–	−140.85	–	−353.09	–	–	200	3.9E-11	2.6E-10	3.9E-07	
K08028F01	52.99	53.99	1	–	−142.41	–	−353.28	–	–	200	3.9E-11	2.6E-10	3.9E-07	
K08028F01	53.99	54.99	1	–	−141.35	–	−353.18	–	–	200	3.9E-11	2.6E-10	3.9E-07	
K08028F01	54.99	55.99	1	–	−141.62	–	−352.96	–	–	200	3.9E-11	2.6E-10	3.9E-07	

Appendix 17.3

Results of sequential flow logging

Borehole ID	Secup L(m)	Seclow L(m)	L_w (m)	Q_0 (m^3/s)	h_{0FW} (masl)	Q_1 (m^3/s)	h_{1FW} (masl)	T_D (m^2/s)	h_i (masl)	Q-lower limit P (mL/h)	TD-measl$_{LT}$ (m^2/s)	TD- measl$_{LP}$ (m^2/s)	TD- measl$_U$ (m^2/s)	Comments
K08028F01	55.99	56.99	1	–	−141.53	–	−353.13	–	–	200	3.9E-11	2.6E-10	3.9E-07	
K08028F01	56.99	57.99	1	–	−140.38	–	−353.32	–	–	200	3.9E-11	2.6E-10	3.9E-07	
K08028F01	57.99	58.99	1	–	−142.64	–	−353.03	–	–	200	3.9E-11	2.6E-10	3.9E-07	
K08028F01	58.99	59.99	1	–	−140.42	–	−352.79	–	–	200	3.9E-11	2.6E-10	3.9E-07	
K08028F01	59.99	60.99	1	–	−138.59	–	−352.92	–	–	200	3.8E-11	2.6E-10	3.8E-07	
K08028F01	60.99	61.99	1	–	−140.90	–	−353.48	–	–	200	3.9E-11	2.6E-10	3.9E-07	
K08028F01	61.99	62.99	1	–	−140.33	–	−353.38	–	–	200	3.9E-11	2.6E-10	3.9E-07	
K08028F01	62.98	63.98	1	–	−142.36	–	−353.93	–	–	200	3.9E-11	2.6E-10	3.9E-07	
K08028F01	63.98	64.98	1	–	−142.35	–	−354.09	–	–	200	3.9E-11	2.6E-10	3.9E-07	
K08028F01	64.98	65.98	1	–	−141.19	–	−353.13	–	–	200	3.9E-11	2.6E-10	3.9E-07	
K08028F01	65.98	66.98	1	–	−139.03	–	−353.57	–	–	200	3.8E-11	2.6E-10	3.8E-07	
K08028F01	66.98	67.98	1	–	−140.28	–	−353.49	–	–	200	3.9E-11	2.6E-10	3.9E-07	
K08028F01	67.98	68.98	1	–	−140.29	–	−353.38	–	–	200	3.9E-11	2.6E-10	3.9E-07	
K08028F01	68.98	69.98	1	–	−140.41	–	−353.93	–	–	200	3.9E-11	2.6E-10	3.9E-07	
K08028F01	69.98	70.98	1	–	−139.61	–	−353.18	–	–	200	3.9E-11	2.6E-10	3.9E-07	
K08028F01	70.98	71.98	1	–	−139.41	–	−352.85	–	–	200	3.9E-11	2.6E-10	3.9E-07	
K08028F01	71.97	72.97	1	–	−137.95	–	−354.77	–	–	200	3.8E-11	2.5E-10	3.8E-07	
K08028F01	72.97	73.97	1	–	−135.61	–	−354.93	–	–	200	3.8E-11	2.5E-10	3.8E-07	
K08028F01	73.97	74.97	1	–	−136.86	–	−354.65	–	–	200	3.8E-11	2.5E-10	3.8E-07	
K08028F01	74.97	75.97	1	–	−136.12	–	−354.31	–	–	200	3.8E-11	2.5E-10	3.8E-07	
K08028F01	75.97	76.97	1	–	−134.57	–	−354.58	–	–	200	3.7E-11	2.5E-10	3.7E-07	
K08028F01	76.97	77.97	1	–	−134.39	–	−353.69	–	–	200	3.8E-11	2.5E-10	3.8E-07	
K08028F01	77.97	78.97	1	–	−134.29	–	−354.77	–	–	200	3.7E-11	2.5E-10	3.7E-07	
K08028F01	78.97	79.97	1	–	−133.33	–	−355.06	–	–	200	3.7E-11	2.5E-10	3.7E-07	
K08028F01	79.96	80.96	1	–	−132.89	–	−354.16	–	–	200	3.7E-11	2.5E-10	3.7E-07	
K08028F01	80.96	81.96	1	–	−134.90	–	−354.08	–	–	200	3.8E-11	2.5E-10	3.8E-07	
K08028F01	81.97	82.97	1	–	−135.03	–	−354.62	–	–	200	3.8E-11	2.5E-10	3.8E-07	

Appendix 17.4

Results of sequential flow logging

Borehole ID	Secup L(m)	Seclow L(m)	L_w (m)	Q_0 (m^3/s)	h_{0FW} (masl)	Q_1 (m^3/s)	h_{1FW} (masl)	T_D (m^2/s)	h_i (masl)	Q-lower limit P (mL/h)	TD-measl$_{LT}$ (m^2/s)	TD- measl$_{LP}$ (m^2/s)	TD- measl$_U$ (m^2/s)	Comments
K08028F01	82.97	83.97	1	–	-135.05	–	-354.64	–	–	200	3.8E-11	2.5E-10	3.8E-07	
K08028F01	83.97	84.97	1	–	-136.21	–	-354.82	–	–	200	3.8E-11	2.5E-10	3.8E-07	
K08028F01	84.97	85.97	1	–	-137.60	–	-354.68	–	–	200	3.8E-11	2.5E-10	3.8E-07	
K08028F01	85.97	86.97	1	–	-137.52	–	-356.66	–	–	200	3.8E-11	2.5E-10	3.8E-07	
K08028F01	86.97	87.97	1	–	-125.20	–	-355.18	–	–	200	3.6E-11	2.4E-10	3.6E-07	
K08028F01	87.96	88.96	1	–	-132.02	–	-356.26	–	–	200	3.7E-11	2.5E-10	3.7E-07	
K08028F01	88.96	89.96	1	–	-131.86	–	-354.88	–	–	200	3.7E-11	2.5E-10	3.7E-07	
K08028F01	89.96	90.96	1	–	-132.11	–	-354.97	–	–	200	3.7E-11	2.5E-10	3.7E-07	
K08028F01	90.96	91.96	1	–	-130.81	–	-353.66	–	–	200	3.7E-11	2.5E-10	3.7E-07	
K08028F01	91.96	92.96	1	–	-130.86	–	-354.30	–	–	200	3.7E-11	2.5E-10	3.7E-07	
K08028F01	92.96	93.96	1	–	-127.94	–	-353.90	–	–	200	3.6E-11	2.4E-10	3.6E-07	

Flow rates of 1 m sections

Äspö, borehole K08028F01

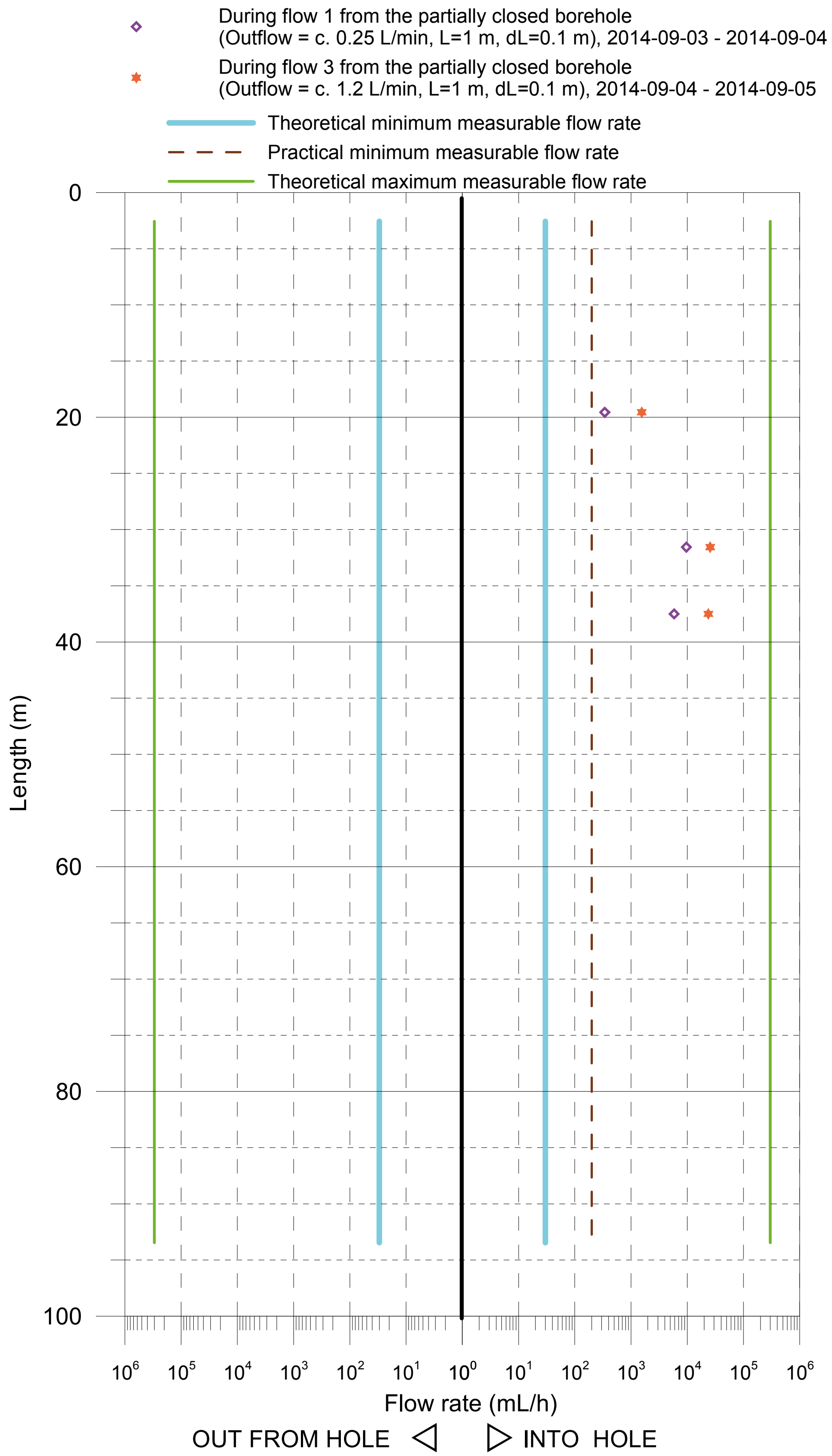

Transmissivity and head of 1 m sections

Äspö, borehole K08028F01

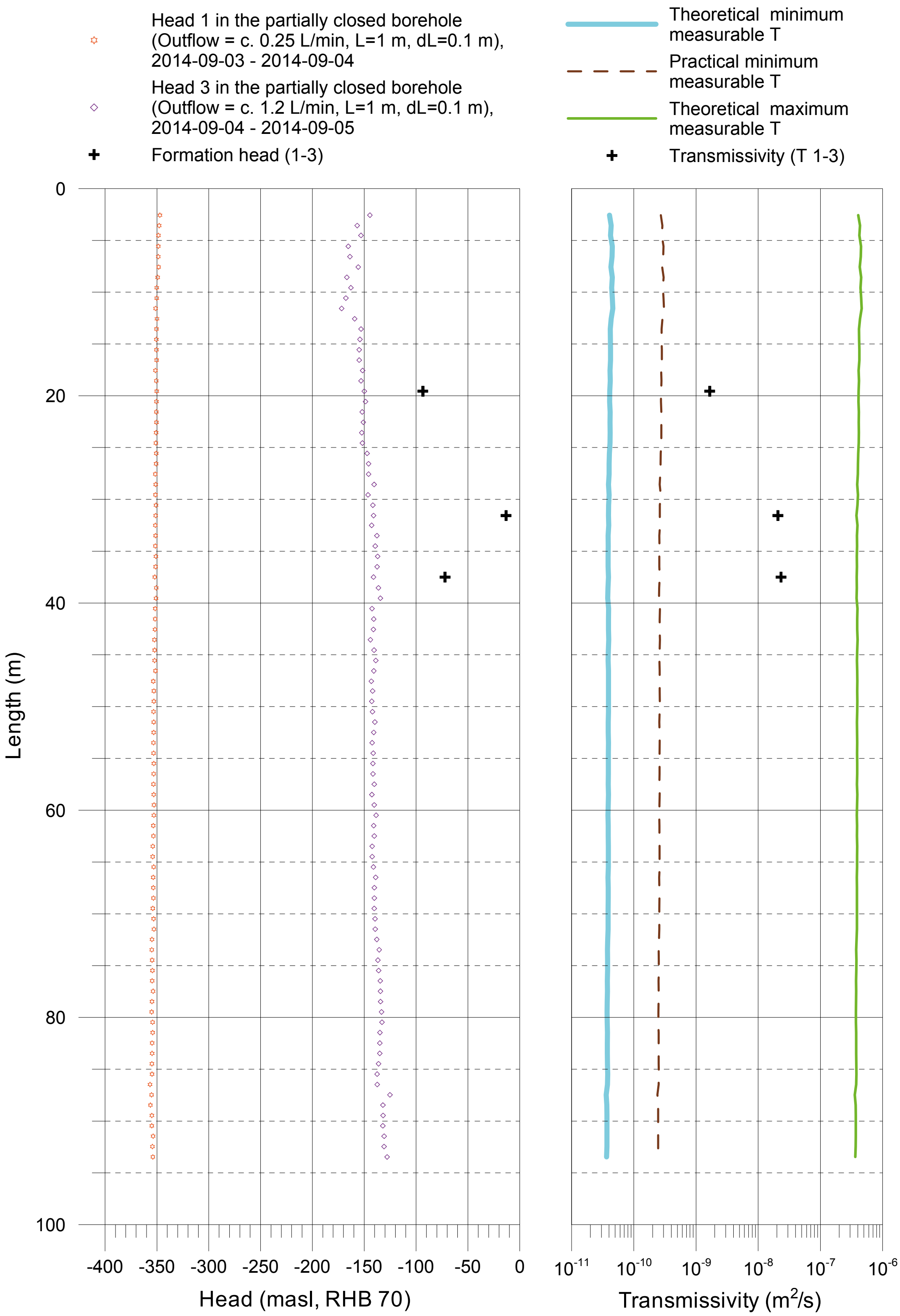

Transmissivity and head of 1 m sections

Äspö, borehole K08028F01

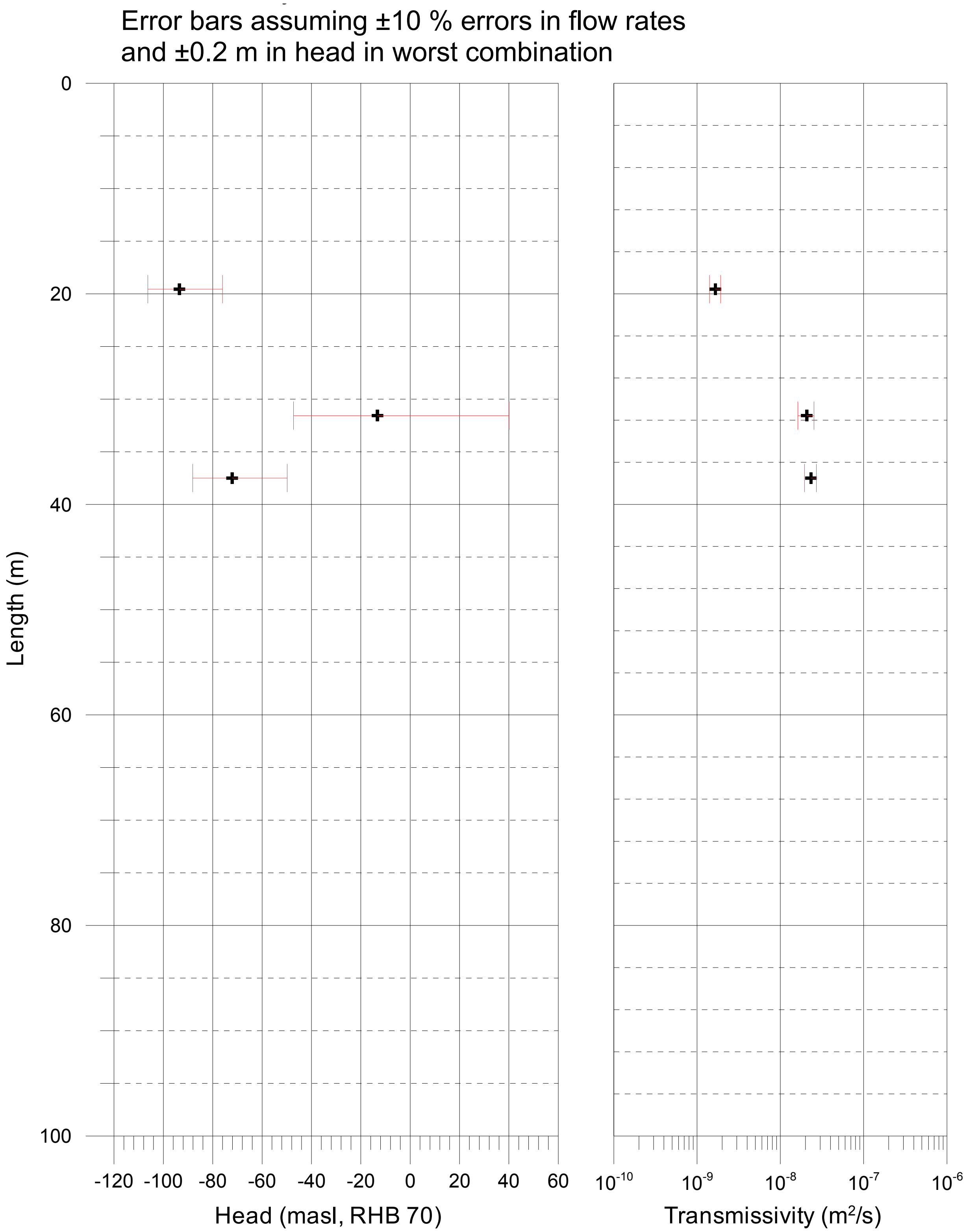

Appendix 19

Results of sequential flow logging

Borehole ID	Secup L(m)	Seclow L(m)	L_w (m)	Q_0 (m^3/s)	h_{0FW} (masl)	Q_1 (m^3/s)	h_{1FW} (masl)	T_D (m^2/s)	h_i (masl)	Q-lower limit P (mL/h)	TD-measl$_{LT}$ (m^2/s)	TD- measl$_{LP}$ (m^2/s)	TD- measl$_U$ (m^2/s)	Comments
K08028F01	3.79	8.79	5	–	−165.36	–	−356.80	–	–	200	4.3E-11	2.9E-10	4.3E-07	
K08028F01	8.79	13.79	5	–	−165.73	–	−359.81	–	–	200	4.3E-11	2.8E-10	4.3E-07	
K08028F01	13.78	18.78	5	–	−154.34	–	−358.62	–	–	200	4.0E-11	2.7E-10	4.0E-07	
K08028F01	18.78	23.78	5	9.47E-08	−150.37	–	−358.32	–	–	200	4.0E-11	2.6E-10	4.0E-07	*
K08028F01	23.78	28.78	5	–	−145.40	–	−358.17	–	–	200	3.9E-11	2.6E-10	3.9E-07	
K08028F01	28.78	33.78	5	2.68E-06	−142.60	7.33E-06	−359.35	2.1E-08	-17.8	200	3.8E-11	2.5E-10	3.7E-07	
K08028F01	33.78	38.78	5	1.62E-06	−137.21	7.38E-06	−356.89	2.6E-08	-75.4	200	3.8E-11	2.5E-10	3.7E-07	
K08028F01	38.77	43.77	5	–	−140.40	–	−360.35	–	–	200	3.8E-11	2.5E-10	3.8E-07	
K08028F01	43.77	48.77	5	–	−142.26	–	−357.85	–	–	200	3.8E-11	2.6E-10	3.8E-07	
K08028F01	48.77	53.77	5	–	−141.35	–	−358.89	–	–	200	3.8E-11	2.5E-10	3.8E-07	
K08028F01	53.77	58.77	5	–	−142.43	–	−357.32	–	–	200	3.8E-11	2.6E-10	3.8E-07	
K08028F01	58.77	63.77	5	–	−140.15	–	−356.83	–	–	200	3.8E-11	2.5E-10	3.8E-07	
K08028F01	63.76	68.76	5	–	−136.26	–	−358.81	–	–	200	3.7E-11	2.5E-10	3.7E-07	
K08028F01	68.76	73.76	5	–	−139.65	–	−361.03	–	–	200	3.7E-11	2.5E-10	3.7E-07	
K08028F01	73.76	78.76	5	–	−135.72	–	−359.71	–	–	200	3.7E-11	2.5E-10	3.7E-07	
K08028F01	78.76	83.76	5	–	−134.37	–	−359.38	–	–	200	3.7E-11	2.4E-10	3.7E-07	
K08028F01	83.76	88.76	5	–	−137.27	–	−360.07	–	–	200	3.7E-11	2.5E-10	3.7E-07	
K08028F01	88.75	93.75	5	–	−130.78	–	−358.79	–	–	200	3.6E-11	2.4E-10	3.6E-07	

* TD could not be calculated as flow was not detected with 5 m section due to high noise level.

Flow rates of 5 m sections

Äspö, borehole K08028F01

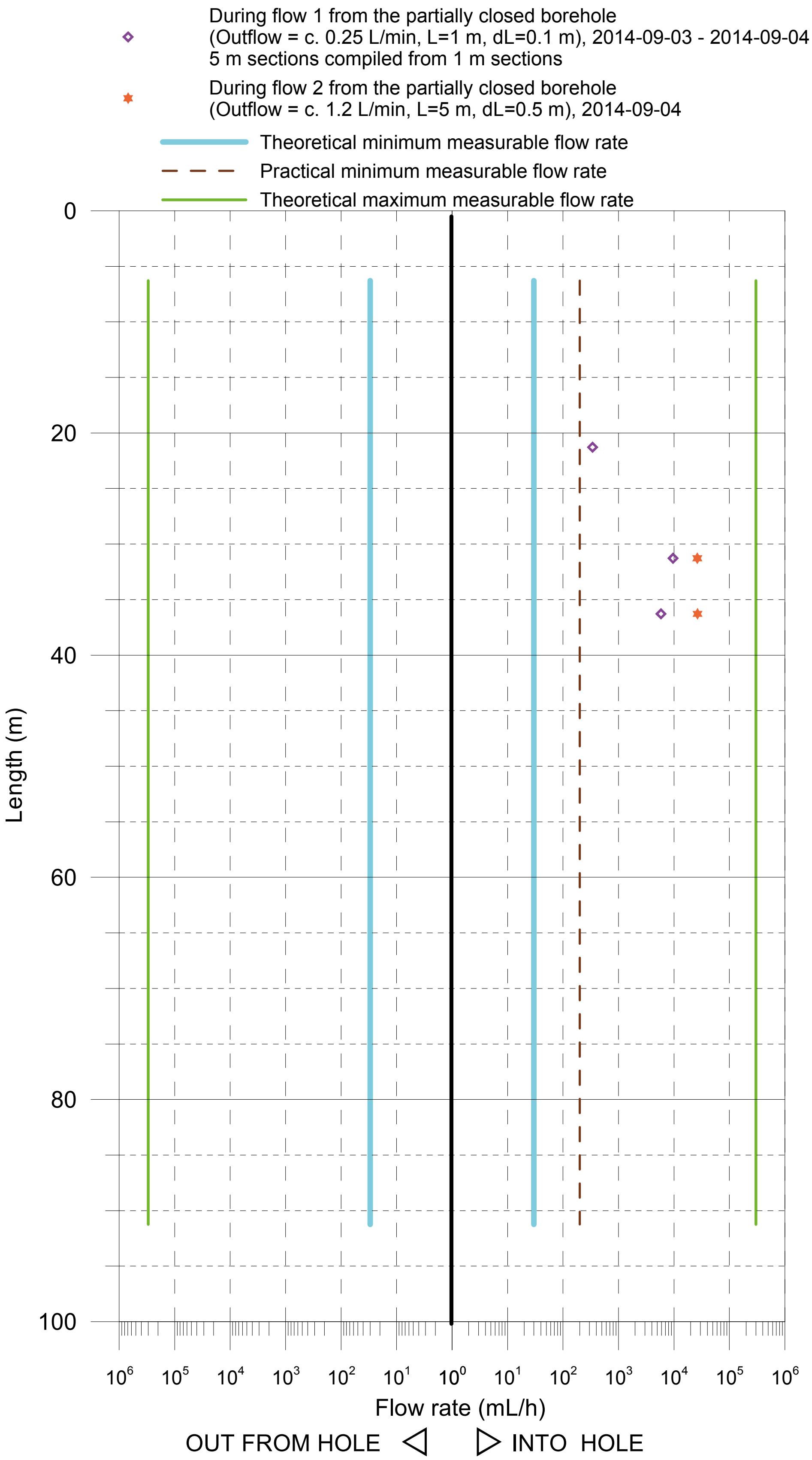

Transmissivity and head of 5 m sections

Äspö, borehole K08028F01

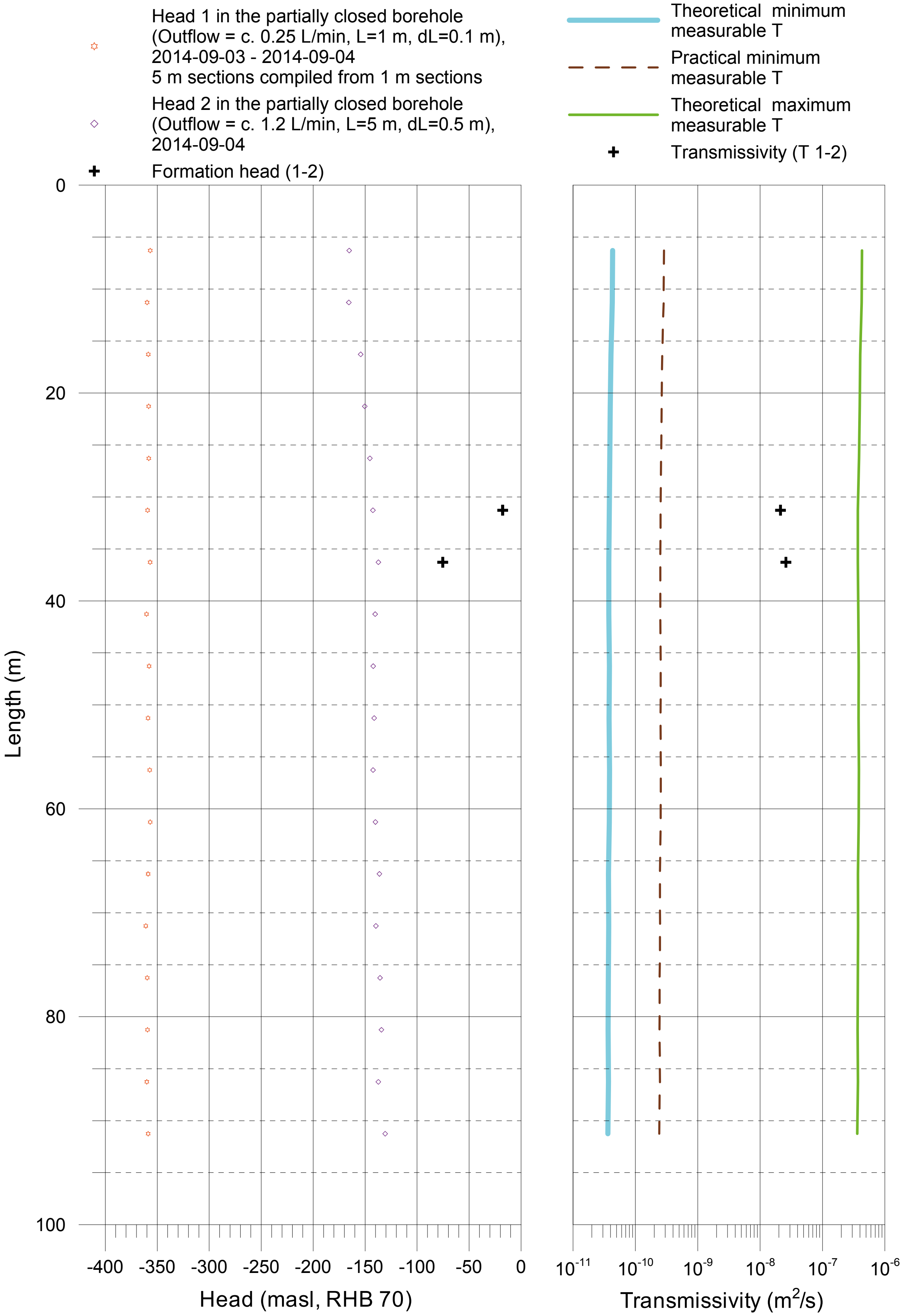

Transmissivity and head of 5 m sections

Äspö, borehole K08028F01

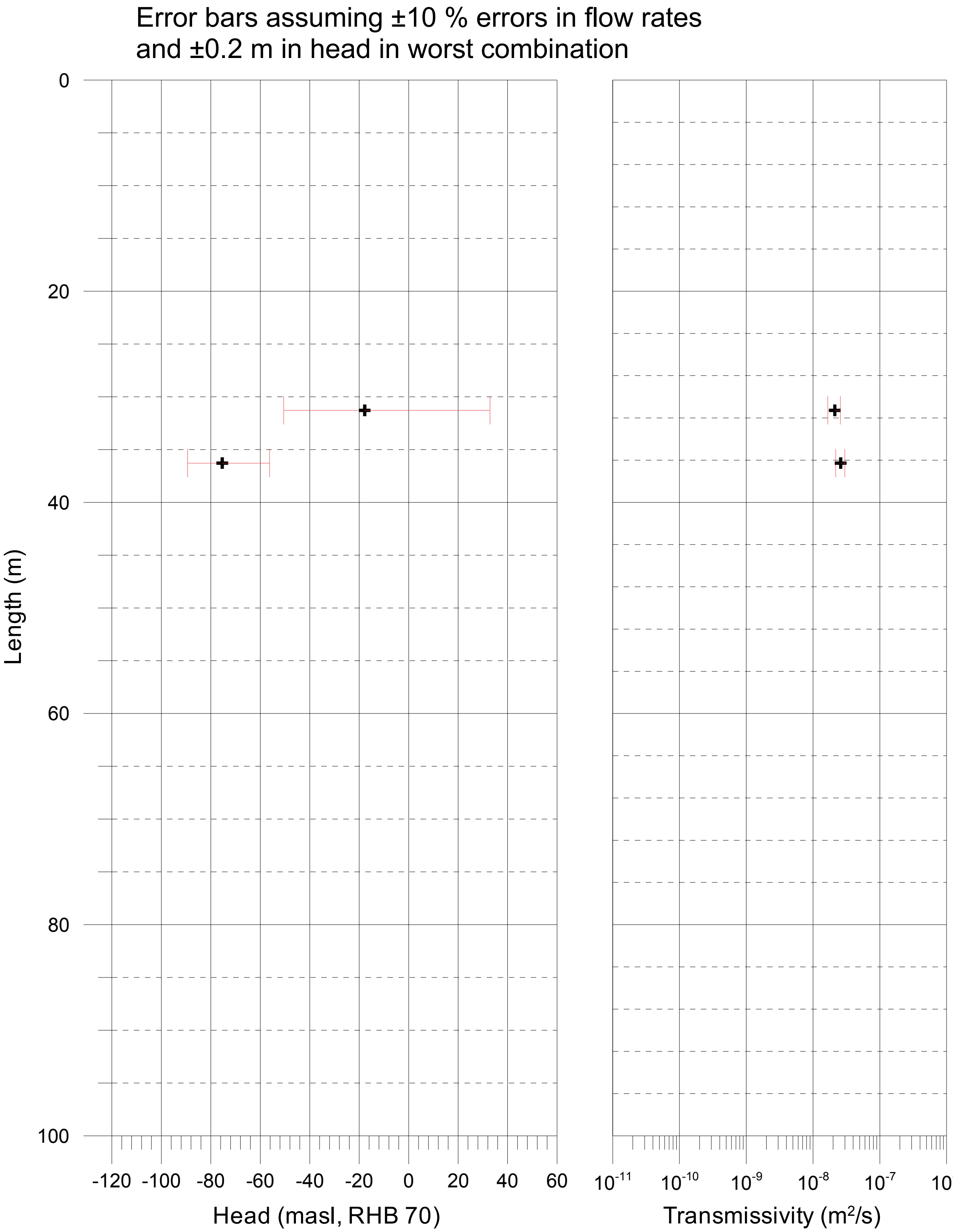

Inferred flow anomalies from overlapping flow logging

Borehole ID	Length to flow anom. L (m)	L_w (m)	dL (m)	Q_0 (m^3/s)	h_{0FW} (masl)	Q_1 (m^3/s)	h_{1FW} (masl)	T_D (m^2/s)	h_i (masl)	Comments
K08028F01	20.0	1	0.1	9.47E-08	−146.26	4.31E-07	−350.38	1.6E-09	−88.7	*
K08028F01	31.4	1	0.1	2.68E-06	−142.16	7.08E-06	−351.14	2.1E-08	−15.1	
K08028F01	37.6	1	0.1	1.62E-06	−141.02	6.58E-06	−352.16	2.3E-08	−72.0	

* Uncertain = The flow rate is less than 30 mL/h or the flow anomalies are overlapping or they are unclear because of noise.

Transmissivity and head of detected fractures

Äspö, borehole K08028F01

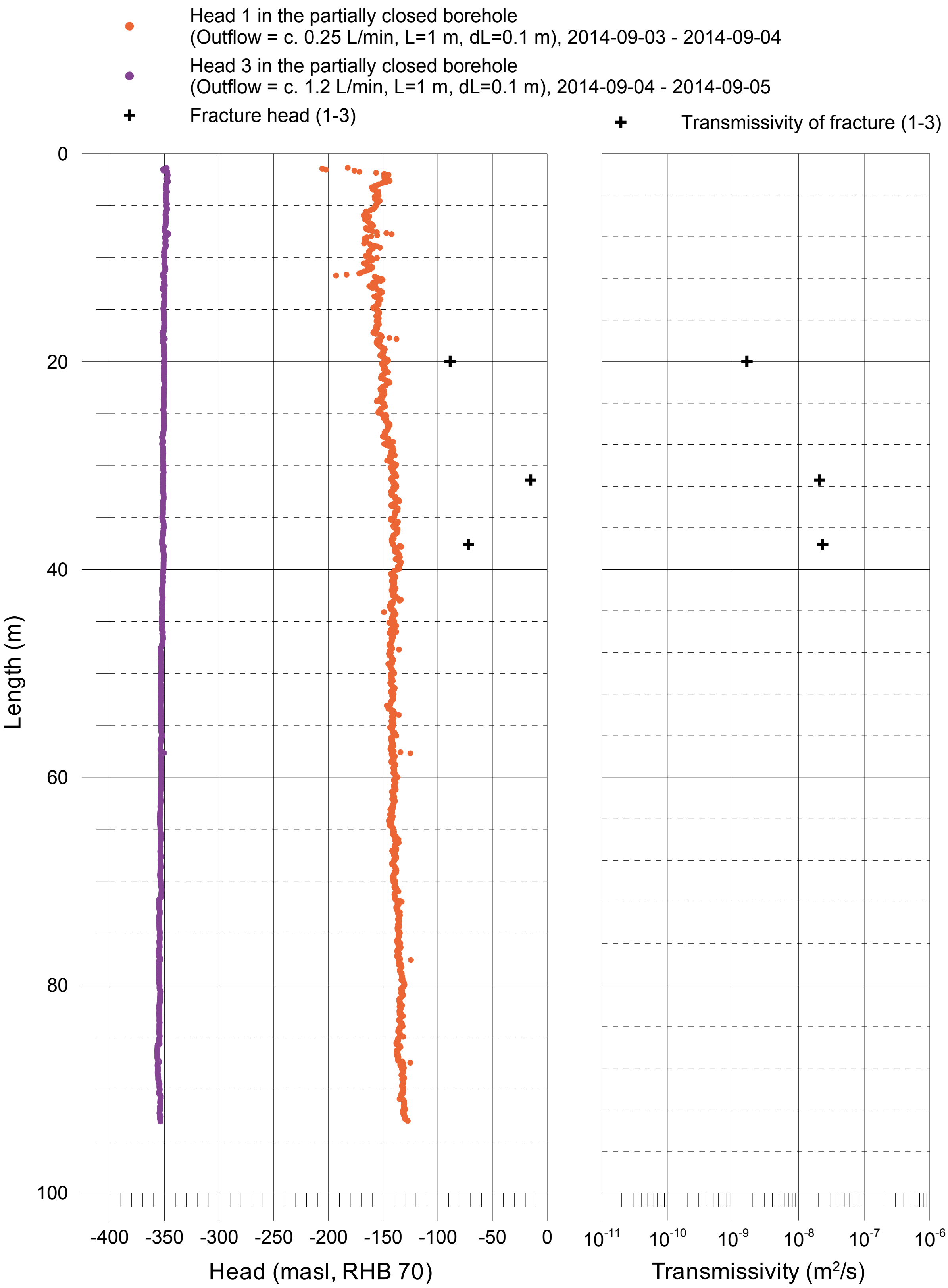

Comparison between section transmissivity and fracture transmissivity

Äspö, borehole K08028F01

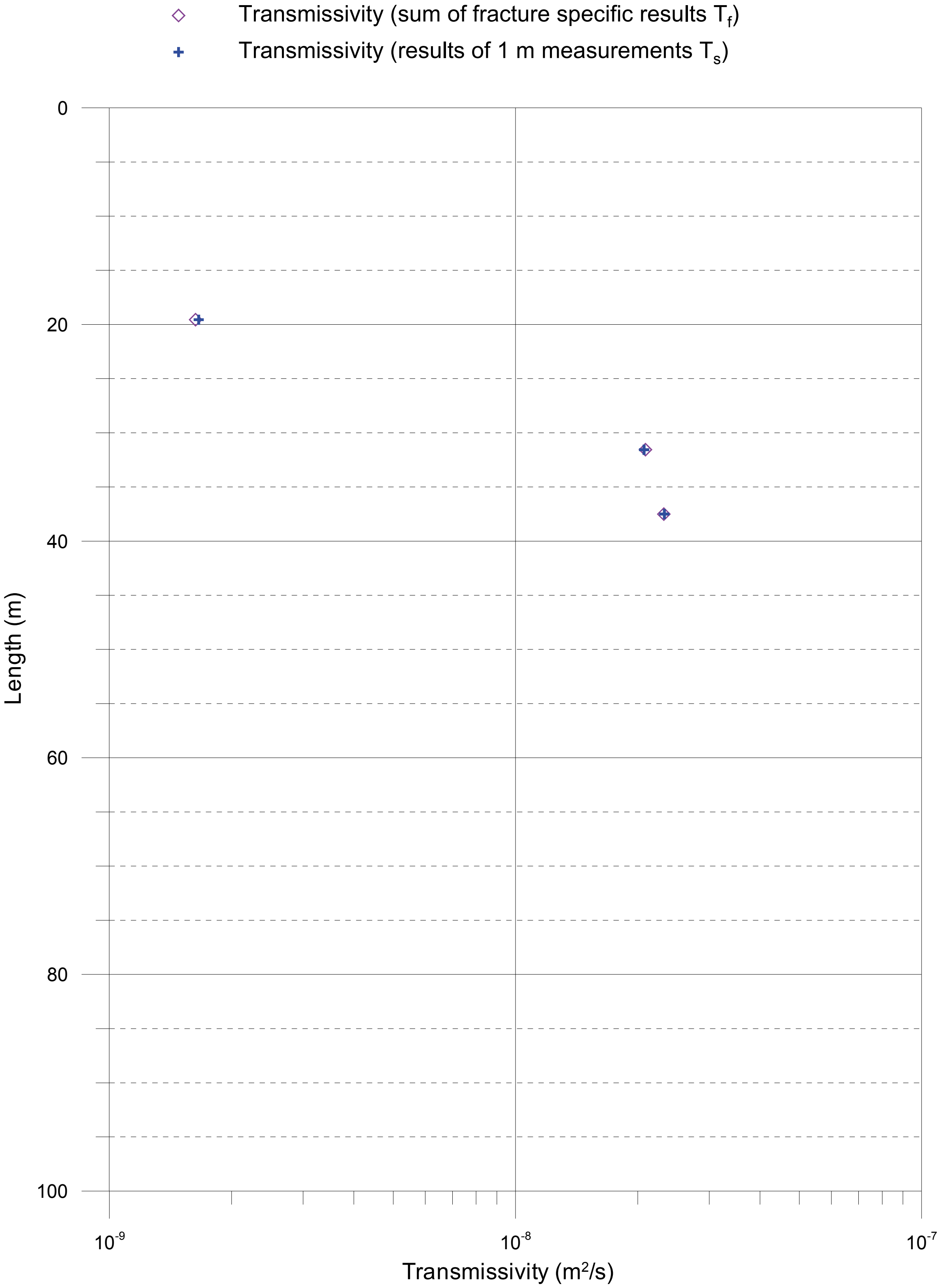

Comparison between section transmissivity and fracture transmissivity

Äspö, borehole K08028F01

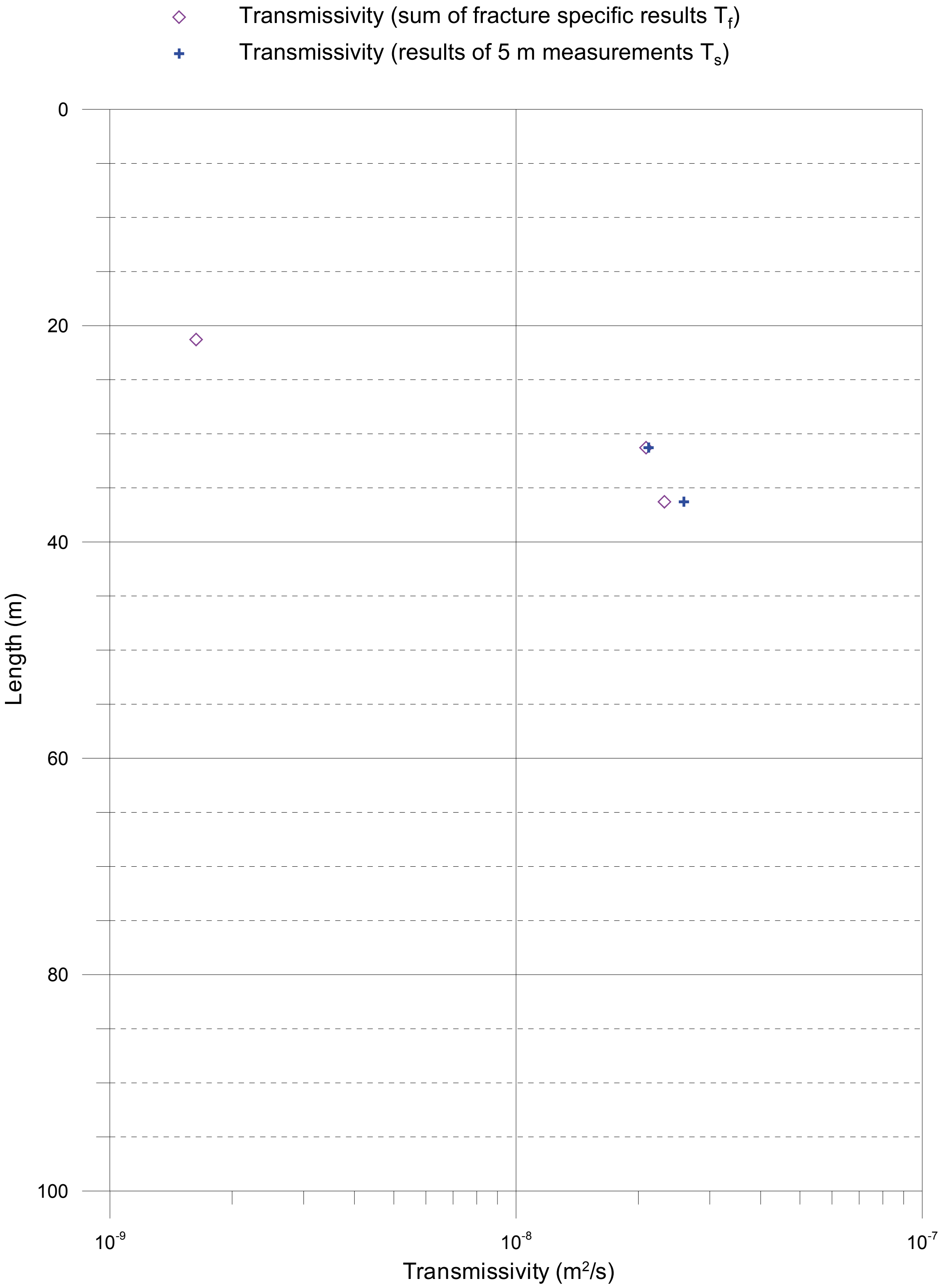

Head in the borehole during flow logging

Äspö, borehole K08028F01

Head(masl)= (Absolute pressure (Pa) - Airpressure (Pa) + Offset) /(1000 kg/m^3 * 9.80665 m/s^2) + Elevation (m)
Offset = 2600 Pa (Correction for absolute pressure sensor)

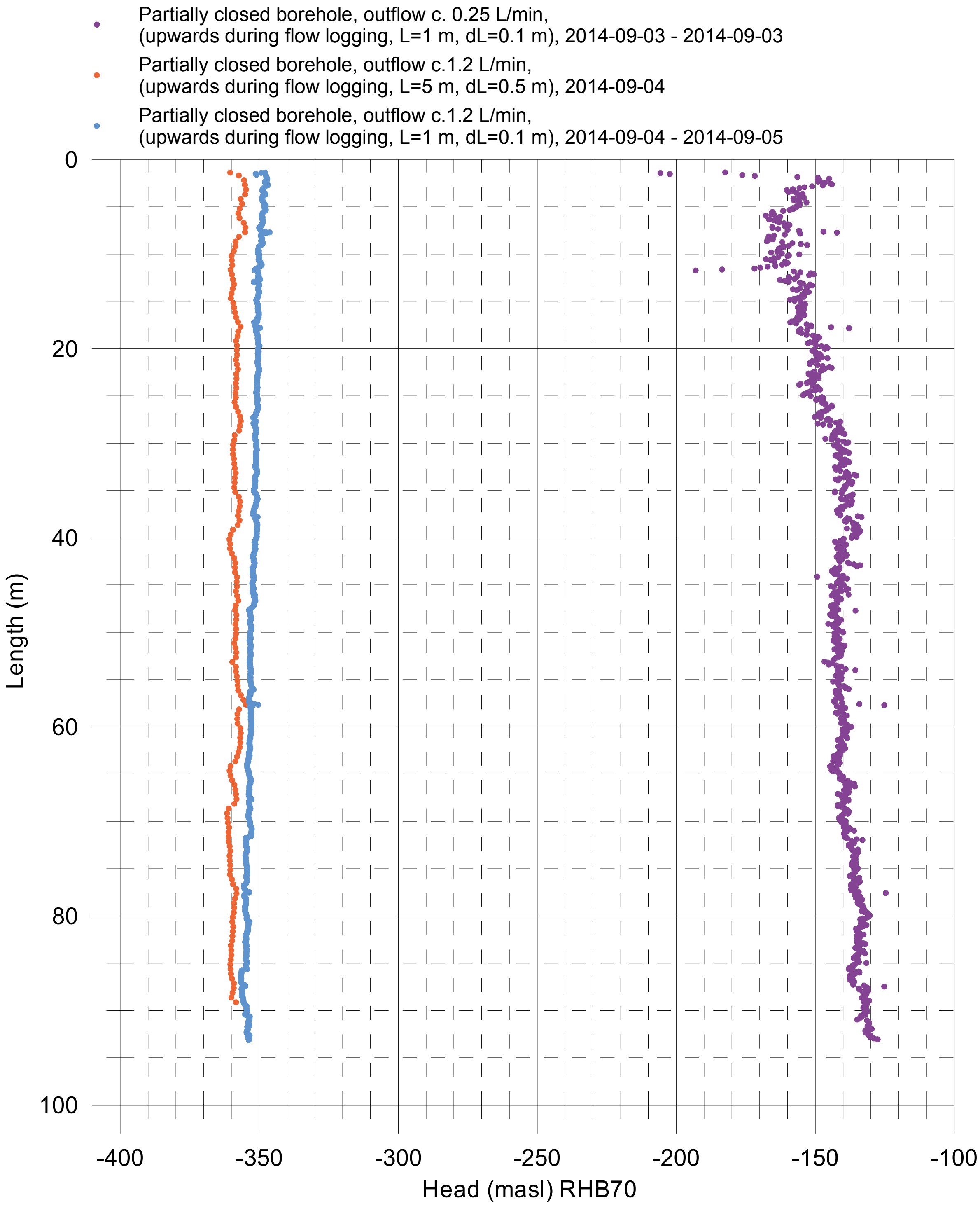

Pressure in the borehole during flow logging

Äspö, borehole K08028F01

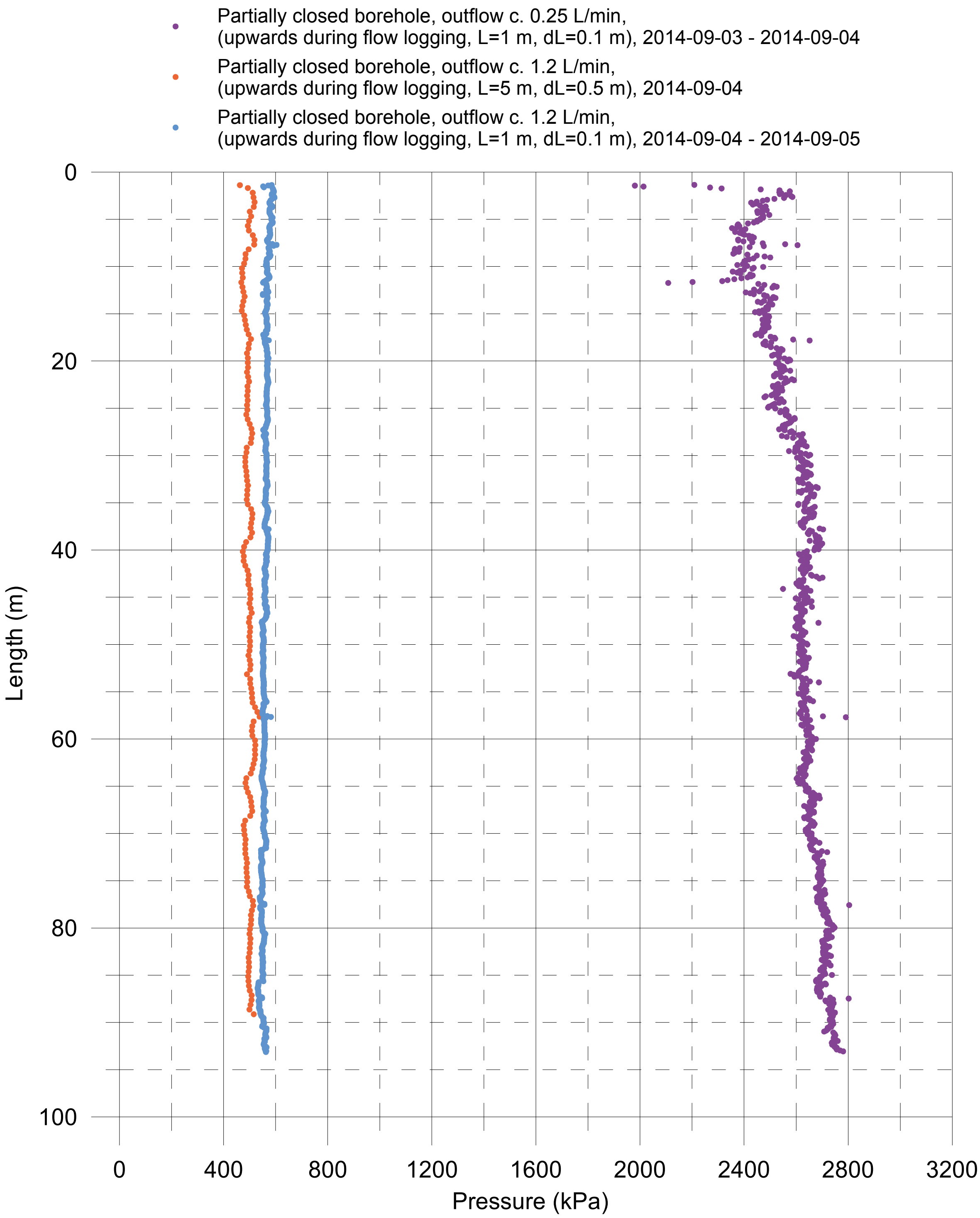

Borehole pressure and outflow from the borehole

Äspö, borehole K08028F01

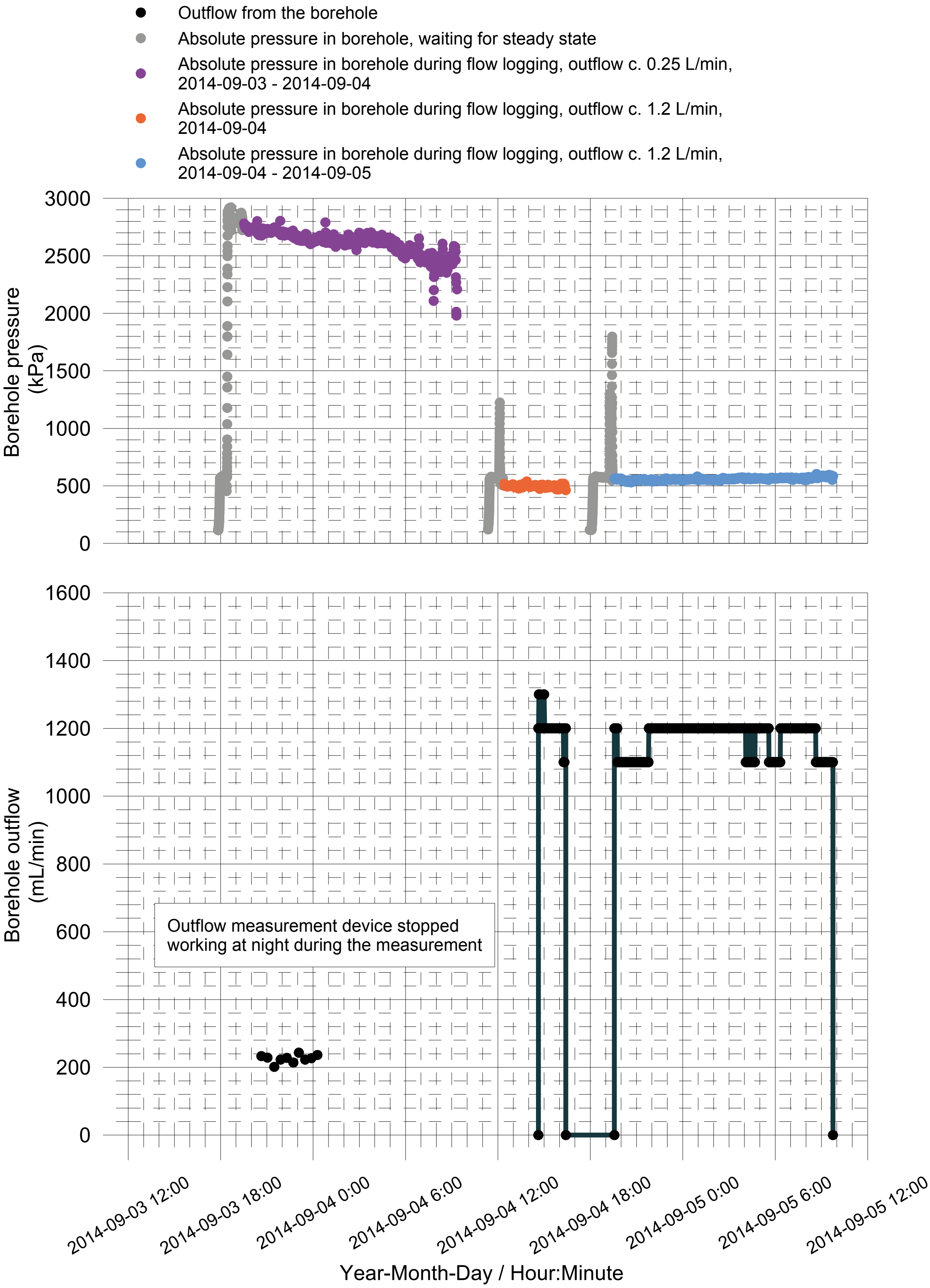

Arkitektkopia AB, Bromma, 2017

SKB is tasked with managing Swedish nuclear and radioactive waste in a safe way.

skb.se